Novel Photoarylation-based Controlled Polymerization of Conjugated Polymers and Its Application for Transparent Electrode

by

Joonkoo Kang

A dissertation submitted in partial fulfillment
of the requirements for the degree of
Doctor of Philosophy
(Macromolecular Science and Engineering)
in the University of Michigan
2019

Doctoral Committee:

Professor Jinsang Kim, Chair
Professor L. Jay Guo
Professor Katsuo Kurabayashi
Associate Professor Timothy Scott

Joonkoo Kang

jkkang@umich.edu

ORCID iD: 0000-0001-7172-8996

To my wife and son, the greatest driving forces of my life

and

To memory of grandmother who passed away during my doctoral studies

Acknowledgements

It took a lot of courage for me to begin a PhD program nearly at 40 years old. I believe it wouldn't be successful without surrounding myself with good people. This dissertation definitely owes much it to a number of great mentors and colleagues I met during my PhD study.

I would first like to thank my advisor, Professor Jinsang Kim for his ingenuous guidance and instruction. He always encouraged me to pursue entire perspective on my research and enjoy scientific challenges to undiscovered area. His insight into nature of conjugated polymers and their synthesis was sincerely instructive to achieve scientific and practical breakthroughs. Not to mention the research achievement, he was very supportive to have a great collaboration with LG Chem to which I am going back. I am pretty sure that his advice will be priceless to persist and maintain a positive attitude to my future research. I should also thank to my committee members, Professor Jay Guo, Professor Katsuo Kurabayashi, Professor Timothy Scott, and former committee member, Professor Shuichi Takayama for giving me very constructive training and feedbacks. Research progress could not be achieved without their insights over various research aspects. I cannot forget very valuable assistance by my program coordinators, Adam Mael and Julie Pollak. Thanks to their dedicated support, I was able to only focus on my research.

It was a great honor to work with the brilliant graduate students and postdocs in Kim Group. It was very exciting to discuss with Apoorv and Daseul about our research progress. They were my research mentors and didn't hesitate to give invaluable instruction and guidance based on solid

research backgrounds. It was extremely helpful to overcome a lot of difficulties I encountered during my experiment such as measurement, analysis, fabrication, and so on. Deokwon's guidance on general procedures of organic molecule synthesis was very instructive so that I was able to successfully settle down in the laboratory. Dr. Kyeongwoon Chung, Dr. Jaehun Jung, Dr. Dohyun Kang, Dr. Seongjun Yoon, Dr. Minsang Kwon, Dr. Gunho Kim, Dr. Youngchang Song, Dr. Byeongseop Song gave me very constructive advice to reduce potential trial and errors. Their professional attitude to science and research played a significant role in demonstrating great research progress. Especially I should not forget Dr. Dongwook Lee who led me into this group and helped me to have settled in the campus and Ann Arbor. I am also thankful to my former and current colleagues, Chen, Steven, Ricardo, Yingying, and Mark for being my great friends and discussing any research issues and advice.

This research was successfully completed by the research interests and continuous assistance of LG Chem. Dr. Youngjun Hong and Youngrae Jang, who were my former group leaders and mentors, are strong supporters and mentors to pursue my research both in academic and industrial areas. Thank to Dr. Sungsoo Yoon and Dr. Jeongrae for their research interests in conducting polymers and I look forward to contributing to their research goals by joining the group after my graduation. My academic and company colleagues, Taesu Kim, Sunghyun Nam, and Wooram Lee. Pleasant memories with you and your family members will be never forgettable.

None of this would be realized without my wife and son who sacrificed themselves to support my PhD study. I am confident to say that all my achievement owes your dedication. Whenever I was struggling with my research, they always encouraged me to stand me in good stead. Thank you for being my supporters.

Finally, give all honor to God.

Table of Contents

List of Figures

Abstract

In order to afford the production of conjugated polymers with uniform and desirable optical and electrical properties on a large scale, much effort have been devoted to light-induced polymerization. Various well-defined conducting polymers are potentially achievable by devising efficient photo-polymerization strategies. Solid-state photo-polymerization of conjugated conducting polymer films not only allows fast thin film fabrication but also is applicable to roll-to-roll process for cost-effective mass production. In spite of these and other invaluable benefits of photo-mediated polymerization, few research papers have reported outstanding optoelectronic values through the photopolymerization.

In this dissertation, a new one-pot photo-mediated polymerization for conjugated polymers with a high molecular weight and narrow polydispersity was devised and its polymerization mechanism was mechanistically investigated. The overall polymerization is composed of two sequential photochemical reactions; 1) photo-arylation between ProDOT molecules and 2,5-diiodo-ProDOT derivatives by 365nm LED irradiation to afford conjugated oligomers, 2) chain extension of diiodinated ProDOT oligomers by addition of iodine source followed by q-switched 532nm pulsed laser to make large molecular weight conjugated polymers. The adoption of the pulsed laser having the longer wavelength not only facilitates photochemical couplings of the diiodinated oligomeric precursors by matching their absorption wavelength but also prevents the

photodegradation of the extended chains by the pulsed illumination. All the photochemical reactions were manipulated by carbon-iodine bonds of growing chain ends that reversibly produce corresponding radical species in the presence of a hydrogen-free solvent, $CBrCl_3$ (bromotrichloromethane), preventing radical consumption by hydrogen-containing solvent molecules. This polymerization process was also successfully employed in the copolymerization of ProDOT monomers with different side chains where the copolymer composition is determined by the feed ratio of the monomers. The characterization of the polymerized products was performed through UV-vis absorption, ^{1}H-NMR, mass spectroscopy, and GPC to analyze the photo-mediated polymerization mechanism for conjugated polymers.

The developed photoarylation-based polymerization for conjugated polymers in solution was adopted in devising solid-state photopolymerization of ProDOT and EDOT derivatives to fabricate conducting and transparent thin polymer films. The composition of the copolymerized thin films from the thiophene derivatives with different side chains was analyzed by XPS and FT-IR. The photochemical coupling between 2,5-diiodo ProDOT or EDOT and a series of heterocyclic molecules in solid states rendered solvent-resistant polymer thin films on glass substrates. A subsequent chemical doping of the polymer thin films with protonic acids provided electric conductivity and optical transparency. Great electrical conductivity (~2,200 S/cm) and high transparency (>80%) were achieved from ProDOT and EDOT derivatives by photo-arylation based UV polymerization. Experimental parameters affecting the polymerization efficiency such as reaction temperature, light source intensity, and side chains of precursors were systematically investigated to enhance the optical and electrical properties of the conducting polymer thin films. In the absence of solvent, mobility of the monomers and growing polymer chains turned out to be critically important to realize large molecular weight polymers and consequential high conductivity. The best optical and electrical properties of the resulting polymer thin films was

achieved from the copolymers of 2,5-diiodo EDOT incorporating a diethylene glycol side chain (DIEDOT-DEG) and EDOT. While the flexible side chain of the former imparts good mobility to the growing polymer chains, the latter without having any side chain contributes to high electrical conductivity by allowing close molecular packing owing to the minimized insulating and steric volume inevitably imposed by side chains.

Chapter 1 Introduction

1.1 Overview of Conjugated Polymers

Since the outstanding electric conductivity from doped polyacetylenes was reported by Heeger, MacDiarmid, and Shirakawa in 1976,[10] conjugated polymers have been extensively studied as a novel class of organic semiconductor showing readily tunable optoelectronic properties with outstanding stability under chemical, thermal, and mechanical stresses. Their nature of plastic, lightweight, easy processability, and flexible semiconducting properties offer new opportunities to replace traditional metallic and inorganic electronic materials for various optoelectronic devices, such as field effect transistors[11,12], light-emitting diodes[13–15], organic solar cells[16,17], and sensors[18–20].

The unique conductivity of the conjugated polymers is originated from the π-conjugation formed by alternating single and double carbon-carbon bonds along the linear polymer backbone and doping mechanism. The conjugation system by the overlapping of π bonds allows the delocalization of unpaired electrons and facilitates charge transfer along the main chains upon doping. When some of the π electrons are removed from conjugated polymers by oxidation, the produced holes are mobile within the conjugated π-orbitals along the polymer backbone through resonance (Figure 1.1 (c)) and between the π-conjugated polymer backbones via hopping. The so-called polaron or bipolaron states of p-doped conjugated polymers afford a several orders increase

in electrical conductivity, resulting in the transition of the conjugated polymers from insulators to semiconductors. Despite of the metallic conductivity of p-doped polyacetylenes (~10^5 S/cm), their inherent insolubility and easy oxidation cause degradation of the π-conjugation, limiting the applicability and practical value of polyacetylenes.

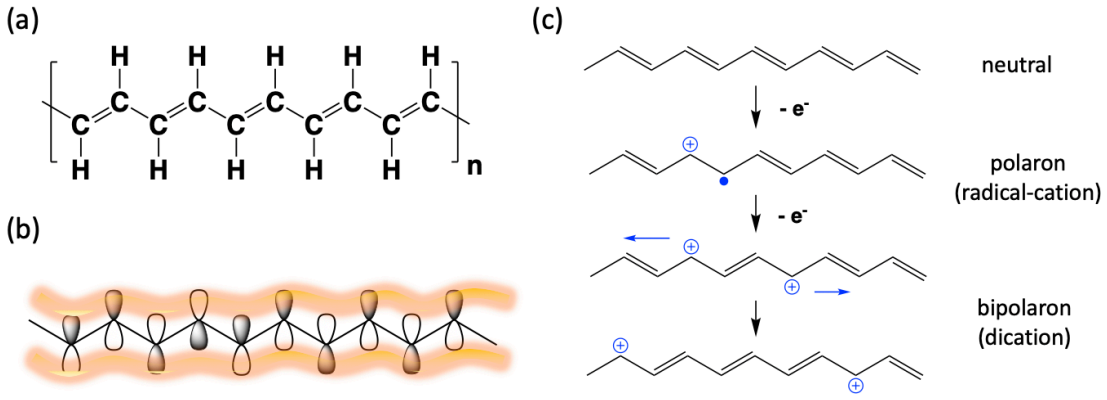

Figure 1.1. Chemical and electronic structure of conjugated polymers. (a) chemical structure of polyacetylene, (b) electron delocalization by π orbital conjugation of polyacetylene, and (c) the formation of cation and dication by electron extraction from neutral polyacetylenes.

Heteroaromatic arylenes such as pyrrole, aniline, and thiophene displayed in Figure 1.2(a) are regarded as a promising monomer to form processable and air-stable conducting polymers having a great potential to demonstrate outstanding optical and electrical properties in doped states. In particular, polythiophene and its derivatives have been extensively investigated due to their easy structural modification to tune the physicochemical and optoelectronic properties through incorporating various functional groups such as alkyl, electron donating, and electron withdrawing groups. While alkyl side chains present solubility to the rigid polymers and prevent the aggregation of polymeric chains, incorporation of electron donating/withdrawing substituents on the thiophene backbone affects the energy levels and bandgap of the polymers so as to manipulate the optical and electrical properties of the polythiophene derivatives. Whereas electron rich side chains reduce

the oxidation potential (or energy bandgap) of conjugated polymers by donating electrons to the conjugated backbones, electron deficient ones withdraw electrons from the main chains, increasing the bandgap of the polymers. A few polythiophene derivatives are shown in Figure 1.2. In particular, 3,4-ethylenedioxythiophene (EDOT) monomer is of great interest for the synthesis of conjugated polymers since the electron donating ethylenedioxy substituent on the thiophene ring not only lower the oxidation potential but also promotes coplanar packing of the resulting polymers in solid state, allowing considerable improvement in optoelectronic property.

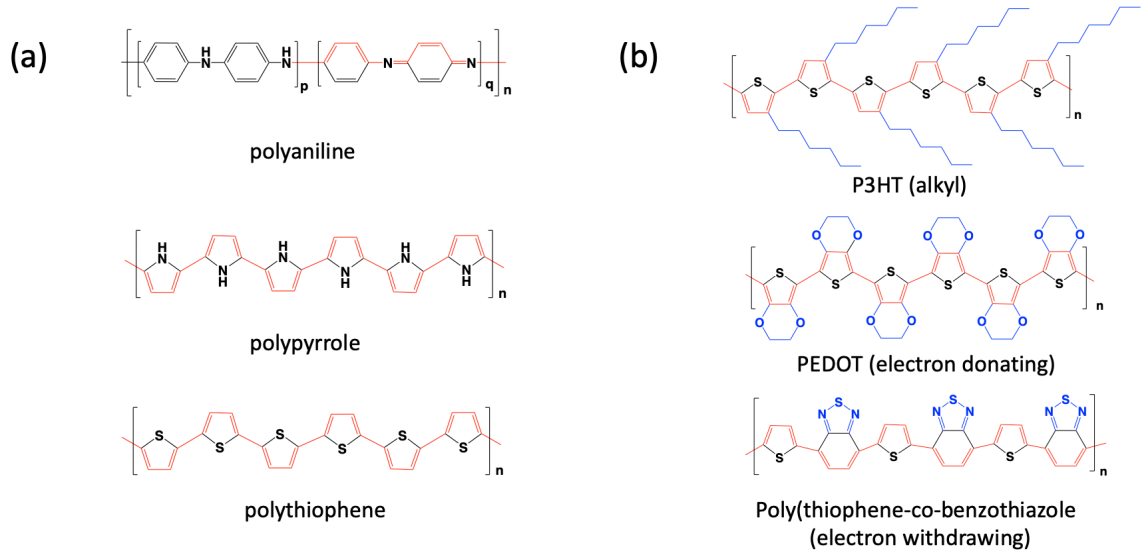

Figure 1.2. Chemical structures of (a) conjugated polyheterocycles and (b) polythiophene derivatives.

1.2 Conventional polymerization for conjugated polymers

1.2.1 Oxidative polymerization

1.2.1.1 Chemical oxidative polymerization

Since PEDOT, poly(3,4-ethylenedioxythiophene), has proven its outstanding electrical properties, there have been numerous efforts to polymerize EDOT and its derivatives. Chemical

oxidative polymerization is one of the most popular PEDOT synthetic routes. It is commonly taken place through the oxidation of EDOT monomer or oligomer in the presence of strong oxidants such as iron(III) chloride ($FeCl_3$)[21], manganese dioxide (MnO_2)[22], copper chloride ($CuCl_2$)[23], or iron tosylate[24]. Heywang et al reported that several thiophene derivatives were oxidatively polymerized by iron(III) chloride as the oxidant in boiling acetonitrile, resulting in the formation of insoluble powders with high conductivity.[21] As depicted in Figure 1.3, the redox reaction between EDOT and $FeCl_3$ manages the polymerization, eventually producing p-doped PEDOT in the presence of $FeCl_4^-$.

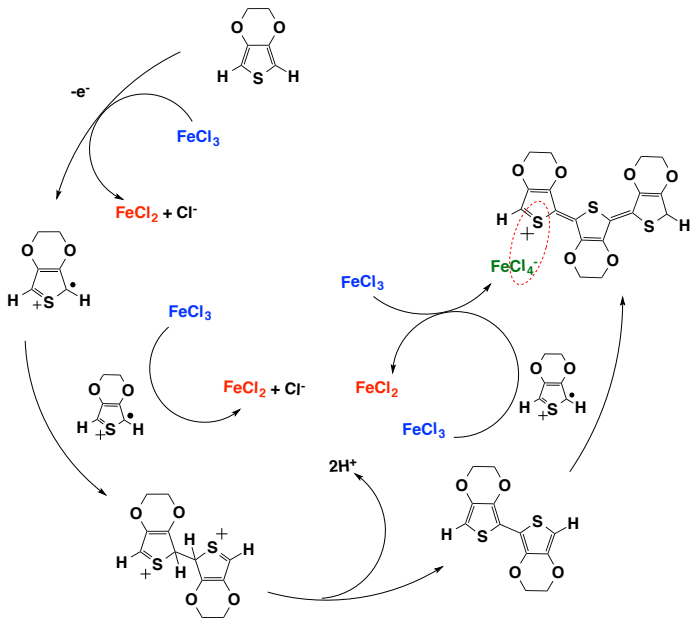

Figure 1.3. The chemical oxidative polymerization for PEDOT based on the coupling of radical cationic species in the presence of iron(III) chloride ($FeCl_3$).

Interestingly, oxidatively polymerized PEDOT powders exhibited excellent conductivity enhancement up to 3000 folds compared to the polypyrrole synthesized in the same manner, while

no polymerized product of polythiophene was observed by the chemical oxidative polymerization. It implies that the electron donating ethylenedioxy substituent on thiophene of EDOT plays a significant role in the efficient polymerization by facilitating the formation of radical cationic EDOT molecules. Despite the unique optical and electrical performances of PEDOT synthesized through the solution based chemical oxidation, the resulting polymers is readily precipitated in solvents during the polymerization due to the intermolecular coulombic interaction between doped polymer chains so that significant loss of the products is inevitable under a dialysis to get rid of small molecular weight species or ion exchanging resins from the dispersed solution[25]. Hence, the chemical oxidative polymerization by the small molecular oxidants is not desirable to the applications of multilayer coating or microelectronic devices[26]

PEDOT can also be polymerized on pre-formed oxidant platforms. The oxidative polymerization of EDOT on a polymeric salt, polystyrene sulfonate (PSS), in the presence of sodium persulfate ($Na_2S_2O_8$) brings about the formation of water soluble PEDOT:PSS which is one of the well-known and commercialized conducting polymers.[27,28] Owing to the good solubility of PSS chains, wet coating process of PEDOT:PSS is possible to fabricate homogeneous conducting polymer thin films. Its electrical properties can be tuned by post-treatment with polar solvents or small molecules such as DMSO or ethylene glycol, which controls charge concentration of the conjugated backbones by screening coulombic interaction between PEDOT and PSS chains.[29–31] A PEDOT film can be formed on pre-deposited ferric chloride ($FeCl_3$) layer by vapor phase polymerization(VPP) or oxidative chemical vapor deposition (o-CVD) of EDOT monomers.[32,33] EDOT monomers deposited on the oxidant layer prepared via spin casting are polymerized to produce a p-doped PEDOT films with conductivity of 25~100 S/cm.

1.2.1.2 Electrochemical polymerization

Electrochemical polymerization is a promising synthetic route to achieve conducting polymer thin films having uniform optical and electrical properties.[34–37] It is carried out in highly acidic electrolytes of water, organic solvents, or ionic liquids with the insertion of counter anions in the presence of monomeric molecules. Under the applied electric fields, EDOT monomers are oxidized by electron transfer to counter anions in electrolytes and polymerized on a conductive electrode. The doping levels of the polymerized film are easily controlled by current density, and the doping/de-doping by external electric field is highly reversible. In addition, the conductivity values of PEDOT films are dependent on the type of counterions used in the in-situ polymerization. While the incorporation of small molecular weight counter anions such as ClO_4^-, BF_4^-, and PF_6^- increases the conductivity of electrochemically polymerized PEDOT films up to 780 S/cm,[34,38] the PEDOT films using polyelectrolytes such as PSS or poly(β-hydroxyethers) in the same manner didn't exhibit compelling conductivity values but showed enhanced mechanical stability of the films.[39,40] However, it is challenging in the electropolymerization to control the physical and chemical properties such as thickness, morphology, and film compositions. Moreover, only conducting electrodes such as ITO coated glasses are eligible for the electropolymerization.

1.2.2 Halogen assisted self-polymerization in solid state

The halogen assisted self-polymerization of EDOT or ProDOT (3,4-propylenedioxythiophene) was suggested as another synthetic strategy to achieve transparent and conducting polymer thin films.[1,41] Wudl group incidentally found 2,5-dibromo EDOT (DBrEDOT) molecules underwent a solid-state polymerization to yield insoluble but conducting product in a prolonged storage at room temperature for 2 years. They found out that the product is bromine doped PEDOT thin films through the characterization of ^{13}C-NMR, FT-IR, and XRD. Based on

ESR monitoring, DSC spectra, and the kinetic study from carbon-halogen bonds, they suggested an autocatalytic solid-state polymerization mechanism initiated by radical cations of DBrEDOT (or DBrProDOT) as described in Figure 1.4, resulting in the formation of higher molecular weight species. Accordingly, the self-doping of DBrEDOT and DBrProDOT precursors gives rise to the formation of a transparent and conducting thin film (0.05~20 S/cm).

It is interesting that any decent self-polymerization of 2,5-diiodo EDOT (DIEDOT) was not observed in the same condition for the DBrEDOT polymerization in spite of the lower dissociation energy of C-I bonds than that of C-Br ones. The difference in the polymerization efficiency was attributed to the distinct molecular packing structure of DBEDOT and DIEDOT in solid state. Owing to the reduced intermolecular distance of the coplanar packing of DBrEDOT, the close π-π stacking of DBrEDOT is expected to be more advantageous to the polymerization than the in-plane molecular arrangement of DIEDOT.

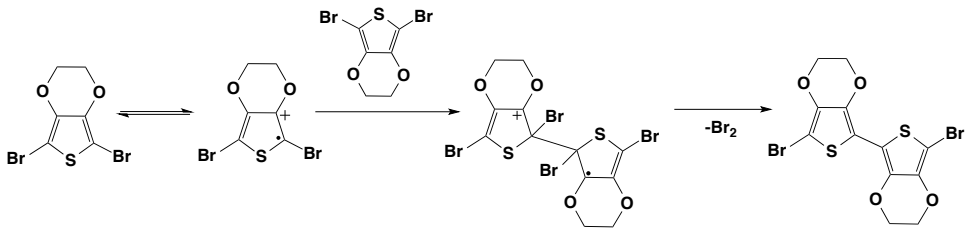

Figure 1.4. The scheme of self-oxidative dimerization of 2,5-dibromo-EDOTs.[1] (Reedited with permission from American Chemical Society publisher (Ref. 32). Copyright 2003)

The bromine assisted solid-state polymerization is also valid for the pristine EDOT monomers deposited via chemical vapor deposition (o-CVD) in a vacuum chamber.[2] They proposed a free radical mediated polymerization mechanism (Figure 1.5), different from the vapor phase polymerization of EDOT on $FeCl_3$ or solid-state self-polymerization of DBrEDOT whose

polymerization is managed by radical cationic precursors. The polymerization was initiated by bromine radicals that are produced from co-deposited Br_2 with EDOT monomers. A bromine radical reacts with EDOT monomer to produce brominated EDOT radical, followed by free radical polymerization to yield PEDOT products. Extra bromine molecules produced by the polymerization are used to dope PEDOT main chains to form a conducting polymer thin film. The doping level of the PEDOT film by bromine was confirmed by the coordination of Br/EDOT from XPS survey scan.

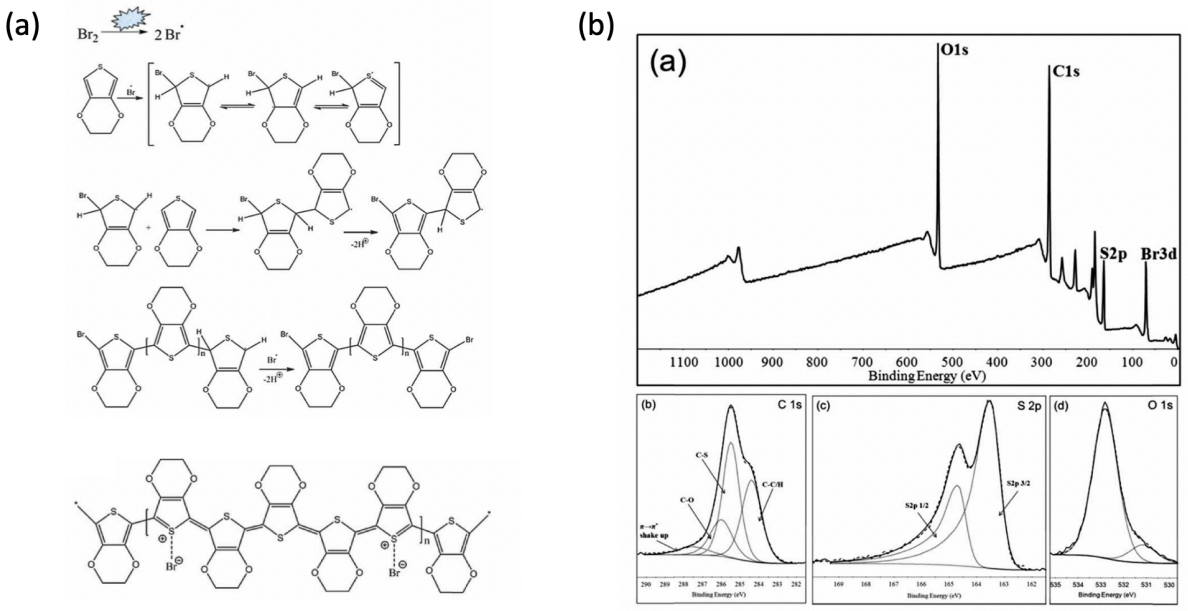

Figure 1.5. Bromine radical assisted polymerization of EDOT. (a) The polymerization scheme and (b) XPS survey scan for bromine doped PEDOT film[2] (Reprinted with permission from Royal Society of Chemistry publishers (Ref. 34). Copyright 2017)

1.2.3 Organo-metallic synthesis

The oxidative or solid-state polymerization commonly give rise to the formation of p-doped conjugated polymers in the presence of counter anions or dopants. Because of the electrically

charged structure and the absence of solubilizing functional groups, the resulting polymers rarely dissolve in organic solvents such as chloroform ($CHCl_3$). Therefore, it is challenging to characterize the resulting polymers by H-NMR, mass analysis (MALDI), and GPC, which are critical to elucidate the polymerization mechanism and the molecular structures of the resulting conjugated polymers.

The synthesis of undoped and soluble conjugated polymers is desirable to engineer and characterize the molecular structures as designed. The synthesis of electrically neutral conjugated polymers can be generally achieved by means of Grignard metathesis (GRIM) polymerization.[42–44] Since McCullough developed this metal catalyst mediated cross-coupling polymerization to synthesize a regioselective poly(3-alkylthiophenes) in 1992,[45,46] it has paved the way for the synthesis of conducting polymers with well-defined molecular structures along with the precise control of molecular weight and polydispersity. 2,5-halogeno-3-alkyl thiophene with an asymmetric molecular structure is employed for the organometallic polymerization owing to its high reactivity in organometallic reactions. The Grignard metathesis was performed using a consecutive two-steps procedure as described in Figure 1.6: (1) iodine-magnesium exchange with alkyl-metallic compound to produce 2-bromo-3-alkyl-5-thienyl magnesium chloride, (2) Nickel-catalyzed reductive polycondensation upon the addition of $Ni(dppp)Cl_2$. It is intriguing that the polymerization revealed a chain-growth behavior in living fashion with a linear increase in molecular weight with excellent thiophene monomer conversion while maintaining low polydispersity. After eliminating extra nickel catalyst and byproducts, the resulting polymer showed its main absorption at 400~500nm corresponding to the π-π^* transition in neutral state. In addition, the regioselective coupling of the asymmetric monomers led to the regioregular poly(3-hexylthiophene) (rr-P3HT) as shown in Figure 1.2(b), demonstrating excellent conductivity of 1000 S/cm by iodine doping.[45]

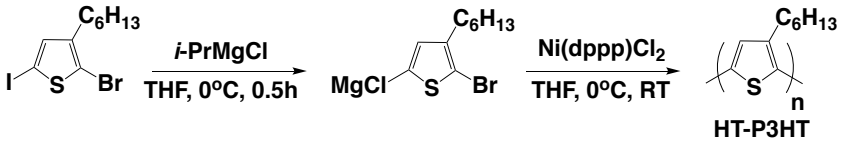

Figure 1.6. Synthetic scheme of a regioregular poly(3-hexylthiophene) by Grignard metathesis.[47]

The nickel-mediated Grignard metathesis is also widely used for the synthesis of PProDOT derivatives having various functional groups. Reynolds group employed Grignard metathesis to synthesize PProDOT incorporating regiosymmetric alkyl side chains for electrochromic device applications.[43,48,49] Although the results indicated a less efficient polymerization efficiency with broader polydispersity over 1.50 compared to the P3HT synthesized in the same manner, they showed excellent solubility in organic solvent due to the long alkyl side chains. The organometallic synthetic route is also available to synthesize dedoped PEDOT.[50–53] The polymerization is managed by dehalogenation of 2,5-dihalogeno-EDOT derivatives by $NiBr_2$-bipyridine complex. However, its inherent insolubility due to the absence of solubilizing side chains is disadvantageous to characterize the molecular structures of the resulting polymers and polymerization mechanism.

1.3 Photopolymerization for conjugated polymers

1.3.1 Photo-induced polymerization for non-conjugated polymers

Besides the conventional synthetic routes to achieve conducting polymers, photo-mediated polymerization to synthesize conjugated polymers has been of great interests in both academia and industries due to its great commercial and practical values. It is not only instantaneous but also less influenced by other environmental factors such as temperature, pH, and type of used solvents. A number of electronic and chemical companies adopt industrial UV curing system for the mass

production of printing, coating, adhesive substances and its market size keeps increasing because of outstanding producibility in a restricted space with small energy consumption. Particularly, solid-state photopolymerization to fabricate conducting polymer thin films is valuable for cost-effective mass production of electronic devices. In addition, it would find very many applications to achieve a conducting layer with sophisticated patterns through area-selective photo-polymerization as such photolithography for semiconducting transistor manufacturing processes.

The photo-mediated polymerization is well established in traditional polymer synthesis; radical polymerization for (meth)acrylates or vinyl ethers, cationic epoxides, thiol-ene reaction, etc.[54] The photopolymerization is usually initiated a photoinitiator molecule. A photoinitiator having π bonds in its molecular structure can be photo-excited by the absorption of proper radiant energy and corresponding electron transfer from ground states (S_0) to excited states (S_1), and/or converted into its triplet state (T_1) via fast inter-system crossing[26,55]. When the excited molecules relax back to the ground states, the molecule generates initiating reactive species by photoscission, dissociation, or hydrogen abstraction.[55–57] Depending on the type of the produced intermediates, photoinitiators are categorized into free radical and cationic photoinitiators. A free radical photoinitiator produces reactive radical species from its triplet state directly or through an encounter interaction with another molecule called co-initiator.[56,57] In contrast, a cationic photoinitiator yields reactive cationic and/or anionic species from its singlet excited state with both hemolytic and heterolytic cleavage of carbon-halogen bonds.[58] Once radical or cationic species are generated by the light irradiation, they readily undergo chain propagation by reacting with neighboring monomers through radical or charge transfer. However, the conventional photopolymerization is disadvantageous to manipulate the molecular structure and size of resulting polymers in a precise manner because of its fast chain propagation, termination, and/or chain transfer reaction.[59]

In contrast, photo controlled radical polymerization (photo-CRP) is allowed to achieve polymers with well-defined structures and controlled molecular weights. By means of ATRP (Atom Transfer Radical Polymerization) and RAFT (Reversible Addition Fragmentation chain Transfer polymerization), vinyl monomers undergo successful controlled radical polymerization in the presence of photoreactive redox agents.[60–62] Hawker group established an ATRP system whose chain propagation is managed by photoredox reaction of an iridium complex, fac-[Ir(ppy)$_3$].[60] Upon visible light irradiation, an excited iridium complex reduces a brominated polymer chain to generate a chain radical and an oxidized Ir(IV)-Br compound. The chain radical is able to extend the chain length by reacting with neighboring monomers until the propagating chain end recaps with bromide by the reduction of the iridium-bromine intermediate. The polymer chain growth is not only switchable between light "on" and "off" states but also manageable the molecular weight and polydispersity of resulting polymers in a precise manner. Johnson group demonstrated a UV mediated controlled radical polymerization of NiPAAm by using bis-norbornene trithiocarbonate as a thiocarbonate base iniferter (initiator-transfer-agent-terminator).[63,64] Its chain growth behavior is similar to that of photomediated-ATRP of vinyl monomers with linear increase in molecular weight with the monomer conversion.

1.3.2 Photo-induced polymerization for conjugated polymers

1.3.2.1 Photo-induced oxidative polymerization of thiophene and pyrrole

In the strong motivation to accomplish efficient and practical polymerization methods for conducting polymers, photo-induced polymerization for conducting polymer has been extensively explored for pyrrole and thiophene derivatives. The researches in the early stage focused on how to efficiently produce radical cation species from thiophene or pyrrole monomers, resulting in the coupling of the charged species.[26] The charged molecules are generated in a ternary system of

electroactive monomers, electron acceptor molecule[65–67], and photocatalyst. When an electron in a ground state of photocatalyst is transferred to its excited states by photo-irradiation and moves to electron acceptor molecules, the photo-generated hole oxidizes an electroactive monomer by electron transfer from the monomer to the catalyst, leading to the polymerization. A variety of photocatalysts ranging from inorganic semiconductors[68–70] to organometallic compounds[71–73] have been widely employed to demonstrate efficient photopolymerization.

Transition metal-coordination complexes such as ruthenium(II) trisbipyridyl chloride, $[Ru(bpy)_3]Cl_2$, could serve as a good photosensitizer to demonstrate photopolymerization of conducting polymers.[68,74–76] The ruthenium complex has not only broad absorption from UV to the visible ranges but also long lifetime in excited states due to the forbidden transition from the triplet excited state to its singlet ground state and its characteristic metal-to-ligand-charge-transfer (MLCT).[73] Polypyrrole was successfully produced in a ternary system of pyrrole, $[Ru(bpy)_3]Cl_2$, and $[Co(NH_3)_5Cl]Cl_2$ under photo-irradiation.[76] According to the proposed mechanism, the triplet excited state of the ruthenium ion, $Ru(bpy)_3^{2+*}$ generated by the photoexcitation of the ruthenium complex is quickly quenched by the cobalt compound, to form oxidized $Ru(bpy)_3^{3+}$ ion. In consequence, monomeric or oligomeric pyrroles in the system are oxidized by electron transfer to the oxidized ruthenium ions to form corresponding radical cationic pyrrole species, followed by the polymerization. In the same manner, the photosensitization of ferrocene, $Fe(C_5H_5)_2$, leads to the UV-mediated polymerization of pyrrole in chlorinated solvents such as CCl_4 or $CHCl_3$.[77] They argued that the polymerization was promoted by the formation of $FeCl_3$ as a result of the photolysis of ferrocene in the chlorinated solvents.

The polymerization of conducting polymers could be initiated from the photoexcitation of onium salts such as diphenyliodonium salt ($Ph_2I^+X^-$, X^-: SbF_6^-, PF_6^-, AsF_6^-).[78] A phenyliodo radical cation ($PhI^{+\bullet}$) species generated from a photoexcited iodonium salt leads to the formation of

thiophene radical cation, followed by the coupling of the radical cation species to yield polythiophenes. Meanwhile, thiophene derivatives having extended conjugation as shown in Figure 1.7 serve as an electron transfer photosensitizer in the near UV and visible region and undergo self-polymerization to produce conducting polymers in the presence of an onium salt, $Ph_2I^+PF_6^-$.[79] According to the proposed mechanism, the electron transfer from a photoexcited precursors to the onium salt is responsible to the formation of radical cation species. The coupling of radical cation intermediates and proton elimination by PF_6^- lead to the self-polymerization of the thiophene derivatives.

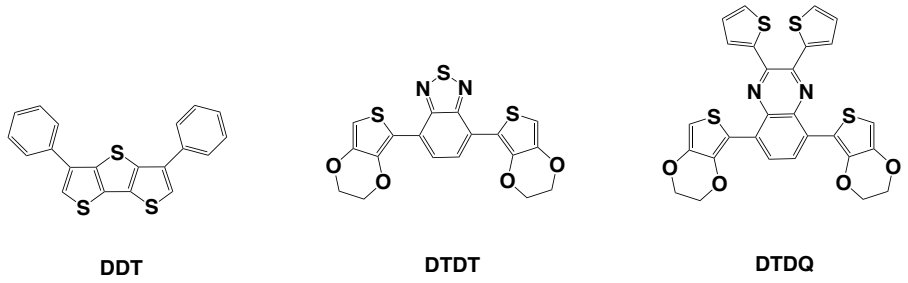

Figure 1.7. Chemical Structures of Conjugated Thiophene Derivatives with extended conjugation: 3,5-Diphenyldithieno[3,2-b:2,3-d]thiophene (DDT), 4,7-Di(2,3-dihydrothieno[3,4-b][1,4]dioxin-5-yl)benzo[1,2,5]thiadiazole (DTDT), and 5,8-Bis(2,3-dihydrothieno[3,4-b][1,4]dioxin-5-yl)-2,3-di(thiophen-2-yl)quinoxaline (DTDQ).[79]

Although the photo-mediated polymerization is initiated from the photoexcitation of a photocatalyst or monomers or a photocatalyst and the generation of radical cationic species, the chain propagation mechanism is identical to the traditional oxidative polymerization in that the polymerization is derived by the coupling of radical cationic species. Unfortunately, the photocatalyst assisted polymerization for conjugated polymers has not demonstrated any decent polymerization efficiency, resulting in the formation of low molecular weight species and poor

electric conductivity of the fabricated thin films. In addition, UV-vis absorption spectrum is presented as the only evidence of the formation of conjugated polymers, which is incomplete to comprehend the overall polymerization mechanism mechanistically.

1.3.2.2 UV-induced radical polymerization of diiodo-thiophenes

UV-mediated radical polymerization is a promising synthetic strategy to achieve conducting polymers owing to the fast response of radical species by photo-irradiation. The UV induced radical polymerization of 2-iodo- or 2,5-diiodo-thiophene was explored to achieve polythiophene based conducting polymer thin films.[80–83] The polymerization is initiated by a thienyl and an iodine radical generation caused from a carbon-iodine bond dissociation of the iodinated thiophenes by light-irradiation. A photoelectronic excitation of the iodo-thiophene and intramolecular energy transfer from the ππ* state of thiophene ring to the nσ* state of the C-I bond leads to the homolytic cleavage of a carbon-iodine bond, followed by the generation of a thienyl and an iodine radical.[84] The generated thienyl radicals are readily reacted with neighboring radicals or other thiophene molecules to produce higher molecular weight species. The reaction can be categorized into two different schemes: i) photomediated cross-coupling reaction (photocondensation) between (di)iodothiophene species[80,81] or ii) photoarylation between an (di)iodothiophene and thiophene.[82,83] Although both reactions commonly yield oligomeric or polymeric thiophene products, there are big differences in polymerization mechanism, efficiency, and resulting products.

1.3.2.2.1 Photo-condensation of diiodo-thiophenes

Polythiophene thin films have been fabricated from 2,5-diiodothiophene through UV light induced in-situ polymerization and their optical and electrical properties were characterized and

compared to those of chemically synthesized polythiophenes.[80,81] The coupling of photodissociated thiophene radicals leads to the polymerization for oligomeric or polymeric thiophene (Figure 1.8(a)). The molecular weight distribution of the resulting oligomeric species follows the Flory model for linear step growth polymerization in that smaller molecular weight species are favored over longer ones.[80] Despite of its simple and instant process, low degree of polymerization and the presence of cross-linked chains produced from α- β' coupling between precursors (Figure 1.8(b)) are not desirable to enhance electrical properties for the application of transparent electrodes. In addition, since iodine species originated from the photodissociation of carbon-iodine bonds of thiophene precursors is not sufficient to fully dope the oligomeric species, additional efforts for post-doping are required to demonstrate compelling optoelectronic properties of conducting polymer thin films.

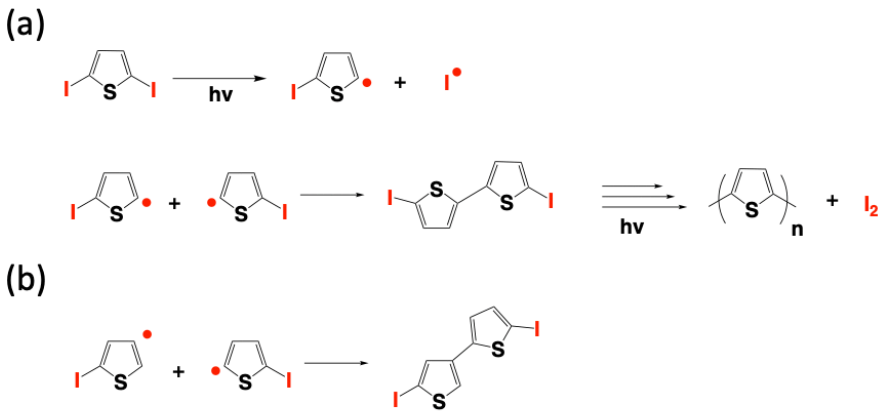

Figure 1.8. The scheme for UV-mediated cross coupling of 2,5-diiodothiophene, resulting in (a) a linear polymerization of polythiophene and (b) α- β' coupling of thienyl radicals.[80]

1.3.2.2.2 Photo-arylation of iodo-thiophene and thiophene

Photo-arylation is another promising photochemical reaction to produce conjugated oligomers or polymers in high yields. It is an aryl group substitution to the halogenated aromatic

molecules by light irradiation. A phenyl radical produced from an iodobenzene reacts with a benzene to yield a conjugated biphenyl molecule with a hydrogen iodide byproduct.[3] In the same manner, 2-iodothiophene in acetonitrile was photoarylated with a pristine thiophene by UV-irradiation to produce a dimeric thiophene molecule in good yields, demonstrating the extension of conjugation.[4] Moreover, the bis-arylation of 2,5-diiodothiophene with two thiophenes was successfully demonstrated in acetonitrile to produce trimeric thiophene with more than 90% yields.[85] Although a number of dimeric or trimeric conjugated molecules have been successfully synthesized through the photoarylation, any noticeable higher molecular weight species have not been reported by the photochemical reaction.[82] It is noteworthy that most of photoarylated products are terminated with C-H bonds at the conjugated chain ends. It is believed that the depletion of carbon-iodine bond of the product prevents sufficient further photochemical reaction leading to the chain extension.

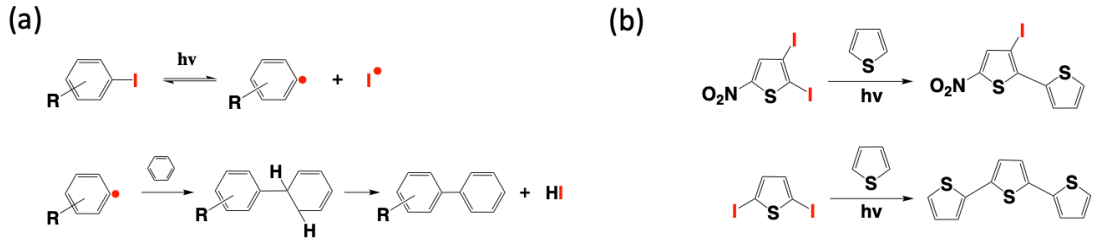

Figure 1.9. Photoarylation scheme of (a) 1-iodobenzene[3] and (b) 2-iodo-5-nitro-thiophene[4] and 2,5-diiodothiophene.[85]

Iodine radicals ($I^{\cdot}$) produced by the photoarylation couple together to produce I_2 or react with other molecules three different pathways. 1) Iodine can be abstracted by organic solvents containing carbon-hydrogen bonds. The halogen radical abstraction by saturated aliphatic

compounds is widely known and the degree of abstraction was evaluated for various type of organic solvents.[86–88] In particular, organic solvents containing electron withdrawing groups (fluorocarbon solvent, $CHCl_3$, or CH_3CN) are highly reactive with halogen radicals. 2) The iodine radicals can be protonated to produce hydrogen iodide (HI) as a result of photochemical reaction, which can serve as dopants for the photoarylated products, 3) Lastly, the photoarylated products or neighboring precursors can be iodinated, which is able to continue the photochemical reaction. Given that most photoarylated products is rarely terminated with carbon-iodine bonds in the references, it is believed that the iodine abstraction by solvents or the formation of hydrogen iodide is dominant in the photoarylation.

1.4 Photodegradation of conjugated polymers

The UV-mediated polymerization for conjugated polymers has not been well-established compared to other synthetic routes such as oxidative polymerization and organometallic synthesis. This is due to the fact that the conjugated molecules are vulnerable to photo-oxidation induced chain degradation in both solution and solid state.[89] In particular, the polymers in solution are susceptible to the fragmentation of conjugated backbones in the exposure to oxygen and light, presented in the reduction in main absorption in the visible range and the decrease in molecular weights.[90] In the same manner, the propagating chains in solution-based photo-induced polymerization could be highly affected by a long term light irradiation, resulting in the photodissociation of the polymer chains and the decrease in their molecular weights.

Most photodegradation of π-conjugated system have to do with the photo-oxidation of conjugated polymers,[89–92] which is attributed to the photoexcitation of conjugated polymers as depicted in Figure 1.10(a). Upon absorbing photon energy, a conjugated polymer is photoexcited and generates a singlet exciton. The excited molecule either returns to a ground state by radiative

(photoluminescence) or non-radiative decay, or transits to a triplet state by intersystem crossing (ISC).[93,94] In the presence of oxygen in the system, the triplet exciton moves to a triplet oxygen by energy transfer, resulting in the formation of an excited singlet oxygen. The singlet oxygen affects the dissociation of the conjugated main chains directly and indirectly.[91] Holdcroft proposed a direct photodegradation mechanism of P3HT in oxygen saturated organic solution that a conjugated polymer chain undergoes 1,4-Diels-Alder addition of singlet oxygen to a thiophene ring to generate a sulfine or a trans-diketone, followed by the loss of conjugation (Scheme 1.10(b)).[95] Manceau suggested a hydroxyl radical mediated photoscission mechanism of P3HT as shown in Scheme 1.10(c).[96] The reaction between a singlet oxygen and a hexyl side chain yields a peroxide on the side chain, followed by the generation of a hydroxyl radical. The radical rapidly reacts with sulfur atom in a thiophene ring, resulting in the formation of a thienyl-oxide (or -dioxide). Finally, the sulfone intermediates undergo the ring opening of the thiophene moiety, leading to the photobleaching of conjugation by the formation of a thienyl dioxide. In order to prevent the photodegradation of conjugated polymers, it is critical to exclude oxygen from the system by inert gas purging with N_2 or Ar or under glovebox condition.

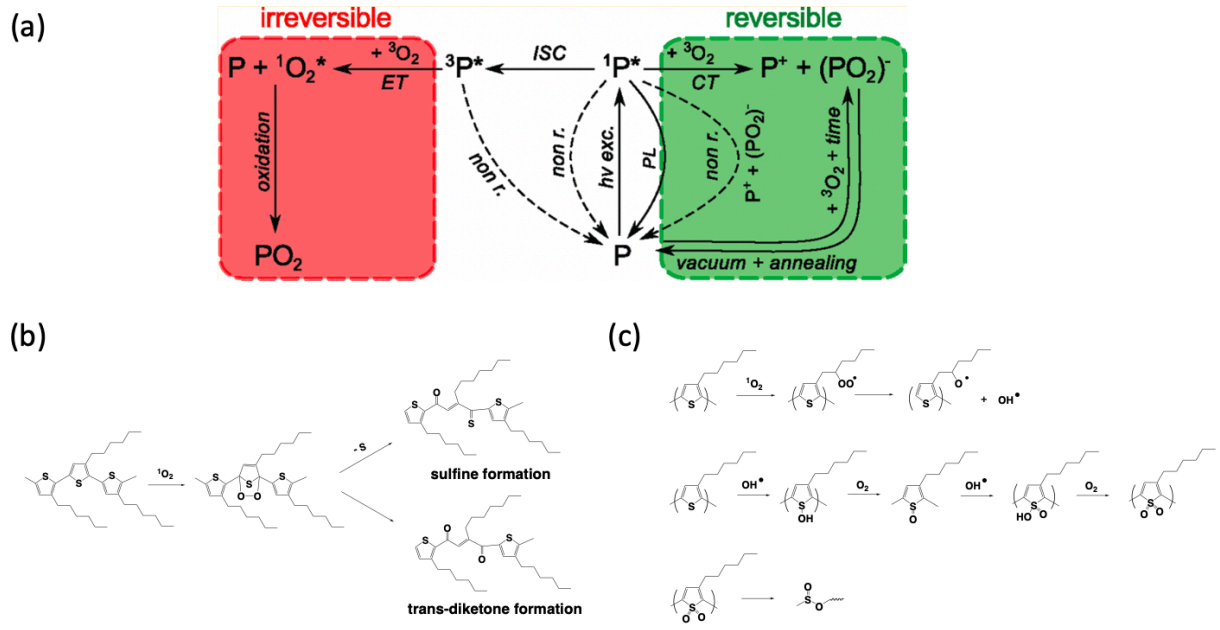

Figure 1.10. Schematic illustration of photooxidation and photodegradation of conjugated polymers. (a) Scheme of photo-oxidation pathway for photoexcited P3HT[93] (Reprinted with permission from American Chemical Society publishers (Ref. 90). Copyright 2011), (b) singlet oxygen mediated direct photodissociation of π-conjugated system[90], and (c) hydroxyl radical induced photodissociation and ring opening reaction.[91]

Light irradiation condition to conjugated polymers also play a significant role in photodegradation of conjugated polymers.[89] Hintz monitored the photodegradation of P3HT thin film irradiated with a high pressure xenon lamp in oxygen rich condition. The degradation rate of P3HT, determined by the decay in its main absorption bands, linearly increases as a function of the light intensity (Figure 1.11(a)). In addition, the photo-oxidation effectiveness is stronger for the polymer films irradiated at the shorter wavelength so that the UV irradiated P3HT film at 320nm exhibited 50 times higher photodegradation than the polymer film irradiated at 550nm (Figure 1.11(b)). It is noteworthy that a photoirradiated P3HT film with a visible 532nm pulsed laser undergoes no degradation both in solution and solid state.[97]

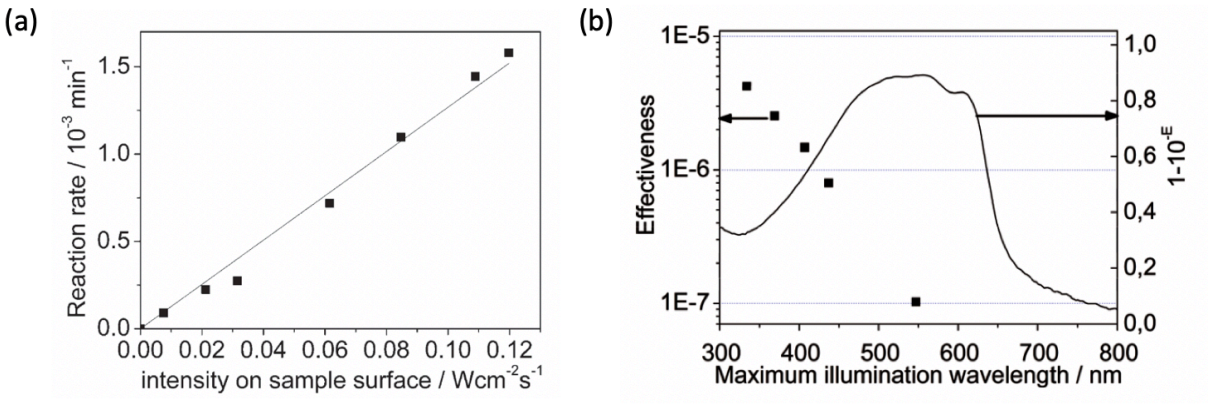

Figure 1.11. Light irradiation condition for the photodegradation of conjugated polymers. (a) Degradation rate depending on light intensity of xenon lamp and (b) Photodegradation effectiveness depending on the irradiation wavelength of the light source and the absorption bands of poly(3-hexylthiophene)[89] (Reprinted with permission from American Chemical Society publishers (Ref. 85). Copyright 2011)

1.5 EDOT and ProDOT as monomers

3,4-ethylenedioxythiophene (EDOT) is widely used to achieve highly conductive polymers with outstanding electrical property and stability in doped state by its unique molecular structure. The electron donating ethylenedioxy moiety on top of the thiophene unit lowers the oxidation potential so that EDOT readily forms a highly reactive radical cation. Its polaron state is stable owing to the resonance of the radical cation encouraged by the alkoxide moiety of EDOT as seen in Figure 1.7. In addition, different from a pristine thiophene containing 4 different accessible reactive sites in the molecular structure, EDOT is susceptible to react with other molecules at 2, 5 position of thiophen moiety so that a linear chain growth is only allowed for the polymerization. This linear chain growth of poly(3,4-ethylenedioxythiophene) (PEDOT) affords excellent optoelectronic property with its longer effective conjugation length and high charge concentration within the 2D structure. Despite of its outstanding conductivity, the intrinsic poor solubility of

PEDOT is not favorable to mass production of conducting polymer thin films through wet coating process.

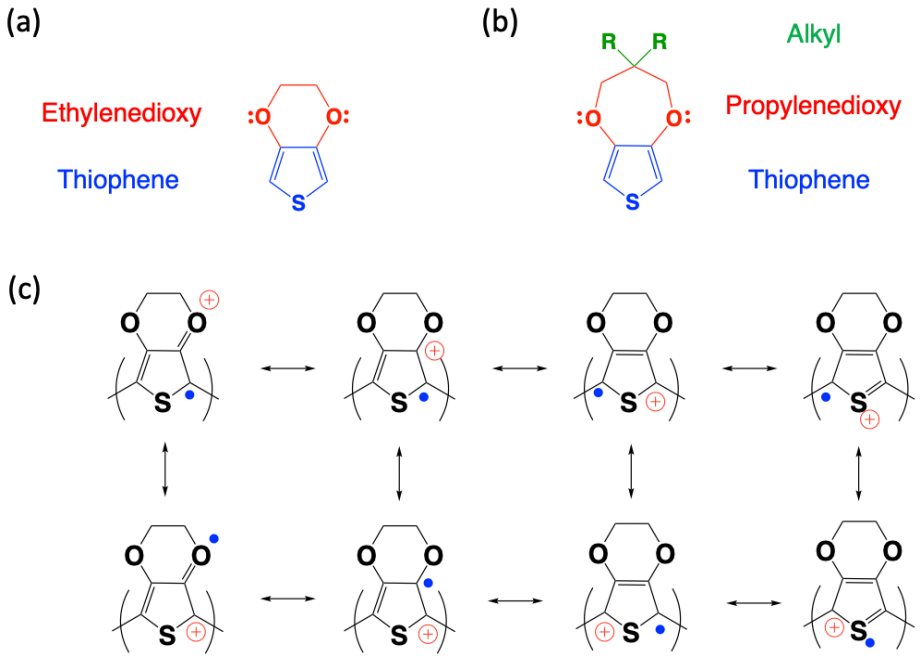

Figure 1.12. Molecular structure of (a) 3,4-ethylenedioxythiophene (EDOT) and (b) 3,4-propylenedioxythiophene (ProDOT), and (c) Resonance of radical cations in EDOT[98].

In contrast, poly(3,4-propylenedioxythiophene) (PProDOT) is highly processable owing to the incorporated two alkyl side chains that also have analogous electron donating character to EDOT. At the same time, since the propylenedioxy ring serves as a spacer to separate the side chains from the conjugated backbone, the intramolecular charge transfer along the polymer backbone is less affected by the insulating side chains. ProDOT-alkyl derivatives are widely used in solution-based polymerization such as Grignard metathesis because of the outstanding solubility of the polymerized precursors during the reaction. It is also advantageous for the characterization of the resulting polymers through GPC, H-NMR, and MALDI to comprehend the polymerization mechanism.

1.6 Doping of conjugated polymer

As an inorganic semiconductor reveals metallic character by introducing small amount of impurity, dopants, p-doped conducting polymers are achieved by removing electrons from the valence bands of the conjugated polymers in the presence of counter anions. The removal of electrons from a polymer chain creates new energy levels within the intrinsic energy gap between HOMO (the highest occupied molecular orbital) and LUMO (the lowest unoccupied molecular orbital) of the neutral states.[99] Depending on the number of electrons taken from the chain or the doping level, it leads to not only the formation of a polaron (radical cation) or bipolaron but also the change in molecular structure of the polymer chain from benzoidal to quinoidal geometry as depicted in Figure 1.13. The evolution of the polaronic states creates holes on top of the valence bands, followed by the delocalization of the positive charge along the polymer chains to exhibit a semiconducting character. The conductivity of doped conjugated polymers increases up to several orders of magnitude compared to that of corresponding neutral ones. Ouyang reported a PEDOT:PSS thin film with excellent conductivity of 3,300 S/cm after methanesulfonic acid (CH_3SO_3H) doping that is comparable to that of ITO films.[100]

In addition, the reduced bandgap by the doping process leads to a red-shift of absorption bands of conjugated polymers. For example, while the main absorption bands between 400~600nm are mostly observed in the neutral states of PEDOT:PSS polymer, they shifted to the long wavelength range (700~1100 nm) in a polaron state or to near-infrared (1250nm~) in a bipolaron state depending on the doping level of the polymer chains.[7] As main absorption bands shift beyond the range of visible light wavelength in a high doping level, the PEDOT film becomes transparent with a high transmittance value, which is applicable to transparent electrodes for organic photovoltaics, flexible display, or smart windows. In particular, the reversible change in colors or

transmittance of the conjugated polymer is of great demands in electrochromic device application.[48,101,102]

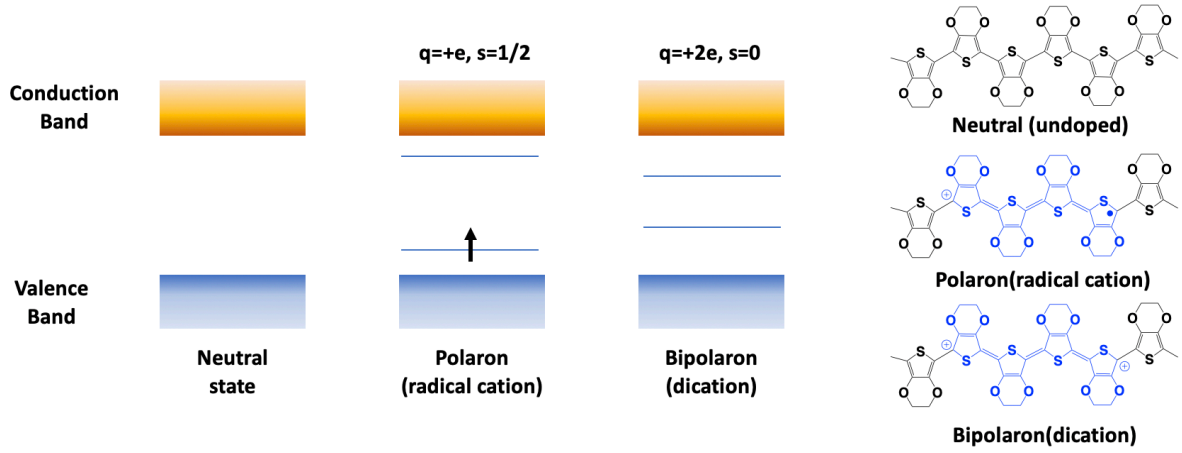

Figure 1.13. Energy level diagram of conjugated polymers (left figures) and chemical structures of neutral and doped PEDOT polymers (right figures).

1.6.1 In-situ doping in oxidative polymerization

Since polyacetylenes exhibited a remarkable metallic conduction in thin films where alkali metals or halides serve as promising dopants for the polymers,[103–105] great efforts have been devoted to developing of efficient doping methods to maximize electric conductivity and obtain its long-term stability in p-doped states. Metallic compounds such as $FeCl_3$, $CuCl_2$, or iron(III) tosylate($FeTos_3$)[21,23,106] are widely adopted in chemical oxidative polymerization for conjugated polymers owing to their outstanding ability to oxidize conjugated molecules. In addition, they serve as strong dopants to make the polymerized products in p-doped state, affording excellent conductivity values. The doped states of conjugated polymer chains are also achieved by electrochemical polymerization in the presence of counter anions such as ClO_4^-, BF_4^-, PF_6^-.[34] The doping anions are embedded on oxidized conjugated polymer chains during the polymerization to acquire electroneutrality of the ion pairs, resulting in the formation of conducting salts on the

substrates. The doping level of conjugated polymers and the conductivity of the polymer films are dependent on the nature of counter anions, electrolyte composition (the concentration of monomers and counter-anions, solvent), and electrode materials.[107] The self-polymerization of brominated EDOT in solid state is reported as a synthetic approach for a conducting polymer (PEDOT) thin film fabrication.[1] The bromine molecules (Br_2) produced by the coupling of dibromo EDOT serve as dopants for the polymerized PEDOT molecules, demonstrating comparable conductivity to PEDOT thin films prepared through oxidative polymerization.

1.6.2 Post-doping by electron withdrawing molecules

Besides oxidative polymerization that doping of growing chains is performed during the polymerization, post-treatment of conjugated polymer films with dopant molecules are proposed as a simple method to enhance electrical conductivity and optical transmittance of non-doped conjugated polymers synthesized through organometallic pathways. A variety of conjugated molecules are efficiently doped by the addition of doping agents to the conjugated polymer system. A suitable dopant molecule for the efficient post-doping of a conjugated polymer is chosen by its electron affinity, the energy offset between the dopant (LUMO) and the polymer (HOMO), and the miscibility in the polymer system.[108–110] Depending on the nature of dopant materials, different doping methods are applied to conducting polymers to enhance their optical and electrical properties.

1.6.2.1 Post-doping by tetrafluorotetracyanoquinodimethane (F_4TCNQ)

Recently, a molecular electron acceptor, tetrafluorotetracyanoquinodimethane (F_4TCNQ) has been widely investigated as a strong organic dopant to oxidize a number of conducting polymers. The LUMO level (-5.2eV) of this dopant is deep enough to take electrons from the

HOMO level of its host organic semiconductor, resulting in the formation of polaron or bipolaron.[109,111,112] Researchers proposed a charge transfer mechanism of the electron acceptor with conducting polymers having various HOMO levels and figured out that the chemical doping by F_4TCNQ is efficient for the conjugated polymers with higher HOMO levels than the LUMO level of the dopant.[110] This chemical doping is available for both the solution mixture of conjugated molecules/dopant and a dopant infiltration into a pre-deposited conjugated polymer thin film. They evaluated electrical conductivity and optical properties for the thin films of p-doped conjugated polymers deposited through the two different pathways.

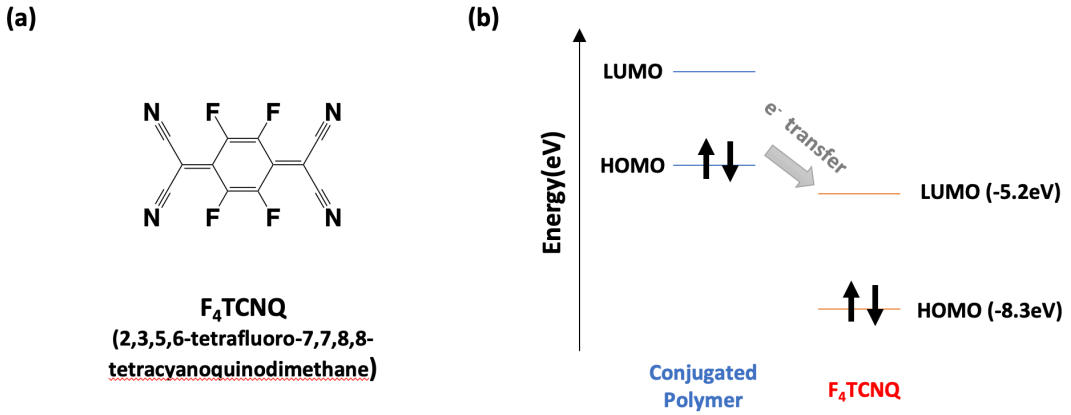

Figure 1.14. F_4TCNQ (a) chemical structure of F_4TCNQ (b) schematic energy level diagram showing the relative HOMO and LUMO levels of conjugated polymers and F_4TCNQ with an electron transfer.

A mixed organic semiconductor:dopant solution is straightforward to prepare p-doped polymer solution to fabricate conductive thin films. While it provides a facile process that F_4TCNQ diluent is added to conjugated polymer solution, the polymer chains readily aggregate and form a gels or large particles by doping induced inter-charge interaction so that the electric conductivity in solid state is underestimated because of its discrete and pre-formed crystalline phase.[109,112,113] The co-deposition of dopant molecules with conjugated polymers results in the formation of

disordered polymer packing structure so that it is challenging to maximize electrical conductivity.[111] In addition, since F_4TCNQ shows a limited solubility in organic solvents, the mixture of polymer/dopant undergoes only small fractional charge transfer so that the doping level of conjugated polymers by the dopant is not uniform to enhance conductivity.

In order to overcome the limitation of polymer/dopant mixture, sequential doping to pre-deposited films is favored to achieve high quality conducting polymer thin films. F_4TCNQ molecule layer is formed on top of a conjugated polymer thin film through wet or dry deposition process, followed by the infiltration of dopants into the polymer film layer. The enhanced electrical conductivity and highly ordered packing structure in solid state were mainly demonstrated in a sequential addition of F_4TCNQ molecules to regioregular poly(3-hexylthiophene) [rr-P3HT][112,114] or poly(2,5-bis(3-tetradecylthiophen-2-yl)thieno-[3,2-b] thiophene) [PBTTT][111,115]. The diffusion of the dopant into the polymer film matrix did not cause significant change in the film morphology and the packing structure. As a result of sequential doping, the doped film exhibited 4~5 orders of increase in conductivity compared to the pristine conjugated polymer film. At the same time, the doped film undergoes the decrease in the absorption bands at 400 ~ 600nm and simultaneous increase in the long wavelength range, which is identical to the redshift in absorption bands of p-doped conjugated polymers except for the absorption band originated from radical anion of F_4TCNQ.[111,112] As the concentration of the dopant increase in the film, the broad polaron absorption band decreases in the long wavelength range and red-shifted to NIR range, but the spectral features of F_4TCNQ both at 350~450nm (neutral) and 750~850nm (radical anion) are apparent so that unfortunately it is technically hard to fabricate transparent and colorless conducting polymer thin films with F_4TCNQ.[111,114,115]

1.6.2.2 Post-doping by fluoroalkyltrichlorosilanes (FTSs)

Calhoun and Kao reported organic semiconductor devices in that a self-assembled monolayer (SAM) of fluoroalkylsilanes is placed on top of a conjugated polymer thin film showing remarkable electrical conductivity and transparency.[116,117] The conductivity values of PBTTT and P3HT are enhanced up to six orders magnitude by the interaction of the hydrolyzed fluoroalkyl trichlorosilane (FTS) with the conjugated polymers (PBTTT/FTS: 1100 S/cm, P3HT/FTS: 30 S/cm). FTS treated conducting polymer films also show excellent transparency with a drastic decrease in absorption bands in the visible range. The FTS induced doping of conjugated polymers is ascribed to an electron transfer from conjugated polymer chains to the self-assembled monolayer of FTS having the strong electron withdrawing ability. However, the FTS induced organic semiconductors underwent the decrease in conductivity by the exposure to polar molecules or humidity, showing unstable electric properties sensitive to the environment. Additionally, the charge transfer in the film is only allowed in-plane direction because of the presence of the insulating SAM layer, which is not applicable to multilayer electronic device requiring interlayer charge transfer.

1.6.2.3 Post-doping by protonic acids

Protonic organic or inorganic acids are also regarded as promising dopants for conjugated polymers to fabricate transparent conductive thin films. PEDOT:PSS thin films treated with sulfuric acid (H_2SO_4) or methanesulfonic acid (CH_3SO_3H) exhibit excellent conductivity of 2000~3000 S/cm which is comparable to that of ITO thin films.[100,118] The conductivity enhancement is originated from the proton transfer from acids to PSS^- of the polymer chains, resulting in the formation of PSSH. The neutral PSSH chains lose the coulombic attraction with PEDOT chains, followed by the phase segregation of hydrophilic PSSH from hydrophobic PEDOT.

The phase separation allows the replacement of PSS^- to acid anions (HSO_4^- or $CH_3SO_3^-$) and conformational change in PEDOT chains from coil to extended structure, resulting in the enhancement in conductivity and optical transparency.[118]

Direct doping of organic semiconductors by protonic acids is also available to enhance electric conductivity.[119] The doping level is determined by acid dissociation constant (pK_a) of acid dopants. A protonic acid with a smaller pK_a value (H_2SO_4:-6.4, CH_3SO_3H: -2.0) is more beneficial to enhancing doping efficiency of conjugated polymers. However, pristine conjugated polymer thin films should be carefully doped via protonic acid treatment to avoid any shrinkage or breakdown of the film caused from mechanical stresses by sudden change in electric states. For this reason, protonic acids are generally diluted with nitromethane to provide a milder doping condition.

1.7 Characterization of conjugated polymers

1.7.1 UV-vis absorption spectrum

Examining the UV-visible absorption behavior of conjugated polymers in solution or solid states gives deep insights about the nature of the conjugated molecules such as chemical and electronic structures, intermolecular interaction, and physical conformation of the polymers. The absorption bands of conjugated polymers have to do with the energy band gap of conjugated molecules corresponding to the energy level difference between the HOMO and LUMO.[120,121] Lin examined the relationship between the energy band gap and the effective conjugation length of ProDOT oligomers.[5] The empirical plot about the energy bandgap (E_g) and the reciprocal value of the number of repeating units (1/n) revealed a linear correlation with a saturated minimum energy bandgap for its infinite conjugation length. This relationship is critical in monitoring the increase in molecular weight of the polymerization for conjugated polymers. In particular, the slope of the

plot reflects the effective conjugation. This value of oligomeric EDOTs or ProDOTs (3.21~3.25) is higher than that of regiorelular thiophene oligomers[6]. They suggested that oligomeric alkylenedioxy thiophenes (EDOT or ProDOT oligomers) afford better coplanarity than oligomeric alkylthiophenes due to a sulfur and oxygen interaction between adjacent EDOT/ProDOT units. The greater coplanar structure of EDOT/ProDOT unit is also supported by the absorption bands with vibrational fine structures in contrast to the single and broad absorption bands of oligothiophenes. In addition, the y-intercept value differences between oligothiophenes (2.54 eV)[6] and EDOT/ProDOT oligomers (2.04~2.05 eV)[5] exhibits the lower energy bandgap of PEDOT/PProDOT than that of polythiophenes. The reduced bandgap is attributed to two oxygen substituents on top of the thiophene moiety that make the HOMO move upwards in energy level more than the LUMO.

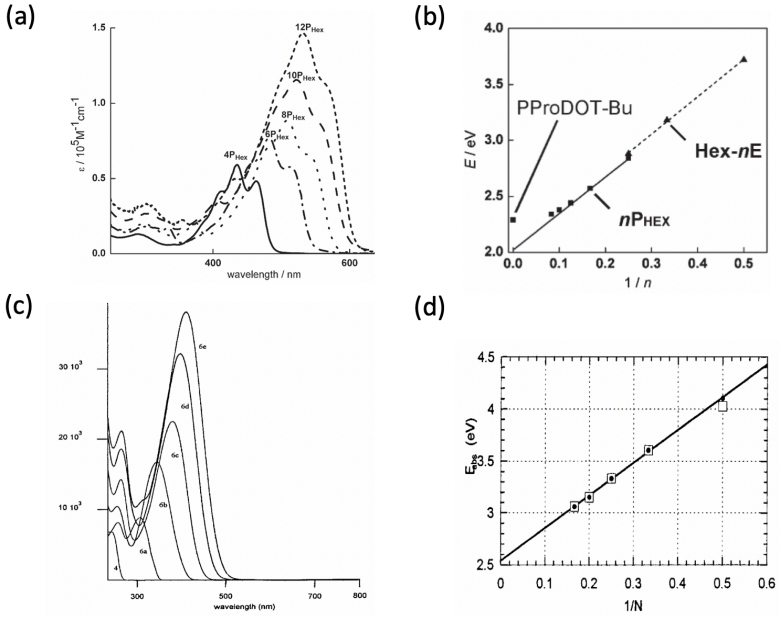

Figure 1.15. UV-vis absorption spectra and the plots of absorption energy vs the reciprocal values of the repeating units of (a), (b) ProDOT[5] (Reprinted with permission from American Chemical Society publishers (Ref. 119). Copyright 2011) and (c), (d) 3-octylthiophene oligomers[6] (Reprinted with permission from ACS publishers (Ref. 120). Copyright 1998).

The decrease in energy bandgap is further encouraged by the oxidation of conjugated polymers in neutral state. The energy transition from a neutral chain to a radical cation or dication by the oxidation of conjugated polymers leads to the reduction in bandgap, resulting in the diminishment of absorption bands in the visible range and the onset polaron and bipolaron bands in the long wavelength and near IR range. Accordingly, it causes to the increase in transmittance of the conjugated polymer complex both in solution and solid state. The UV-vis-NIR absorption bands and electronic structures of PEDOT:PSS is well described in Figure 1.16.

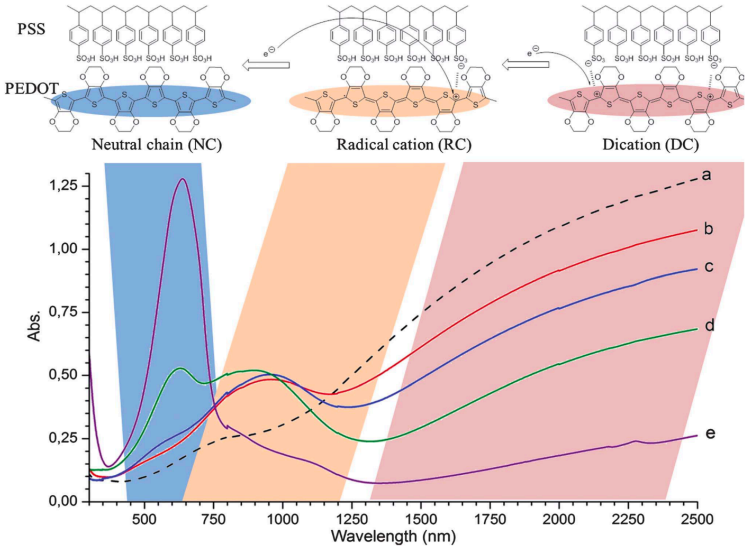

Figure 1.16. Chemical and electronic structures of PEDOT:PSS and UV-vis-NIR absorption spectra in neutral, radical cation, and dication states.[7] (Reprinted with permission from Royal Society of Chemistry publishers (Ref. 97). Copyright 2014)

1.7.2 Gel Permeation Chromatography (GPC)

The molecular weight and polydispersity of conjugated polymers are generally characterized by chloroform GPC. They are generally determined by a retention time that is calibrated with a series of polystyrene standards with discrete molecular weights. However,

flexible polystyrene and rigid conjugated polymers show different behaviors in solution so that the molecular size output of conjugated polymers tends to be overestimated compared to polystyrene standards. Hence, it is required to take into account the nature of rigid conjugated polymers when estimating the molecular weights.

In general, GPC characterization is allowed for the conjugated polymers soluble in organic solvents such as chloroform, THF, chlorobenzene. For conjugated polymers with a high molecular weight or polyaniline not containing any soluble side chains, N-methyl-2-pyrrolidinone (NMP) or dichlorobenzene are employed as eluent solvents. Poly(3,4-ethylenedithiathiophene) (PEDTT) synthesized through chemical and electrochemical oxidative polymerization was characterized with eluents containing LiCl in NMP.[122] Li^+ ion is believed to help to separate the polymer aggregates into single chains via Lewis acid-base interactions and reveal the correct molecular weight in GPC. The effect of Li^+ ion is also proved for the GPC characterization of polyaniline.[123] The incorporation of long and bulky side chains into thiophene derivatives is another approach to allow GPC characterization by inhibiting the formation of aggregates in chloroform. While PEDOT synthesized by chemical or electrochemical oxidative polymerization is not favorable for GPC characterization due to the insolubility of the polymer products in the absence of side chain, P3HT[47] or PProDOT incorporating long alkyl side chains[48,124] allow the molecular weight estimation of the resulting polymers through chloroform GPC.

The mechanistic study based on GPC trace of polymerized products offers important clues to understand the nature of polymerization. Yokoyama demonstrated a controlled radical polymerization chain growth behavior of conducting polymers through GPC.[47] The chain growth behavior of poly(3-hexylthiophene) synthesized via Grignard metathesis is confirmed by the shift of retention time to higher molecular weight while maintaining narrow PDI. The increase in

molecular weight of the resulting polymers is accompanied by monomer conversion showing a linear relation.

1.7.3 ^{1}H-NMR characterization

^{1}H-NMR offers important clues in identifying the molecular structure of conjugated polymers. Polythiophene derivatives exhibit their own unique ^{1}H-NMR spectra in $CDCl_3$ (Deuterated chloroform). For example, PProDOT derivatives commonly exhibited a single broad peak in the range of δ 3.4-4.5 assigned to the CH_2O protons of the propylenedioxy bridge on top of the thiophene unit.[43,124] When linear alkyl side chains are symmetrically incorporated at the center of the bridge, other broad signals are shown in the range of δ 0.7-1.5 attributed to the CH_2 and CH_3 protons of the alkyl chains.[48] The broad signal of the conjugated polymers is typical for the polymers due to the overlapping of a number of protons on the molecules. Because of the numerous protons on the thiophene substituents, protons at the conjugated chain ends in δ 6.0-6.5 are negligible.

The formation of block copolymers consisting of two different blocks is also confirmed by ^{1}H-NMR. Noonan group demonstrated a polythiophene block copolymer having two different side chains of hexyl (C_6H_{13}) and hexylester ($COOC_6H_{13}$).[8] The addition of 3-hexylesterthiophene monomer (3HET) to poly(3-hexylthiophene) (P3HT) leads to the formation of P3HT-b-P3HET via Suzuki polycondensation in the presence of nickel catalyst. The production of the block copolymer was determined by the coexistence of proton signals originated from P3HT (7.00ppm: CH of β position of thiophene, 2.80ppm: CH_2 of hexyl side chains closed to thiophene unit) and P3HET (7.86ppm: CH of β position of thiophene, 4.30ppm: CH_2 of the hexylester side chain closed to ester group) blocks. In particular, we can estimate the composition ratio of the two polythiophene blocks from the integration of those peaks.

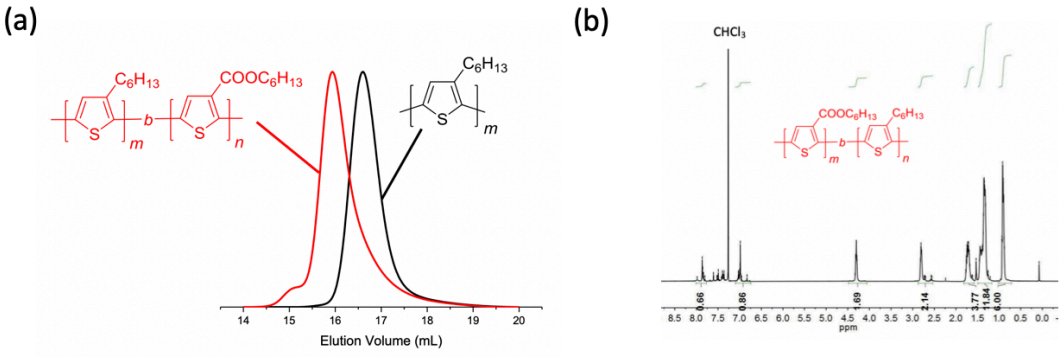

Figure 1.17. Characterization of P3HT-b-P3HET. (a) GPC and (b) ^{1}H-NMR(500MHz, $CDCl_3$) spectra.[8] (Reprinted with permission from ACS publishers (Ref. 124). Copyright 2016)

1.7.4 MALDI-TOF

In order to understand the chain extension mechanism of conjugated polymers synthesized via organometallic pathways, the chain end group of the resulting polymers is commonly characterized via MALDI-TOF mass analysis.[8,9,43,47,48,123,124] As presented in Figure 1.6, the formation of undoped polythiophenes is ascribed to the polycondensation of 2-bromothiophene derivatives catalyzed by a nickel complex. The MALDI-TOF mass spectrum of the neutral polythiophene derivatives revealed the presence of the C-Br bonds as described in Figure 1.18.[8,9] Every main peak is separated with an identical m/z value corresponding to the mass of the repeating unit of thiophene derivatives. At the same time, the m/z values of the primary peaks are precisely expressed as $n \times (mass\ of\ repeat\ unit) + 79.9(Br) + 1.0(H)$, implying that most of the polymers have the same end group (H-M_n-Br). Given the H/Br end groups, the linear correlation of molecular weight and monomer conversion, and low polydispersity of resulting polymers, it is believed that the polymerization was performed in a living fashion and most of polymer products are terminated with C-Br bonds at the chain ends.

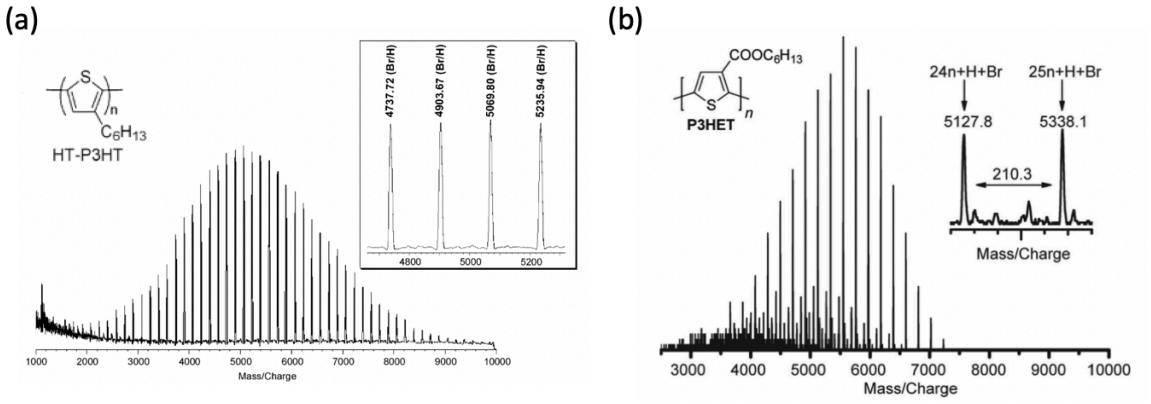

Figure 1.18. MALDI-TOF mass spectrum of (a) regioregular poly(3-hexylthiophene)[9] and (b) poly(3-hexylesterthiophene)[8] synthesized via nickel catalyzed Grignard metathesis. (Reprinted with permissions from American Chemical Society publishers (Ref. 124). Copyright 2016 and (Ref. 125). Copyright 2005)

1.8 Dissertation Outline

Chapter 1 offers a general overview of conventional polymerization for conjugated polymers as well as photo-mediated polymerization. The polymerization mechanisms and the nature of resulting polymers are analyzed with the characterization results of UV-vis absorption spectra, GPC, ^{1}H-NMR, and MALDI-TOF. Depending on the type of reacting intermediates, photo-mediated polymerization is categorized into i) oxidative polymerization: managed by the coupling of radical cation species and ii) halogen mediated radical polymerization: derived by thienyl and halogen radicals. Oxidative polymerization is generally determined by the ability of photocatalyst to withdraw electrons from monomers and demonstrates a poor polymerization efficiency with a low conversion ratio of the reagents compared to the conventional polymerization. In contrast, photo-induced radical polymerization is managed by highly reactive radical species, resulting in better polymerization efficiency. Systematic comparison between photocondensation and photoarylation of conjugated polymers is given as important background of the dissertation.

In particular, photoarylation presents excellent monomer conversion to yield oligomeric conjugated molecules.

Chapter 2 presents an one-pot photopolymerization of ProDOT derivatives in solution to achieve conjugated polymers with a high molecular weight and narrow polydispersity. Photoarylation is an essential photochemical reaction to achieve conjugated polymers and largely influenced by the monomer composition, solvent choice, light source, and irradiation time. The main factors affecting the polymerization efficiency are thoroughly discussed based on the characterization data of the resulting polymers. We propose a polymerization mechanism in which chain growth is controlled by the reversible activation of C-I bonds at the growing chain ends and the electronic state of propagating chains under proper illumination conditions. Electrophilic halogenation of the growing chains with newly replenished iodine sources and switching light source to promote chain propagation through coupling and to prevent oxidative photodegradation are systematically investigated and logically presented.

Chapter 3 demonstrates an one-pot fabrication strategy to realize transparent conducting polymer thin films through UV mediated polymerization. A facile photoarylation with 2,5-diiodo thiophene derivatives and other heteroaryl compounds in solid state by UV light irradiation leads to the formation of insoluble and robust conjugated polymer thin films. We examined how the mobility of monomers in solid state affects the polymerization efficiency and electric conductivity by adjusting the reaction temperature and side chain design of ProDOT (or EDOT) monomers. Chemical doping of the PEDOT derivative copolymer films with protonic acids affords outstanding conductivity and transparency to the polymerized films.

1.9 References

1. Meng, H., Perepichka, D. F., Bendikov, M., Wudl, F., Pan, G. Z., Yu, W., Dong, W., Brown, S. Solid-State Synthesis of a Conducting Polythiophene via an Unprecedented Heterocyclic Coupling Reaction. *J. Am. Chem. Soc.* **125,** 15151–15162 (2003).
2. Pistillo, B. R., Menguelti, K., Desbenoit, N., Arl, D., Leturcq, R., Ishchenko, O. M., Kunat, M., Baumann, P. K., Lenoble, D. Pistillo, B. R. One step deposition of PEDOT films by plasma radicals assisted polymerization via chemical vapour deposition. *J. Mater. Chem. C* **4,** 5617–5625 (2016).
3. Wolf, W., Kharasch, N. Photolysis of Iodoaromatic Compounds in Benzene. *J. Org. Chem.* **30,** 2493–2498 (1965).
4. D'Auria, M., Distefano, C., D'Onofrio, F., Mauriello, G., Racioppi, R. Photochemical substitution of polyhalogenothiophene and halogenothiazole derivatives †. *J. Chem. Soc. Perkin Trans. 1* 3513–3518 (2000).
5. Lin, C., Endo, T., Takase, M., Iyoda, M., Nishinaga, T. Structural, Optical, and Electronic Properties of a Series of 3,4-Propylenedioxythiophene Oligomers in Neutral and Various Oxidation States. *J. Am. Chem. Soc* **133,** 11339–11350 (2011).
6. Bidan, G., Nicola, A. De, Ene, V., Guillerez, S. Synthesis and UV-Visible Properties of Soluble Regioregular Oligo(3-octylthiophenes), Monomer to Hexamer. *Chemistry of Materials* **10,** 1052–1058 (1998).
7. Massonnet, N., Carella, A., Jaudouin, O., Rannou, P., Laval, G., Celle, C., Simonato, J. P. Improvement of the Seebeck coefficient of PEDOT:PSS by chemical reduction combined with a novel method for its transfer using free-standing thin films. *J. Mater. Chem. C* **2,** 1278–1283 (2014).

8. Qiu, Y., Worch, J. C., Fortney, A., Gayathri, C., Gil, R. R., Noonan, K. J. T. Nickel-Catalyzed Suzuki Polycondensation for Controlled Synthesis of Ester-Functionalized Conjugated Polymers. *Macromolecules* **49,** 4757–4762 (2016).

9. Miyakoshi, R., Yokoyama, A., Yokozawa, T. Catalyst-transfer polycondensation. Mechanism of Ni-catalyzed chain-growth polymerization leading to well-defined poly(3-hexylthiophene). *J. Am. Chem. Soc.* **127,** 17542–17547 (2005).

10. Chiang, C. K., Fincher, C. R., Park, Y. W., Heeger, A. J., Shirakawa, H., Louis, E. J., Gau, S. C.; MacDiarmid, A. G. Electrical Conductivity in Doped Polyacetylene. *Phys. Rev. Lett.* **39,** 1098–1101 (1977).

11. Kline, R. J., McGehee, M. D., Toney, M. F. Highly oriented crystals at the buried interface in polythiophene thin-film transistors. *Nat. Mater.* **5,** 222–228 (2006).

12. Kim, B. G., Jeong, E. J., Chung, J. W., Seo, S., Koo, B., Kim, J. A molecular design principle of lyotropic liquid-crystalline conjugated polymers with directed alignment capability for plastic electronics. *Nat. Mater.* **12,** 659–664 (2013).

13. Romero, D. B., Schaer, M., Zuppiroli, L., Cesar, B., François, B. An iodine-doped polymer light-emitting diode. *Appl. Phys. Lett.* **67,** 1659 (1995).

14. Adachi, C., Baldo, M. A., Thompson, M. E., Forrest, S. R. Molecular organic light-emitting diodes using highly conducting polymers as anodes. *J. Appl. Phys.* **90,** 5048–5051 (2001).

15. Levermore, P. A., Chen, L., Wang, X., Das, R., Bradley, D. D. C. Highly conductive poly(3,4-ethylenedioxythiophene) films by vapor phase polymerization for application in efficient organic light-emitting diodes. *Adv. Mater.* **19,** 2379–2385 (2007).

16. Torabi, S., Jahani, F., Van Severen, I., Kanimozhi, C., Patil, S., Havenith, R. W. A., Chiechi, R. C., Lutsen, L., Vanderzande, D. J. M., Cleij, T. J. Strategy for enhancing the dielectric

constant of organic semiconductors without sacrificing charge carrier mobility and solubility. *Adv. Funct. Mater.* **25,** 150–157 (2015).

17. Gu, Z., Tan, Y., Tsuchiya, K., Shimomura, T., Ogino, K. Synthesis and Characterization of Poly(3-hexylthiophene)-b-Polystyrene for Photovoltaic Application. *Polymers (Basel).* **3,** 558–570 (2011).
18. Setiadi, D., He, Z., Hajto, J., Binnie, T. D. Application of a conductive polymer to self-absorbing ferroelectric polymer pyroelectric sensors. *Infrared Phys. Technol.* **40,** 267–278 (1999).
19. Yoon, H., Chang, M., Jang, J. Formation of 1D poly(3,4-ethylenedioxythiophene) nanomaterials in reverse microemulsions and their application to chemical sensors. *Adv. Funct. Mater.* **17,** 431–436 (2007).
20. Lee, K., Mandal, S., Morry, J., Srivannavit, O.,Gulari, E., Kim, J. A conjugated polymer-peptide hybrid system for prostate-specific antigen (PSA) detection. *Chem. Commun.* **49,** 4528–4530 (2013).
21. Heywang, B. G., Jonas, F. Poly(alkylenedioxythiophene)s-New, Very Stable Conducting Polymers. *Adv. Mater.* **4,** 116–118 (1992).
22. Wolf, G. D., Jonas, F., Schomaecker, R. EP707440. (1994).
23. Im, S. G., Kusters, D., Choi, W., Baxamusa, S. H., van de Sanden, M. C. M., Gleason, K. K. Conformal coverage of poly(3,4-ethylenedioxythiophene) films with tunable nanoporosity via oxidative chemical vapor deposition. *ACS Nano* **2,** 1959–1967 (2008).
24. Merker, U., Kirchmeyer, S., Wussow, K. Specipic oxidation agents for producing conductive polymers, WO/2004/088672. (2004).

25. Louwet, F., Groenendaal, L., Dhaen, J., Manca, J., Van Luppen, J., Verdonck, E., Leenders, L. PEDOT/PSS: Synthesis, characterization, properties and applications. *Synth. Met.* **135–136,** 115–117 (2003).

26. Heydarnezhad, H. R., Pourabbas, B., Tayefi, M. Conducting Electroactive Polymers via Photopolymerization: A Review on Synthesis and Applications. *Polym. Plast. Technol. Eng.* **57,** 1093–1109 (2018).

27. Jonas, F., Krafft, W., AG, B. EP440957. (1990).

28. Jonas, F., Krafft, W.,Muys, B. Poly(3, 4-ethylenedioxythiophene): Conductive coatings, technical applications and properties. *Macromolecules Symposium* 169–173 (1995).

29. Ahlswede, E., Mühleisen, W., Wahinuddin, M., Wahi, M., Hanisch, J., Powalla, M. Highly efficient organic solar cells with printable low-cost transparent contacts. *Appl. Phys. Lett.* **92,** 183 (2008).

30. Kim, G. H., Lee, D., Shanker, A., Shao, L., Kwon, M. S., Gidley, D., Kim, J., Pipe, K. P. High thermal conductivity in amorphous polymer blends by engineered interchain interactions. *Nat. Mater.* **14,** 295–300 (2015).

31. Sun, K., Zhang, S., Li, P., Xia, Y., Zhang, X., Donghe, D., Isikgor, H. F., Ouyang, J. Review on application of PEDOTs and PEDOT:PSS in energy conversion and storage devices. *J. Mater. Sci. Mater. Electron.* **26,** 4438–4462 (2015).

32. Kim, J., Kim, E., Won, Y., Lee, H., Suh, K. The preparation and characteristics of conductive poly(3,4-ethylenedioxythiophene) thin film by vapor-phase polymerization. *Synth. Met.* **139,** 485–489 (2003).

33. Lock, J. P., Im, S. G., Gleason, K. K. Oxidative chemical vapor deposition of electrically conducting poly(3,4-ethylenedioxythiophene) films. *Macromolecules* **39,** 5326–5329 (2006).

34. Groenendaal, L., Zotti, G., Aubert, P. H., Waybright, S. M., Reynolds, J. R. Electrochemistry of poly(3,4-alkylenedioxythiophene) derivatives. *Adv. Mater.* **15,** 855–879 (2003).

35. Wang, Y., Lucht, B. L., Euler, W. B. Investigation of the oxidative coupling polymerization of 3-alkylthiophenes with iron(III) chloride. in *American Chemical Society, Polymer Preprints, Division of Polymer Chemistry* **43,** 1160 (2002).

36. Xia, J., Masaki, N., Lira-Cantu, M., Kim, Y., Jiang, K., Yanagida, S. Influence of doped anions on poly(3,4-ethylenedioxythiophene) as hole conductors for iodine-free solid-state dye-sensitized solar cells. *J. Am. Chem. Soc.* **130,** 1258–1263 (2008).

37. Romero, D. B., Schaer, M., Zuppiroli, L., Cesar, B., François, B. Effects of doping in polymer light-emitting diodes. *Appl. Phys. Lett.* **67,** 1659 (1995).

38. Granström, M., Inganäs, O., Electrically conductive polymer fibres with mesoscopic diameters: 1. Studies of structure and electrical properties. *Polymer* **36,** 2867-2872 (1995).

39. Yamato, H., Ohwa, M., Wernet, W. Stability of polypyrrole and poly(3,4_ethylene dioxythiophene) for biosensor application. *Journal of Electroanalytical Chemistry* **397,** 163-170 (1995).

40. Yamato, H., Kai, K. I., Ohwa, M., Wernet, W., Matsumura, M. Mechanical, electrochemical and optical properties of poly(3,4-ethylenedioxythiophene)/sulfated poly(β-hydroxyethers) composite films. *Electrochim. Acta* **42,** 2517–2523 (1997).

41. Kim, B., Koh, J. K., Kim, J., Chi, W. S., Kim, J. H., Kim, E. Room temperature solid-state synthesis of a conductive polymer for applications in stable I2-free dye-sensitized solar cells. *ChemSusChem* **5,** 2173–2180 (2012).

42. Weng, B., Ashraf, S., Innis, P. C., Wallace, G. G. Colour tunable electrochromic devices based on PProDOT-(Hx)2 and PProDOT-(EtHx)2 polymers. *J. Mater. Chem. C* **1,** 7430–7439 (2013).

43. Welsh, D. M., Kloeppner, L. J., Madrigal, L., Pinto, M. R., Thompson, B. C., Schanze, K. S., Abboud, K. A., Powell, D., Reynolds, J. R. Regiosymmetric dibutyl-substituted poly(3,4-propylenedioxythiophene)s as highly electron-rich electroactive and luminescent polymers. *Macromolecules* **35,** 6517–6525 (2002).

44. Loewe, R. S., Khersonsky, S. M., McCullough, R. D. A simple method to prepare head-to-tail coupled, regioregular poly(3-alkylthiophenes) using grignard metathesis. *Adv. Mater.* **11,** 250–253 (1999).

45. Lowe, R. D., McCullough, R. D. Enhanced Electrical Conductivity in Regioselectively Synthesized Poly(3-alkylthiophenes). *J. Chem. Soc. Chem. Commun.* **12,** 70–72 (1992).

46. McCullough, R. D., Lowe, R. D., Tristram-Nagle, S., Jayaraman, M., Anderson, D. L., Ewbank, P. C. Design and Control of Conducting Polymer Architectures: Synthesis and Properties of Regiochemically Well-Defined Poly(3-alkyl-thiophenes). *J . Org. Chem* **58,** 904–912 (1993).

47. Yokoyama, A., Miyakoshi, R., Yokozawa, T. Chain-Growth Polymerization for Poly(3-hexylthiophene) with a Defined Molecular Weight and a Low Polydispersity. *Macromolecules* **37,** 1169–1171 (2004).

48. Reeves, B. D., Grenier, C. R. G., Argun, A. A., Cirpan, A., McCarley, T. D., Reynolds, J. R. Spray coatable electrochromic dioxythiophene polymers with high coloration efficiencies. *Macromolecules* **37,** 7559–7569 (2004).

49. Grenier, C. R. G., George, S. J., Joncheray, T. J., Meijer, E. W., Reynolds, J. R. Chiral ethylhexyl substituents for optically active aggregates of π-conjugated polymers. *J. Am. Chem. Soc.* **129,** 10694–10699 (2007).

50. Yamamoto, T., Abla, M. Synthesis of non-doped poly(3,4-ethylenedioxythiophene) and its spectroscopic data. *Synth. Met.* **100,** 237–239 (1999).

51. Yamamoto, T., Shiraishi, K., Abla, M., Yamaguchi, I., Groenendaal, L. B. Neutral poly(3,4-ethylenedioxythiophene-2,5-diyl)s: Preparation by organometallic polycondensation and their unique p-doping behavior. *Polymer (Guildf).* **43,** 711–719 (2001).

52. Tran-Van, F., Garreau, S., Louarn, G., Froyer, G., Chevrot, C. A fully undoped oligo(3,4-ethylenedioxythiophene): Spectroscopic properties. *Synth. Met.* **119,** 381–382 (2001).

53. Tran-Van, F., Garreau, S., Louarn, G., Froyer, G., Chevrot, C. Fully undoped and soluble oligo(3,4-ethylenedioxythiophene)s: Spectroscopic study and electrochemical characterization. *J. Mater. Chem.* **11,** 1378–1382 (2001).

54. Decker, C. The use of UV irradiation in polymerization. *Polym. Int.* **45,** 133–141 (1998).

55. Turro, N. J., Ramamurthy, V., Scaino, J. C. Modern Molecular Photochemistry of Organic Molecules. *University Science Phublishers* (2010).

56. Fouassier, J. P., Allonas, X., Laleve, J., Dietlin, C. Photoinitiators for Free Radical Polymerization Reactions. *Photochemistry and Photophysics of Polymer Materials.* 351–419 (2010).

57. Hageman, H. J. Photoinitiators for free radical polymerization. *Prog. Org. Coatings* **13,** 123–150 (1985).

58. Crivello, James V. The Discovery and Development of Onium Salt Cationic Photoinitiators. *J. of Polymer Sci.: Part A: Polymer Chemistry* **37,** 4241–4254 (1999).

59. Young, R. J., Lovell, P. A. Introduction to polymers. *CRC Press* (2011).

60. Fors, B. P., Hawker, C. J. Control of a living radical polymerization of methacrylates by light. *Angew. Chem. Int. Ed.* **51,** 8850–8853 (2012).

61. Xu, J., Jung, K., Atme, A., Shanmugam, S., Boyer, C. A robust and versatile photoinduced living polymerization of conjugated and unconjugated monomers and its oxygen tolerance. *J. Am. Chem. Soc.* **136,** 5508–5519 (2014).

62. Treat, N. J., Sprafke, H., Kramer, J. W., Clark, P. G., Barton, B. E., Read De Alaniz, J., Fors, B. P., Hawker, C. J. Metal-free atom transfer radical polymerization. *J. Am. Chem. Soc.* **136,** 16096–16101 (2014).

63. Zhou, H., Johnson, J. A. Photo-controlled growth of telechelic polymers and end-linked polymer gels. *Angew. Chem. Int. Ed.* **52,** 2235–2238 (2013).

64. Chen, M., Zhong, M., Johnson, J. A. Light-Controlled Radical Polymerization: Mechanisms, Methods, and Applications. *Chem. Rev.* **116,** 10167–10211 (2016).

65. Kijewska, K., Blanchard, G. J., Szlachetko, J., Stolarski, J., Kisiel, A., Michalska, A., Maksymiuk, K., Pisarek, M., Majewski, P., Krysiński, P. Kijewska, K. Photopolymerized polypyrrole microvessels. *Chem. A Eur. J.* **18,** 310–320 (2012).

66. Zhang, S., Lv, G., Wang, G., Zhu, K., Yu, D., Shao, J. Effects of UV radiation on the preparation of polypyrrole in the presence of hydrogen peroxide. *Radiat. Eff. Defects Solids* **170,** 821–831 (2015).

67. Piletsky, S. A., Piletska, E. V., Karim, K., Davis, F., Higson, S. P. J., Turner, A. P. F. Photochemical polymerization of thiophene derivatives in aqueous solution. *Chem. Commun.* 2222–2223 (2004).

68. Huisman, C. L., Huijser, A., Donker, H., Schoonman, J., Goossens, A. UV polymerization of oligothiophenes and their application in nanostructured heterojunction solar cells. *Macromolecules* **37,** 5557–5564 (2004).

69. Okano, M., Itoh, K., Fujishima, A., Honda, K. Generation of organic conducting patterns on semiconductors by photoelectrochemical polymerization of pyrrole. *Chem. Lett.* 469–472 (1986).

70. Yoneyama, H., Kitayama, M. Photocatalytic Deposition of Light-localized Polypyrrole Film Pattern on n-type Silicon Wafers. *Chem. Lett.* 657–660 (1986).

71. Kalyanasundaram, K. Photophysics, photochemistry and solar energy conversion with tris(bipyridyl)ruthenium(II) and its analogues. *Coord. Chem. Rev.* **46,** 159–244 (1982).

72. Tyson, D. S., Bialecki, J., Castellano, F. N. Ruthenium(II) complex with a notably long excited state lifetime. *Chem. Commun.* 2355–2356 (2000).

73. Zeitler, K. Photoredox catalysis with visible light. *Angew. Chem. Int. Ed.* **48,** 9785–9789 (2009).

74. Tepavcevic, S., Darling, S. B., Dimitrijevic, N. M., Rajh, T., Sibener, S. J. Improved hybrid solar cells via in situ UV polymerization. *Small* **5,** 1776–1783 (2009).

75. Norihisa Kobayashi. Conducting polymer image formation with photoinduced electron transfer reaction. *J. Mater. Chem* **8,** 497–506 (1998).

76. Segawa, H., Shimidzu, T., Honda, K. A novel photo-sensitized polymerization of pyrrole. *J. Chem. Soc. Chem. Commun.* 132–133 (1989).

77. Rabek, J. F., Lucki, J., Qu, B. J., Shi, W. F. Photopolymerization of pyrrole initiated by the ferrocene- and iron-arene saltchlorinated solvents complexes. *J. Macromol. Sci. Part A* **29,** 297–310 (1992).

78. Yagci, Y., Yilmaz, F., Kiralp, S., Toppare, L. Photoinduced polymerization of thiophene using iodonium salt. *Macromol. Chem. Phys.* **206,** 1178–1182 (2005).

79. Aydogan, B., Yagci, Y., Toppare, L., Jockusch, S., Turro, N. J. Photoinduced electron transfer reactions of highly conjugated thiophenes for initiation of cationic polymerization and conjugated polymer formation. *Macromolecules* **45,** 7829–7834 (2012).

80. Natarajan, S., Kim, S. H. Photochemical oligomerization pathways in 2,5-diiodothiophene film. *J. Photochem. Photobiol. A Chem.* **188,** 342–345 (2007).

81. Natarajan, S., Kim, S. H. Photochemical conversion of 2,5-diiodothiophene condensed on substrates to oligothiophene and polythiophene thin films and micro-patterns. *Thin Solid Films* **496,** 606–611 (2006).

82. D'Auria, M. Photochemical and Photophysical Behavior of Thiophene. *Adv. Heterocycl. Chem.* **104,** 127–390 (2011).

83. D'Auria, M., Distefano, C., D'Onofrio, F., Mauriello, G., Racioppi, R. Photochemical substitution of polyhalogenothiophene and halogenothiazole derivatives. *J. Chem. Soc. Perkin Trans.* **1,** 3513–3518 (2000).

84. Sage, A. G., Oliver, T. A. A,; Murdock, D., Crow, M. B., Ritchie, G. A. D., Harvey, J. N., Ashfold, M. N. R. nσ* and πσ* excited states in aryl halide photochemistry: a comprehensive study of the UV photodissociation dynamics of iodobenzene. *Phys. Chem. Chem. Phys.* **13,** 8075 (2011).

85. D'Auria, M., De Mico, A., D'Onofrio, F., Piancatelli, G. Italian Pat. Appl., 479799A90. (1990).

86. Tedder, J. M. The interaction of free radicals with saturated aliphatic compounds. *Q. Rev. Chem. Soc.* **14,** 336–356 (1960).

87. Herrera, O. S., Nieto, J. D., Olleta, A. C., Lane, S. I. The photoinduced reaction of 2-iodothiophene in solutions of n-heptane, dichloromethane and methanol. *J. Phys. Org. Chem.* **24,** 398–406 (2011).

88. Fox, R. J., Evans, F. W., Szwarc, M. Abstraction of Halogen Atoms by Methyl Radicals Part 2. *Trans. Faraday Soc.* **57,** 1915–1927 (1961).

89. Hintz, H., Egelhaaf, H. J., Lüer, L., Hauch, J., Peisert, H., Chassé, T. Photodegradation of P3HT - A systematic study of environmental factors. *Chem. Mater.* **23,** 145–154 (2011).

90. Abdou, A., Holdcroft, S. Mechanisms of Photodegradation of Poly(3-alkylthiophenes) in Solution. *Macromolecules* **26,** 2954–2962 (1993).

91. Ohta, H., Koizumi, H. Mechanisms of photo-induced degradation of polythiophene derivatives: re-examination of the role of singlet oxygen. *Polym. Bull.* **74,** 2319–2330 (2017).

92. Koch, M., Nicolaescu, R., Kamat, P. V. Photodegradation of polythiophene-based polymers: Excited state properties and radical intermediates. *J. Phys. Chem. C* **113,** 11507–11513 (2009).

93. Sperlich, A., Kraus, H., Deibel, C., Blok, H., Schmidt, J., Dyakonov, V. Reversible and irreversible interactions of poly(3-hexylthiophene) with oxygen studied by spin-sensitive methods. *J. Phys. Chem. B* **115,** 13513–13518 (2011).

94. Dhoot, A. S., Ginger, D. S., Beljonne, D., Shuai, Z., Greenham, N. C. Triplet formation and decay in conjugated polymer devices. *Chem. Phys. Lett.* **360,** 195–201 (2002).

95. Holdcroft, S. A photochemical study of poly(3-hexylthiophene). *Macromolecules* **24,** 4834–4838 (1991).

96. Manceau, M., Rivaton, A., Gardette, J. L. Involvement of singlet oxygen in the solid-state photochemistry of P3HT. *Macromol. Rapid Commun.* **29,** 1823–1827 (2008).

97. Neto, N. M. B., Silva, M. D. R., Araujo, P. T., Sampaio, R. N. Photoinduced Self-Assembled Nanostructures and Permanent Polaron Formation in Regioregular Poly(3-hexylthiophene). *Adv. Mater.* **30,** 1705052 (2018).

98. Elschner, A., Kirchmeyer, S., Lovenich, W., Merker, U., Reuter, K. *PEDOT:* Principles and Applications of an Intrinsically Conductive Polymer. *CRC Press* (2011).

99. Bredas, J. L., Street, G. B. Polarons , Bipolarons , and Solitons in Conducting Polymers. *Acc. Chem. Res.* **18,** 309–315 (1985).

100. Ouyang, J. Solution-Processed PEDOT:PSS Films with Conductivities as Indium Tin Oxide through a Treatment with Mild and Weak Organic Acids. *Appl. Mater. interfaces* **5,** 13082–13088 (2013).

101. Welsh, D. M., Kumar, A., Meijer, E. W., Reynolds, J. R. Enhanced contrast ratios and rapid switching in electrochromics based on poly(3,4-propylenedioxythiophene) derivatives. *Adv. Mater.* **11,** 1379–1382 (1999).

102. Beaujuge, P. M., Ellinger, S., Reynolds, J. R. The donor-acceptor approach allows ablack-to-transmissive switching polymeric electrochrome. *Nat. Mater.* **7,** 795–799 (2008).

103. Heeger, A. J. Semiconducting and Metallic Polymers: The Fourth Generation of Polymeric Materials. *Angew. Chem. Int. Ed.* **40,** 2591–2611 (2001).

104. Derivatives, H., Louis, J., Macdiarmid, A. G. Synthesis of Electrically Conducting Organic Polymers : *J.C.S Chem. Comm.* **100,** 578–580 (1977).

105. Chiang, C. K., Druy, M. A., Gau, S. C., Heeger, A. J., Louis, E. J., MacDiarmid, A. G., Park, Y. W., Shirakawa, H. Synthesis of highly conducting films of derivatives of polyacetylene, (CH)x. *J. Am. Chem. Soc.* **100,** 1013–1015 (1978).

106. Jonas, F., Heywang, G., Schmidtberg, W., Heinze, J., Dietrich, M. EP339340. (1988).

107. Heinze, J., Frontana-Uribe, B. A., Ludwigs, S. Electrochemistry of conducting polymers-persistent models and new concepts. *Chem. Rev.* **110,** 4724–4771 (2010).

108. Smith, L. K., Fantella, S. L. N., Pellis, S. M. Quantitative Dedoping of Conductive Polymers. *Chem. Mater.* **29,** 832–841 (2017).

109. Cochran, J. E., Junk, M. J. N., Glaudell, A. M., Miller, P. L., Cowart, J. S., Toney, M. F., Hawker, C. J., Chmelka, B. F., Chabinyc, M. L. Molecular interactions and ordering in electrically doped polymers: Blends of PBTTT and F4TCNQ. *Macromolecules* **47,** 6836–6846 (2014).

110. Yim, K. H., Whiting, G. L., Murphy, C. E., Halls, J. J. M., Burroughes, J. H., Friend, R. H., Kim, J.-S. Controlling Electrical Properties of Conjugated Polymers via a Solution-Based p-Type Doping. *Adv. Mater.* **20,** 3319–3324 (2008).

111. Kang, K., Watanabe, S., Broch, K., Sepe, A., Brown, A., Nasrallah, I., Nikolka, M., Fei, Z., Heeney, M., Matsumoto, D. 2D coherent charge transport in highly ordered conducting polymers doped by solid state diiusion. *Nat. Mater.* **15,** 896–903 (2016).

112. Scholes, D. T., Hawks, S. A., Yee, P. Y., Wu, H., Lindemuth, J. R., Tolbert, S. H., Schwartz, B. J. Overcoming Film Quality Issues for Conjugated Polymers Doped with F4TCNQ by Solution Sequential Processing: Hall Effect, Structural, and Optical Measurements. *J. Phys. Chem. Lett.* **6,** 4786–4793 (2015).

113. Zhang, Y., Boer, B. De, Blom, P. W. M. Controllable molecular doping and charge transport in solution-processed polymer semiconducting layers. *Adv. Funct. Mater.* **19,** 1901–1905 (2009).

114. Jacobs, I. E., Aasen, E. W., Oliveira, J. L., Fonseca, T. N., Roehling, J. D., Li, J., Zhang, G., Augustine, M. P., Mascal, M., Moulé, A. J. Comparison of solution-mixed and sequentially processed P3HT:F4TCNQ films: Effect of doping-induced aggregation on film morphology. *J. Mater. Chem. C* **4,** 3454–3466 (2016).

115. Fujimoto, R., Watanabe, S., Yamashita, Y., Tsurumi, J., Matsui, H., Kushida, T., Mitsui, C., Yi, H. T., Podzorov, V., Takeya, J. Control of molecular doping in conjugated polymers by thermal annealing. *Org. Electron. physics, Mater. Appl.* **47,** 139–146 (2017).

116. Kao, C. Y., Lee, B., Wielunski, L. S., Heeney, M., McCulloch, I., Garfunkel, E., Feldman, L. C., Podzorov, V. Doping of conjugated polythiophenes with alkyl silanes. *Adv. Funct. Mater.* **19,** 1906–1911 (2009).

117. Calhoun, M. F., Sanchez, J., Olaya, D., Gershenson, M. E., Podzorov, V. Electronic functionalization of the surface of organic semiconductors with self-assembled monolayers. *Nat. Mater.* **7,** 84–89 (2008).

118. Xia, Y., Sun, K., Ouyang, J. Solution-processed metallic conducting polymer films as transparent electrode of optoelectronic devices. *Adv. Mater.* **24,** 2436–2440 (2012).

119. Han, C. C., Elsenbaumer, R. L. Protonic Acids: Generally Applicable Dopants for Conducting Polymers. *Synth. Met.* **30,** 123–131 (1989).

120. Meier, H., Stalmach, U., Kolshorn, H. Effective conjugation length and UV/vis spectra of oligomers. *Acta Polym.* **48,** 379–384 (1997).

121. Botelho, A. L., Shin, Y., Liu, J., Lin, X. Structure and optical bandgap relationship of π-conjugated systems. *PLoS One* **9,** 1–8 (2014).

122. Wang, C., Schindler, J. L., Kannewurf, C. R., Kanatzidis, M. G. Poly(3,4-ethylenedithiathiophene). A New Soluble Conductive Polythiophene Derivative. *Chem. Mater.* **7,** 58–68 (1995).

123. Lawrence, J., Goto, E., Ren, J. M., Mcdearmon, B., Kim, D. S., Ochiai, Y., Clark, P. G., Laitar, D., Higashihara, T., Hawker, C. J. A Versatile and Efficient Strategy to Discrete Conjugated Oligomers. *J. Am. Chem. Soc.* **139,** 13735–13739 (2017).

124. Bonillo, B., Swager, T. M. Chain-growth polymerization of 2-chlorothiophenes promoted by lewis acids. *J. Am. Chem. Soc.* **134,** 18916–18919 (2012).

Chapter 2. Facile Fabrication of Conjugated Polymers through One-pot Photo-mediated Polymerization based on Photoarylation of Thiophene Derivatives

2.1 Introduction

Since PEDOT [poly(3,4-ethylenedioxythiophene)] and water soluble PEDOT:PSS were commercially manufactured by Beyer AG early in the 1990s,[1,2] numerous synthetic methods for π-conjugated conducting polymers have been extensively investigated including chemical oxidative polymerization in solution[3–6], in vapor phase[7,8], electrochemical[9,10], organometallic polymerization[11–14] for various applications such as antistatic coatings[2], electrochromics[15], light-emitting diodes[16,17], and sensors[18–20] owing to their excellent transparency and conductivity in doped states. Although significant development with respect to the polymerization for conjugated polymers has been achieved, there still remains a great demand to develop a versatile and efficient synthetic route for the synthesis of well-defined conjugated polymers with enhanced optical and electrical properties. Given that conjugated molecules are highly reactive to light irradiation and the electronic states are photochemically tunable, photo-mediated polymerization has great potential to engineer the molecular structures of conjugated polymers. Photo-mediated radical polymerization is also significantly advantageous such as facile and instantaneous reaction and cost-effective mass production capability through a roll-to-roll process.

Light-induced radical polymerization has been widely investigated and well established for a variety of vinyl monomers in the last few decades. In particular, photo-controlled radical polymerization (photo-CRP) to engineer the polymer structure with a designed molecular weight and narrow polydispersity has been of great interests. The polymerization managed by the photoredox reaction of metal-ligand catalysts is able to produce aliphatic polymers with well-defined linear structures. The polymerization mechanism of photo-CRP has been well-established by means of various characterization methods such as GPC, ^{1}H-NMR, and MALDI.

Motivated by the promising results from photo-controlled radical polymerization of vinyl monomers, extensive efforts have also been devoted to developing a variety of conjugated polymers through photochemical polymerization. Yagci and coworkers established photo-induced cationic polymerization for conjugated polymers, which is driven by electron transfer from thiophene derivatives or their conjugated molecules to iodonium salts, followed by the coupling of corresponding radical cation species.[24–26] Polypyrrole or polyaniline were obtained through the coupling between photo-oxidized monomeric or oligomeric precursors in the presence of photoactivated Ruthenium complexes by light illumination.[27–29] Those synthetic approaches took advantages of the oxidation of the precursors to achieve conjugated polymers so that the polymerization mechanisms are similar to that of the chemical oxidative polymerization. Step growth polymerization with iodinated thiophenes is another synthetic approach to synthesize conjugated polymers. The coupling of thienyl radical species, which is originated from the photodissociation of carbon-iodine bonds of 2,5-diiodothiophenes by UV irradiation, results in the formation of oligomeric or polymeric thiophenes.[30–32] Although a linear step growth mechanism was proposed through optical and physical property analyses, the monomer conversion and polymerization efficiency were still unsatisfactory, not suitable for high molecular weight polymers.

The photoarylation between thiophenes and their iodothienyl derivatives is regarded as a promising synthetic strategy to efficiently produce thiophene oligomers in high yields.[33–36] UV light irradiation to 2,5-diiodothiophenes in the presence of thiophene monomers in acetonitrile gives thiophene trimers with a high conversion yield through the photo-arylation mechanism.[37] However, higher molecular weight species have not been achieved by the photochemical reaction. It is believed that the resulting oligomers are terminated with carbon-hydrogen bonds and become unreactive to light irradiation. If reversible carbon-iodine bonds are manageable at the chain ends after the photo-arylation, the trimers are expected to grow further by the photo-arylation in the presence of additional monomers, eventually reaching to higher molecular species. Here, we have devised a photo-mediated radical polymerization in solution to achieve conducting polymers with a high molecular weight and low polydispersity by reviving carbon-iodine bonds at the growing chain ends. A series of 3,4-propylenedioxythiophenes (ProDOT) having two symmetrically incorporated solubilizing alkyl chains are designed, synthesized, and used to investigate the novel photopolymerization. The alkyl side chains not only render good solubility to the growing polymer chains during the solution polymerization but also enable the characterization of resulting products by GPC, MALDI Mass, UV-vis absorption spectroscopy, and ^{1}H-NMR.[38,39] The polymerization mechanism was systematically investigated by correlating the molecular weight, absorption properties, and the molecular structure of the resulting polymers.

2.2 Experimental

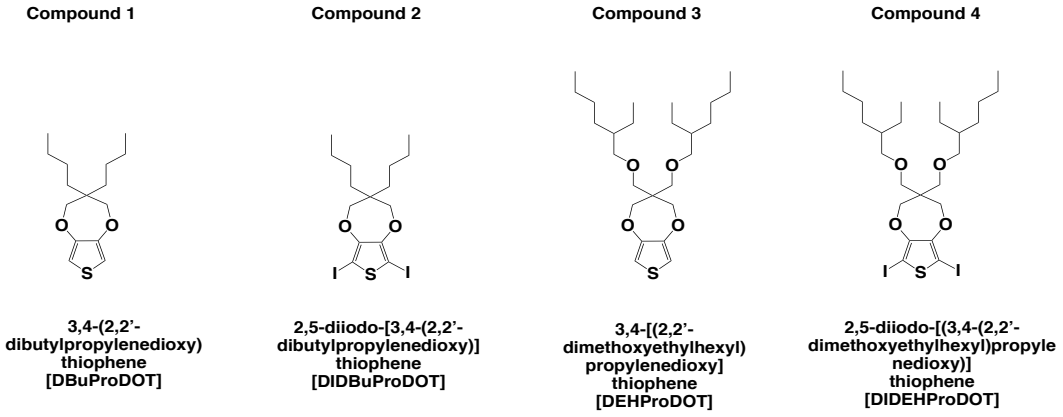

Figure 2.1. ProDOT derivatives synthesized for the photomediated polymerization.

3,4-propylenedioxythiophene molecules incorporating dibutyl or dimethoxyethylhexyl side chains on the center of the propylene bridge (DBuProDOT or DEHProDOT) and the diiodinated ProDOT derivatives (DIDBuProDOT or DIDEHProDOT) were prepared as a precursor according to the literature procedures (Figure 2.1).[39,40] The photo-polymerization was initiated by means of the 365nm LED in the 1.0 mM solution of the ProDOT monomers and DIProDOT derivatives in argon purged bromotrichloromethane ($CBrCl_3$). After confirming that most monomers were consumed by the UV irradiation, 2.0 mmol of iodine (I_2) and a few drops of perchloric acid ($HClO_4$) were subsequently added and the light source was switched to a 532nm q-switched pulsed laser. Aliquots of the photo-reacted samples were taken at a regular interval and their UV-vis absorption was measured after dilution with chloroform. The aliquots were also rinsed with an aqueous solution of sodium thiosulfate ($Na_2S_2O_3$) and dedoped with hydrazine (N_2H_4) to remove extra iodine molecules and neutralize the polymer products, followed by dissolution in chloroform for UV-vis absorption and Gel Permeation Chromatography (GPC) analysis. In addition, after removing residual monomers from the polymerized products, H-NMR

($CDCl_3$) and MALDI-TOF were employed to investigate the molecular structures. All the samples for GPC analysis were stirred and annealed in a chloroform solution at 50°C for 3 hours before the sample injection to prevent polymer aggregation for accurate molecular weight analysis.

2.3 Results and discussion

The photoarylation efficiency of the thiophene derivatives is determined by how iodo-thiophene molecules promptly generate radical species via the selective homolytic cleavage of the carbon-iodine bonds without hampering π-conjugation upon UV irradiation[31,41] and efficiently react with neighboring thiophenes to yield thiophene dimers or trimers in a high yield[35]. As depicted in Figure 2.2, an iodine radical produced by the photoarylation could react with other molecules in three different ways; 1) halogen abstraction by organic solvents containing carbon-hydrogen bonds[41–43], 2) coupling with a hydrogen radical to give corresponding hydrogen iodide (HI)[44], and 3) coupling with thienyl radical or electrophilic iodination.

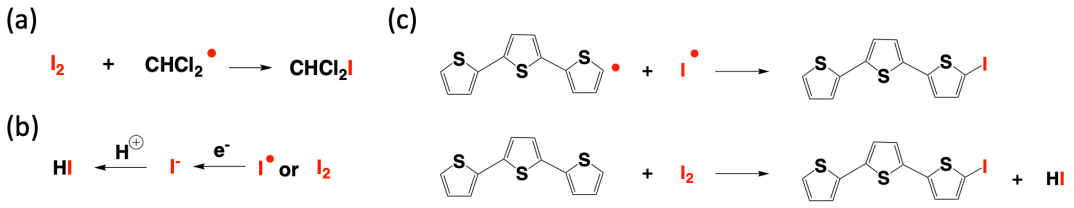

Figure 2.2. Schematic iodine consumption in three different ways; (a) abstraction by hydrogen donating solvents[41–43], (b) hydrogen iodide formation[44], (c) coupling with thienyl radicals/electrophilic iodination.

In order to achieve conjugated molecules having a higher molecular weight, it is required to recover carbon-iodine bonds at the growing chain ends to continue photoarylation between the iodinated molecules and neighboring thiophene precursors under continuous photoirradiation. Organic solvents having hydrogen atoms on their molecular structures, however, will likely

consume iodine radical during the reaction by means of halogen abstraction by carbon-hydrogen bonds.[42,45–47] Therefore, $CBrCl_3$ was chosen as a hydrogen-free organic solvent to avoid the iodine abstraction by solvent during the reaction and allow iodine radical exchange between the growing chain ends and thiophene precursors. In order to examine the validity of these assumptions, a photo-polymerization with DBuProDOT and DIDBuProDOT was carried out.

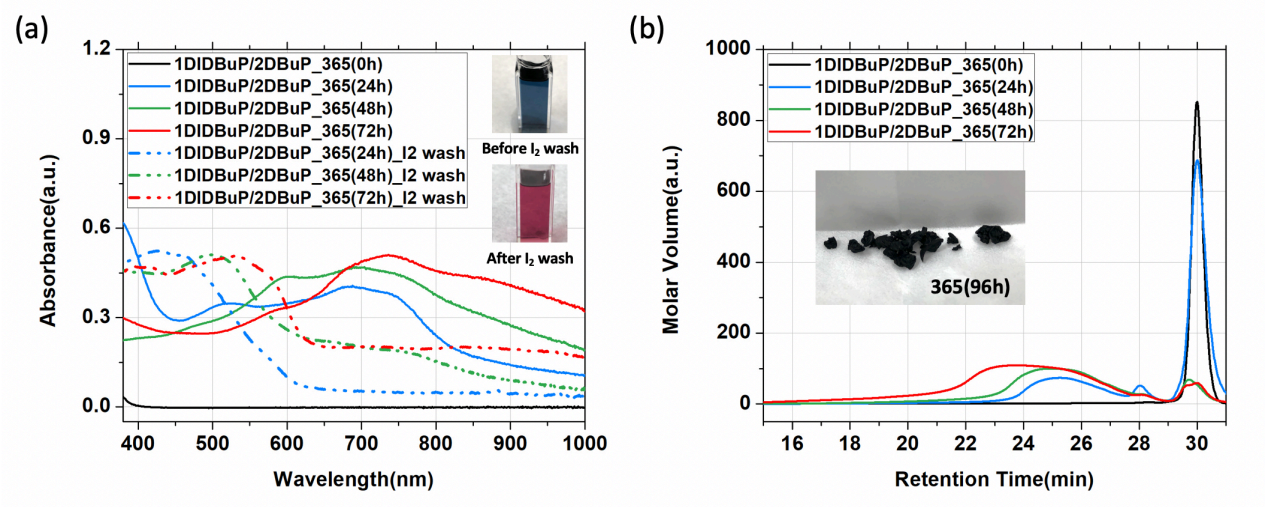

Figure 2.3. Characterization of 365nm UV-irradiated products from DIDBuProDOT and DBuProDOT solution by (a) UV-vis absorption spectra in a diluted chloroform solution and (b) GPC traces.

The UV-vis absorption spectra of the photopolymerized product of DIDBuProDOT and DBuProDOT by 365nm UV light are presented as solid lines in Figure 2.3(a). The UV irradiated solution exhibited the main absorption in the 600~1000nm wavelength range and the absorption λ_{max} redshifted as the UV irradiation time increased, suggesting a gradual increase in the conjugation length and the doped state of the product. The de-doped products after the I_2 washing also demonstrate vibronic and redshifted absorption spectra in the 400~600nm range in solution with an increasing irradiation time as displayed as the dashed lines. In particular, a shoulder peak at around 570nm corresponds to the enhanced intermolecular π-π* transition of the higher

molecular weight species. This vibrational fine structure is comparable to the absorption spectrum of the poly(DBuProDOT) in solution where the polymer was synthesized through the organometallic pathway.[48] Although extra iodine species were eliminated by rinsing with sodium thiosulfate and de-doping, the appearance of the broad absorption bands across the long wavelength region over 700nm was observed when 48 hours of the UV-irradiation time was longer than 48 hours, which indicates the polaron formation and delocalization of charge carriers due to the interchain interaction of the growing polymer chains[49–51]. This transition behavior in the long wavelength region is similar to the result of the photo-induced P3HT aggregation.[52]

The changes in the optical properties of the solution are consistent with the change in the molecular weight distributions. GPC traces of the photopolymerized products of DBuProDOT showed that the retention time gets smaller with an increasing UV irradiation time as presented in Figure 2.3(b). The GPC traces also shows that the increase in the molecular weight of the polymerized products is accompanied with the consumption of ProDOT monomers. Hence, the photopolymerization trait resembles the typical chain growth polymerization mechanism in that the molecular weight increase is attributed to the progressive addition of monomer to the chain end. The number average molecular weight (M_n) of the photo-polymerized product for 72 hours of reaction is 2,200 g/mol (PDI=1.20) corresponding to the octamer length with monomer conversion up to 95%. Further UV irradiation led to the precipitation of the resulting products in the solution as shown in the inset of Figure 2.3(b). This observation suggests that the p-doped oligomer species undergo significant intermolecular interactions and that the dibutyl side chains of the polymer are not bulky enough to effectively prevent the intermolecular aggregation.

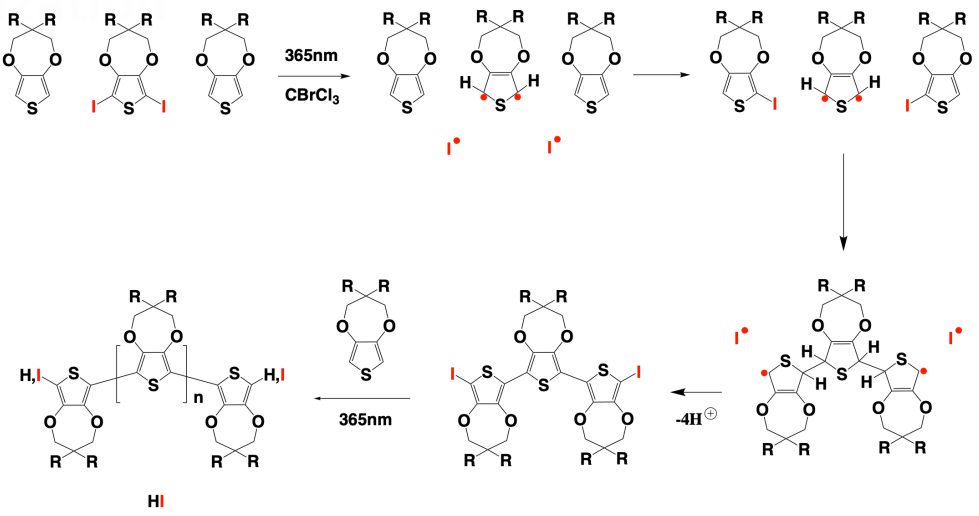

Figure 2.4. Schematic showing photoarylation based polymerization of Poly(DBuProDOT).

Based on the UV-vis absorption and GPC results, we propose the photoarylation-based polymerization mechanism described in Figure 2.4. Upon UV 365nm irradiation, DIDBuProDOT undergoes photodissociation of the carbon-iodine bonds to generate the DBuProDOT radical and iodine radicals. Then the produced ProDOT radical rapidly reacts with the idodinated monomers generated from the iodine radical and two neighboring DBuProDOT monomers to form a ProDOT trimer in the same manner a thiophene trimer formation by photoarylation.[34,37] In particular, when the trimer ProDOT recovers carbon-iodine bonds at the chain ends, the photoarylation by UV irradiation would continue between the oligomeric species and DBuProDOT monomers to yield higher molecular weight species. Along with the growing conjugated products, photogenerated iodine species ($I^{\bullet}$ or I_2) transform into iodide complexes (I^- or I_2^-) by electron transfer from the oligomeric ProDOT,[32] followed by the formation of hydrogen iodide (HI) by the protonation of the iodide species. Electron charge transfer from the growing chains and the presence of HI promote the produced oligomers to be doped in the solution evidenced by the broad absorption spectra in the long wavelength range as shown in Figure 2.3(a).

Another photo-polymerization mechanism possible for iodinated thiophene molecules is photo-induced polycondensation [30,31]. In this scheme, only DIDBuProDOT monomers serve as reactants in a hydrogen-free $CBrCl_3$ solution. As suggested in Figure 2.5, photogenerated 2-iodoProDOT radical by 365nm UV irradiation reacts with another ProDOT radical or neighboring 2,5-diiodoProDOT to form a diiodo ProDOT dimer with iodine species. Due to the absence of hydrogen radical in the system, hydrogen iodide (HI) is not formed by the photo-mediated coupling. In the same manner, all the growing chains remain active with carbon-iodine bonds at the chain ends along with iodine byproducts.

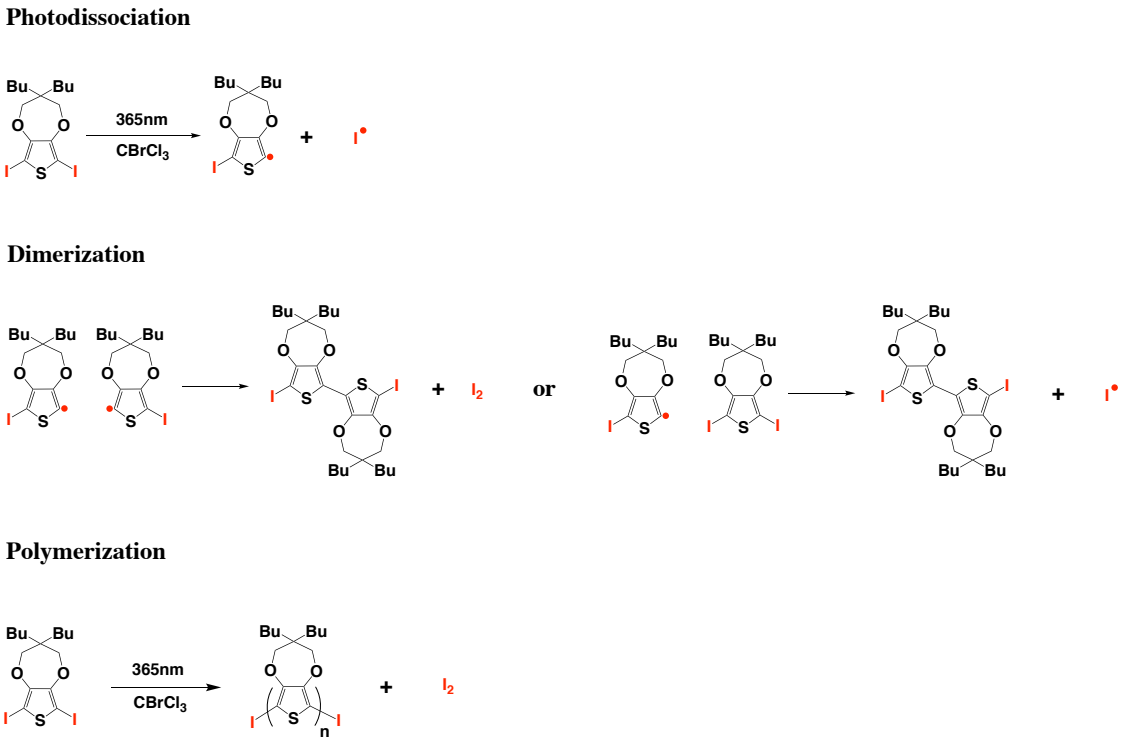

Figure 2.5. Schematic showing photocondensation of DIDBuProDOT under 365nm LED irradiation.

The UV-vis absorption spectra and GPC trace of the photopolymerized products of DIDBuProDOT (Figure 2.6) support the proposed photo-induced polycondensation scheme. The reaction products were recovered from the $CBrCl_3$ solution and diluted in chloroform for UV-vis absorption measurement. Two main absorption bands appear in the 400~700nm wavelength range as presented in solid lines in Figure 2.6(a). The absorption bands centered at around 450 and 520nm are assigned to π-π^* transition of ProDOT oligomers and iodine species, respectively, in the chloroform solution. As the reaction time gets longer, the absorption intensity increases, indicating the increasing concentration of photopolymerized products and iodine molecules as a result of the photo-condensed polymerization. However, absence of any noticeable absorption redshift during the long-term UV irradiation suggests that further chain extension through condensation among the oligomers is not attainable by the photocondensation. The limited molecular weight of photo-condensation products is also confirmed by the GPC trace in Figure 2.6(b). The molecular weight data show that ProDOT dimers (retention time: ~28min) are dominant regardless of the reaction time, shorter oligomers are favored over longer ones, and molecular weight distribution gets broaden with increasing reaction time. This result is consistent with the finding in the polythiophenes photopolymerized from 2,5-diiodothiophene,[30] which is also in good agreement with the Flory's model for linear step growth polymerization assuming that all the species in the system have equal chances of reacting with other molecules regardless of their size.

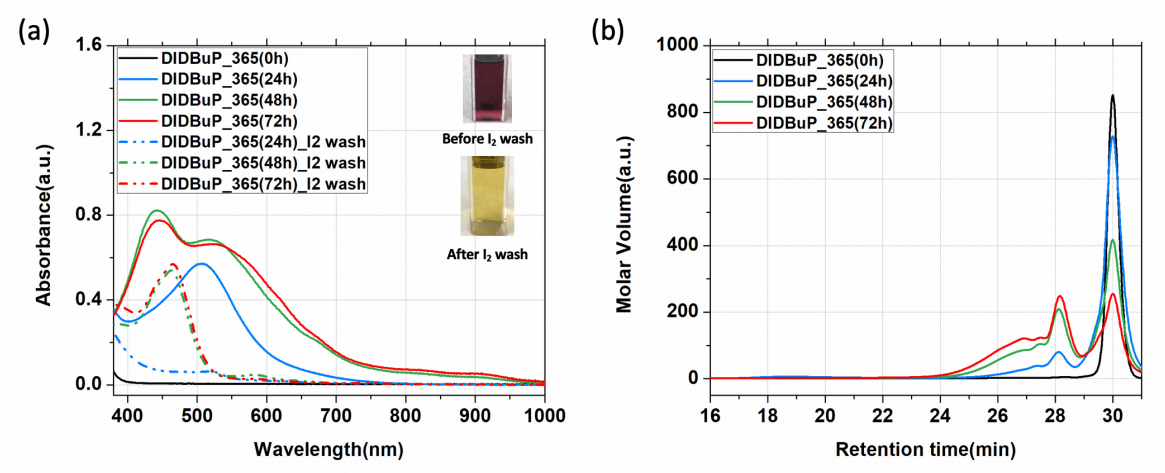

Figure 2.6. Characterization of 365nm UV-irradiated products from DIDBuProDOT solution by (a) UV-vis absorption spectra and (b) GPC traces.

Judging from the monomer conversion efficiency and the number average molecular weights of the photopolymerized products as shown in Figure 2.7, the photo-arylation of DIDBuProDOT/DBuProDOT is believed to provide a more efficient photochemical pathway to yield higher molecular weight species than the photo-condensation. The polymerization efficiency is generally determined by the reactivity of the growing chain ends produced by the reversible photo-dissociation of carbon-iodine bonds in this system. The efficient photo-dissociation of carbon-iodine bonds is ascribed to the photo-excited species absorbing sufficient photon energy exceeding the energy bandgap and subsequent energy transfer to the chain ends.[53] Therefore, it is reasonable that conjugated molecules with a low oxidation potential is beneficial to produce radical species by the C-I fission of chain ends. It is noteworthy that the polymerized ProDOT oligomers by the photo-arylation are p-doped by hydrogen iodide (HI) so that the growing chains having a reduced HOMO-LUMO band gap are readily photo-excited. In other words, the facile photo-excitation of growing oligomer chains in p-doped states promotes the photo-dissociation of

carbon-iodine bonds at the chain ends and corresponding radical generation so as to extend their chain length by further reacting with available monomers.

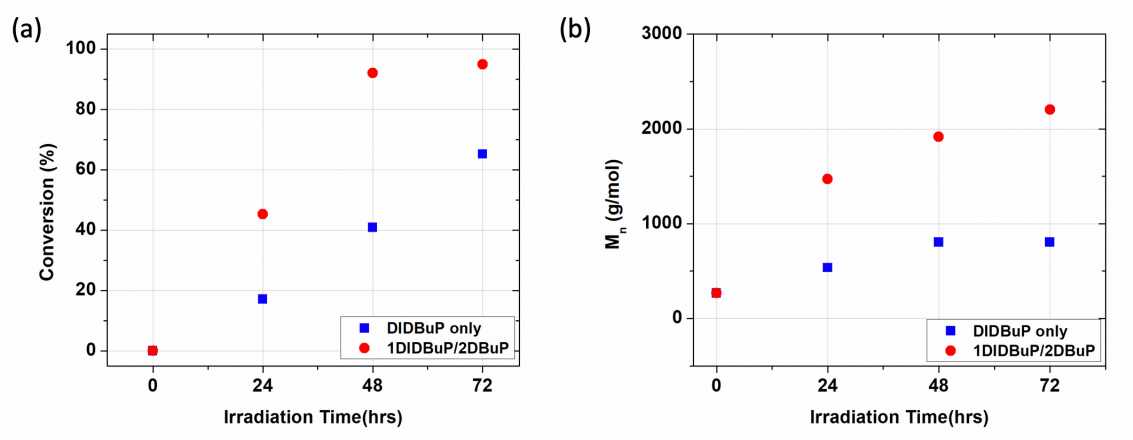

Figure 2.7. The comparison of the photocondensation from DIDBuProDOT (blue) and the photoarylation from DIDBuProDOT and DBuProDOT with (a) Monomer conversion and (b) number average molecular weights.

ProDOT incorporating the bulky diethylhexylmethoxy side chains (DEHProDOT) was designed to prevent the precipitation observed in the prolonged photo-polymerization of DBuProDOT. Photo-polymerization of DIDEHProDOT/DEHProDOT demonstrated a chain growth behavior with analogous UV-vis absorption spectra and GPC results to those of DIDBuProDOT/DBuProDOT as shown in Figure 2.8. No precipitation of polymerized products was observed even after a prolonged UV irradiation owing to the longer and bulkier alkyl side chains than the dibutyl ones. However, no additional increase in the molecular weight was achieved by a long-term irradiation for over 72 hours, rather a slight increase in the retention time was observed in the GPC trace, indicating a decrease in the molecular weight. It is suspicious that the growing chains undergo photo-degradation by the continuous UV irradiation. We assumed that the chain growth would continue as long as the growing chain ends retain carbon-iodine bonds.

However, when the growing chain ends fail to retain carbon-iodine bonds and terminate with carbon-hydrogen bonds, the oligomeric or polymeric chains not only stop growing but also are susceptible to photo-degradation in the photoexcited states by UV irradiation.

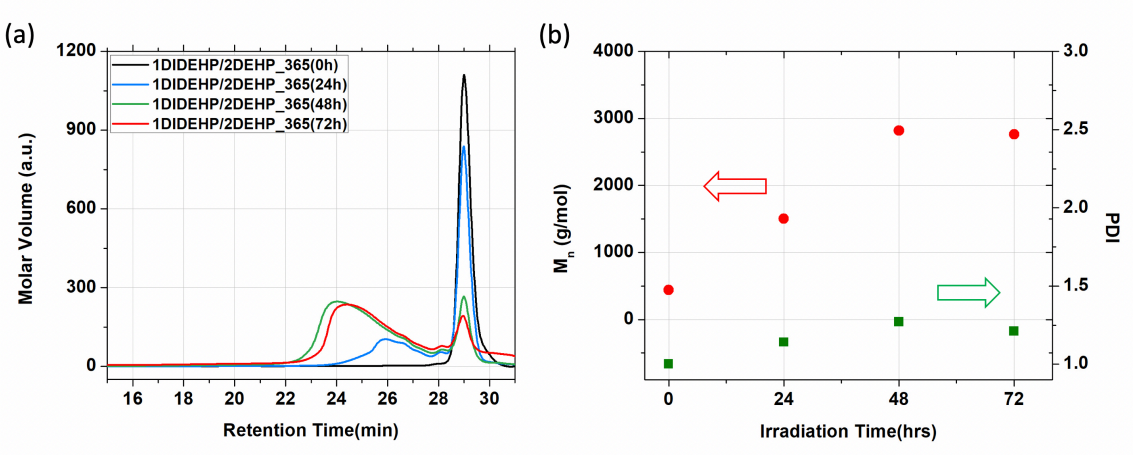

Figure 2.8. Characterization of 365nm UV-irradiated products from DIDEHProDOT and DEHProDOT solution by (a) GPC results and (b) number average molecular weight and PDI depending on UV irradiation time.

The chain end group of the photo-polymerized products of DBuProDOT and DEHProDOT was identified by MALDI-TOF to investigate that the constraint of chain growth is originated from the loss of the iodine as depicted in Figure 2.9. The consistent mass difference shown in the MALDI-TOF data corresponds to the molecular weight of the monomer repeat unit of the polymers; 266 amu for DBuProDOT and 438 for DEHProDOT, and the mass spectra results are consistent with the literature characterizations.[39,48,54] It is noteworthy that the minute residual peaks of two ion series (438n+127 or 438n+254) are observed in the poly(DEHProDOT) sample corresponding to I-M_n-H or I-M_n-I as shown in the inset of Figure 2.9(b). Since most of oligomer

chains have carbon-hydrogen end groups, the oligomer chains are expected to lose the ability to continue their chain extension and would be prone to photodegradation by UV irradiation.

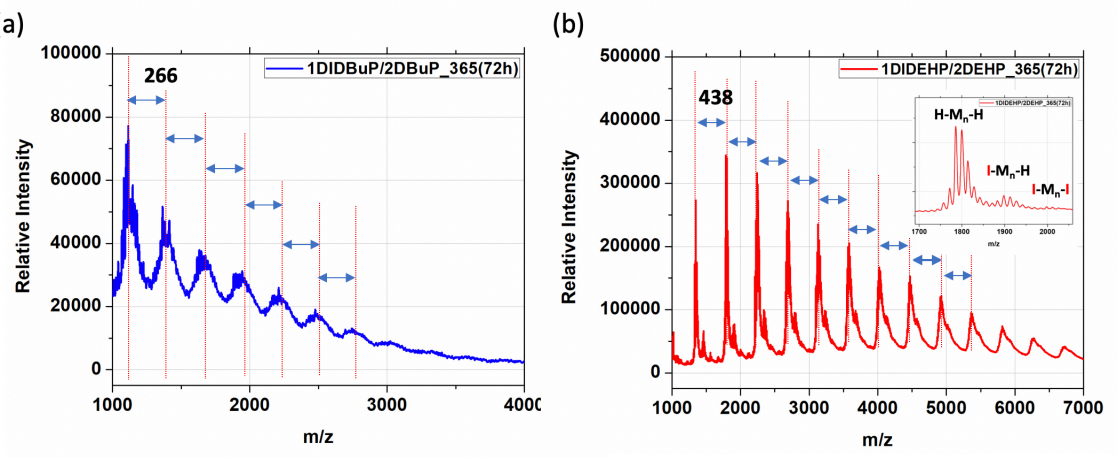

Figure 2.9. MALDI-TOF results of the photopolymerization of (a) DBuProDOT and (b) DEHProDOT.

Feasible reduction in oxidation potential of conjugated oligomers by hydrogen iodide (HI) doping can stimulate the photo-dissociation of carbon-iodine bonds at the chain ends, promoting chain extension from the conjugated oligomers. This implies that the radical states of the growing chain are preferred to the reversible deactivation by the recovery of living groups (C-I) as the conjugation is extended. At the same time, the photogenerated iodine radicals readily transform to hydrogen iodide as explained in Figure 2.4, resulting in the depletion of iodine species by the long-term UV irradiation. Continuous UV irradiation does not lead to additional chain extension of the oligomers, rather the growing chains are liable to terminate with carbon-hydrogen bonds by protonation. The absence of living groups at the chain ends is responsible for the termination of chain growth.

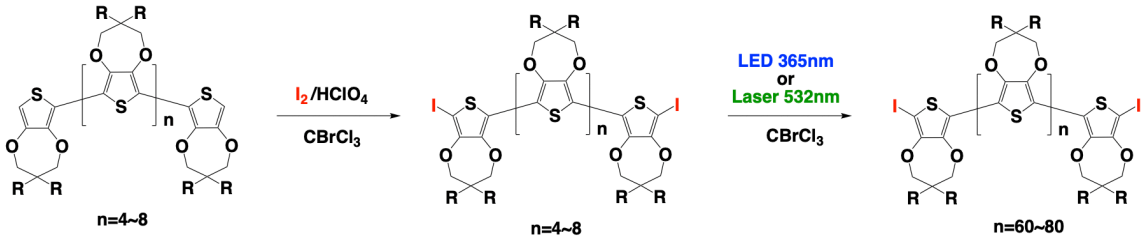

Figure 2.10. Schematic showing the recovery of carbon-iodine bonds at the oligomer chain ends and the photochemical coupling between the oligomer species to produce PProDOT with a higher molecular weight.

Electrophilic halogenation of the growing chains with newly replenished iodine sources is a promising strategy to resume the chain propagation. Recovery of living features of carbon-iodine bonds at the end of growing chains was pursued by adding iodine (I_2) and perchloric acid ($HClO_4$) to catalyze iodine substitution of the growing chain ends.[55] The achieved iodination of the oligomer chain ends was confirmed by MALDI-TOF analysis as one can see in Figure 2.11. While DEHProDOT oligomers have mainly carbon-hydrogen bonds at the chain ends, the iodinated oligomers having I/H and I/I end groups are observed after the iodine replenishment. Although not all oligomer species are iodinated, continuous carbon-iodine bond recovery by the electrophilic halogenation is anticipated in the iodine-rich solution. We assumed that if the iodinated oligomers successfully resume the photochemical reaction by additional light irradiation, the chain growth would continue to yield higher molecular weight species as described in Figure 2.10. The additional chain growth was examined by GPC analysis before and after photoirradiation of the iodinated oligomers.

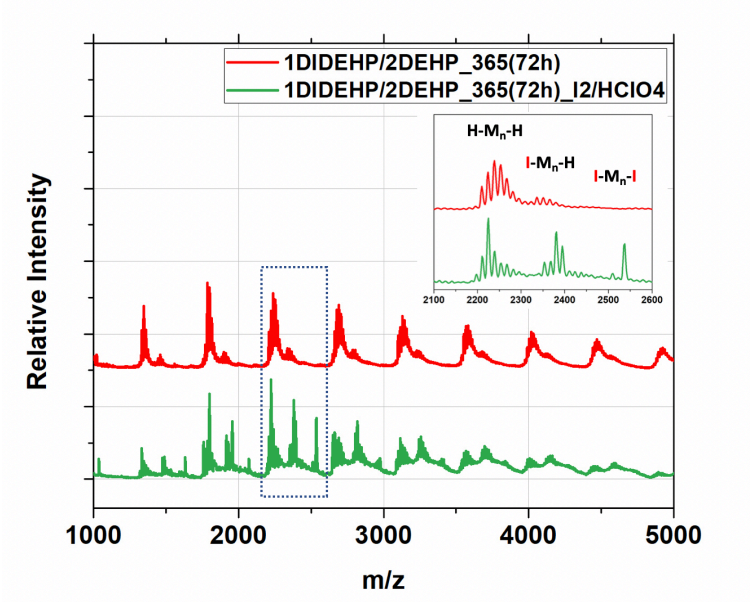

Figure 2.11. The MALDI-TOF results before and after iodination of DEHProDOT oligomers with the addition of iodine/chloroform solution and perchloric acid ($HClO_4$), followed by stirring for 3 hours and extra iodine washing with sodium thiosulfate.

The iodinated oligomers irradiated with 365nm LED light, however, turned out to undergo photodegradation to yield monomer or dimer species as depicted in Figure 2.12(a). Photodegradation of conjugated polymers is largely affected by the light intensity and wavelength, not to mention the presence of oxygen in the system.[56–58] Photodissociation of conjugated backbone becomes more significant with increasing light intensity. Even though the oligomers recover carbon-iodine bonds at the chain ends, the absorbed photon energy from the 365nm UV light likely dissociate not only the C-I bonds to generate radicals but also conjugated backbones of growing chains.

A q-switched 532nm pulsed laser is a promising light source to overcome the photodegradation and continue the photopolymerization of the iodinated ProDOT oligomers. The high pulsed energy of the laser source with 10~10,000 W/mm^2 should be large enough to dissociate

carbon-iodine bonds considering that the energy of carbon-iodine bond is comparable to those of iodobenzenes (63.7 kcal/mol). In addition, the longer irradiation wavelength not only overlaps well with the absorption spectra of the ProDOT oligomers to excite them to promote C-I cleavage, but also lessens the photodegradation of the conjugated backbone. A photoexcited polymeric chain under continuous light absorption readily forms a peroxide radical intermediate in the presence of oxygen molecules, photo-oxidation, resulting in the polymer degradation, the major photodegradation of conjugated organic molecules.[52,56] In contrast, an excited conjugated molecule by a pulsed laser with a short pulse width of a few nanoseconds undergoes an emissive decay with a high quantum yield and recovers its ground state when the pulsed laser is in its longer incubation time up to 20 μs between every pulses than a typical fluorescence lifetime of conjugated polymers in a nanosecond regime.[52] It is also expected that a limited short excitation time by pulse laser for the growing chains prevents their photodegradation by impeding the production of singlet oxygen molecules.[59]

A solution of iodinated DEHProDOT oligomers was photopolymerized in the presence of I_2 and $HClO_4$ by a q-switched 532nm pulsed laser having 2mJ/cm^2 of pulsed energy and 10 Hz of repetition rates. As shown in Figure 2.12(b), the GPC trace reveals that the molecular weight of the iodinated ProDOT oligomers (24~28 minutes, M_n~3,000 g/mol) shifts to a higher molecular weight regime, 16~20 minutes, corresponding to M_n~ 29,500 g/mol and a narrow PDI of 1.35. It is intriguing that neither the photodegradation nor additional chain growth by the laser irradiation was observed after a longer irradiation time than 12 hours.

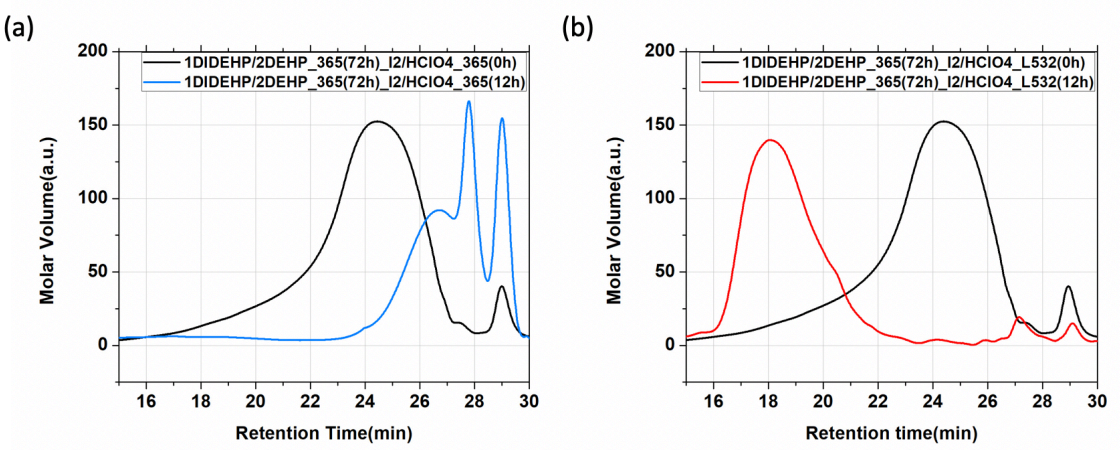

Figure 2.12. GPC trace of the photopolymerized samples from diiodinated DEHProDOT oligomers by (a) 365nm LED and (b) q-switched 532nm Laser irradiations. The products were prepared with iodine washing, drying, and annealing at 50°C for 3 hours.

We postulate that the limited molecular weight of resulting DEHProDOT polymers at ~ 30K stems from the depletion of carbon-iodine bonds by hydrogen substitution. The reaction mixture was replenished with additional iodine and illuminated further with the pulse laser. However, no more polymer growth was observed (Figure 2.13), implying that the recovered carbon-iodine chain ends no longer renders any additional chain growth. The end group analysis by means of MALDI-TOF before and after the laser irradiation in Figure 2.14 shows that the recovered carbon-iodine chain ends after the iodine replenishment are hydrogenated. These results suggest that the dissociation of C-I is dominant compared to the recovery of the carbon-iodine bonds even in the iodine rich condition and consequently the chain end carbon-iodine bonds are replaced by carbon-hydrogen bonds.

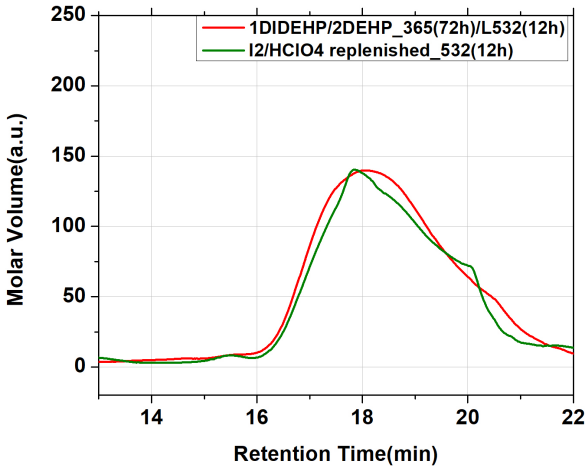

Figure 2.13. GPC results for poly(DEHProDOT) before and after q-switched 532nm Laser irradiations.

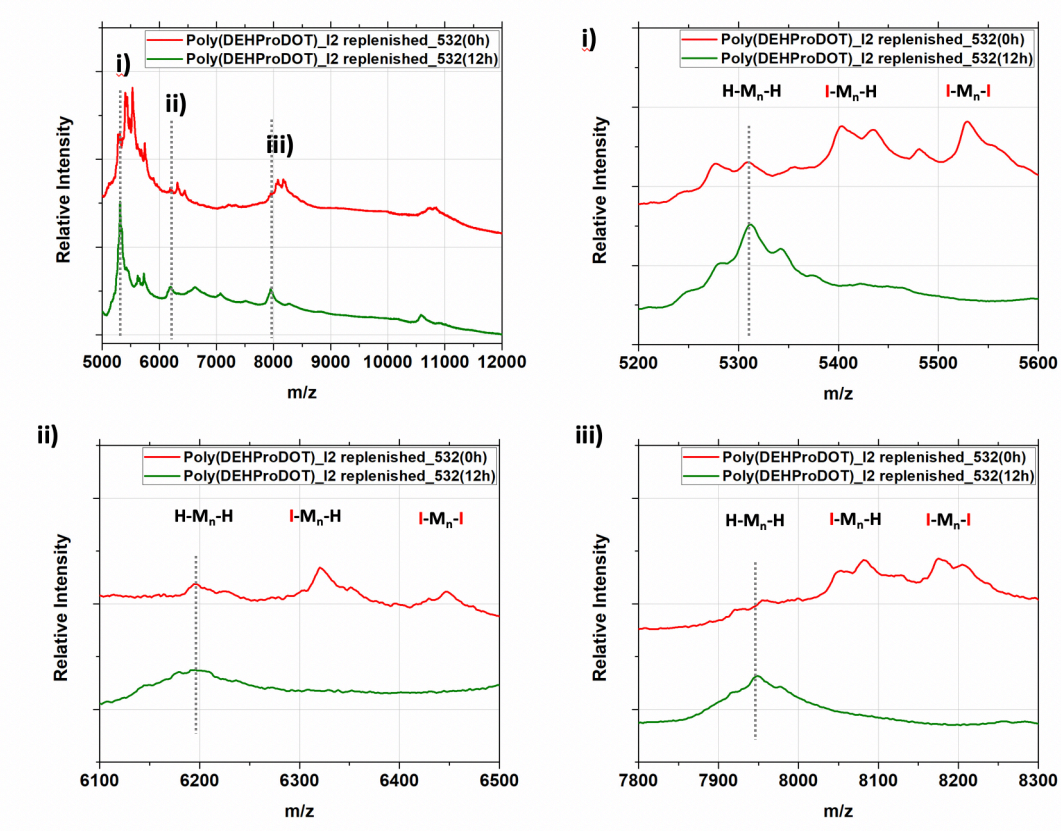

Figure 2.14. MALDI-TOF results of the iodine replenished poly(DEHProDOT) before and after pulse laser irradiation.

The photoarylation-based polymerization of DIDBuProDOT/DEHProDOT at an 1:2 molar feed ratio was carried out to investigate the copolymerization feasibility as depicted in Figure 2.15. The bulkier DEHProDOT had the GPC retention time at 29 minutes shorter than 30 minutes of DIDBuProDOT, which allows quantitative analysis of the monomer conversion ratio (Figure 2.16). The GPC traces showed that both DEHProDOT and DIDBuProDOT are consumed together to form ProDOT oligomer chains under UV-induced photoarylation. It also exhibited a controlled radical polymerization behavior showing a linear increase in molecular weight with monomers conversion as well as low polydispersity (<1.30) until most of DIDBuProDOT are depleted. This implies that the activation and deactivation of the living groups (C-I) of the growing chains are efficient through the oligomer regime. It is noteworthy that the depletion of DIDBuProDOT monomers, the radical source, is accompanied by the decrease in the molecular weight of ProDOT oligomers (from 72 hours to 96 hours in Figure 2.16(a)). It is believed that low oxidation potential of the oligomeric products in solution, when the oligomer chain ends fail to retain C-I bonds by shortage of iodine species at the depletion of DIDBuProDOT, is responsible for the photodegradation by additional UV irradiation. The same trend was also observed in the copolymerization of DIDBuProDOT/DEHProDOT with different monomer feed ratios (Figure 2.17).

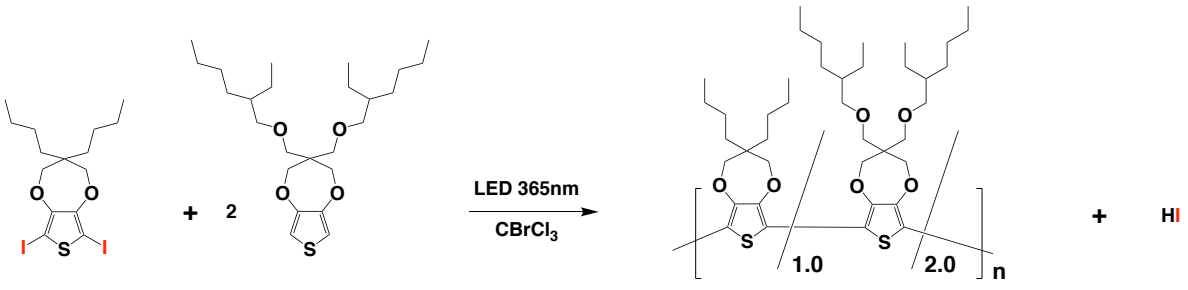

Figure 2.15. Schematic showing photoarylation based copolymerization for poly(DBuProDOT-co-DEHProDOT).

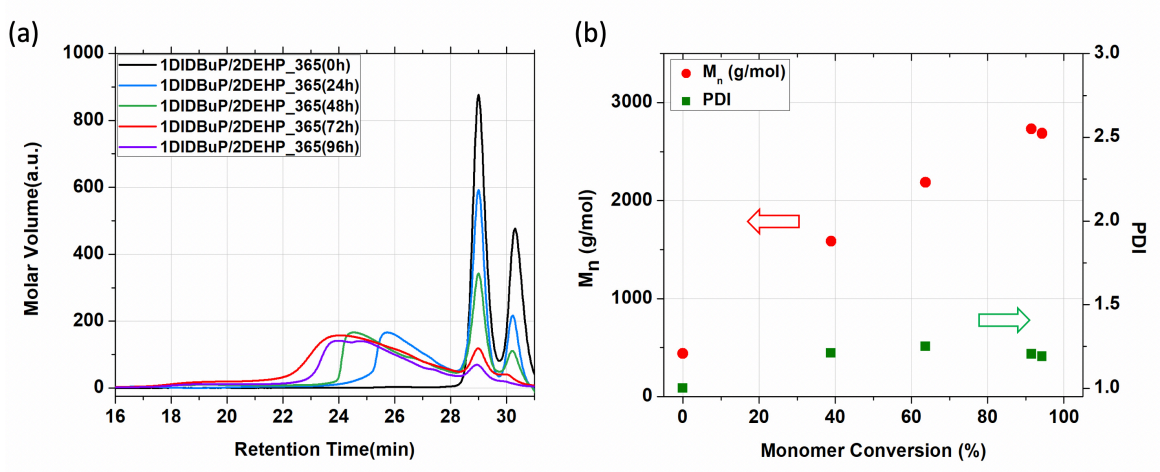

Figure 2.16. Characterization of DBuProDOT/DEHProDOT copolymers by (a) GPC results and (b) M_n and PDI as a function of monomer conversion. Retention time of monomers: DEHProDOT (29 minutes) and DIDBuProDOT (30 minutes).

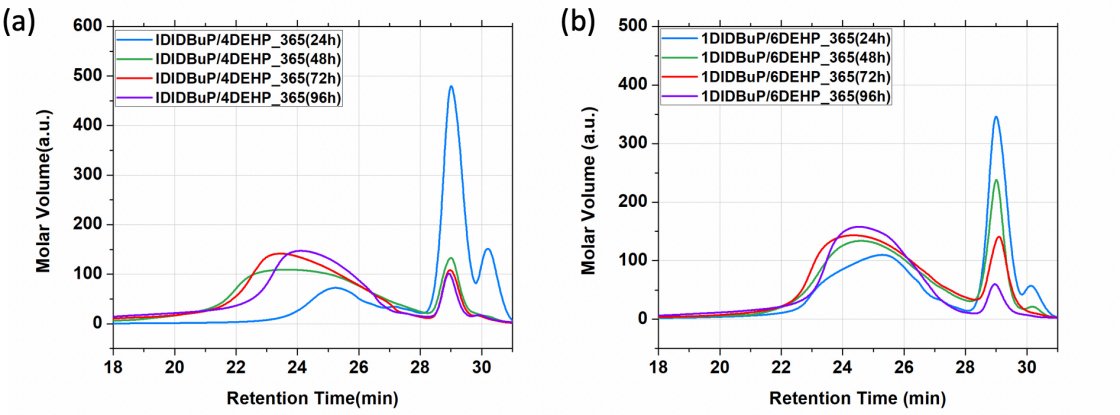

Figure 2.17. GPC traces of the photopolymerized ProDOT products by 365nm LED irradiation with different monomer feed ratios of DIDBuProDOT/DEHProDOT (a) 1:4 and (b) 1:6.

The oligomers produced by the homo- and co-polymerization were characterized by ^{1}H-NMR ($CDCl_3$) after the purification by Soxhlet extraction with methanol (Figures 2.18 and 2.19). The broader spectra of the samples than those of their monomers are comparable to the ^{1}H-NMR spectra of poly(DBuProDOT)[12] and poly(DEHProDOT)[39] prepared by organometallic pathways.

The repeating ProDOT units have different chemical shifts depending on the side chains. The CH_2 shifts at 3.94 and 4.11 ppm are assigned to 2,4 positions of the propylenedioxy moiety of DBuProDOT and DEHProDOT, respectively. While a butyl side chain has broad chemical shifts at CH_2 (1.25 ppm) and CH_3 (0.88 ppm), a diethylhexylmethoxy side chain has additional CH_2 (3.70~3.15 ppm) and CH (1.48 ppm) shifts originated from the methoxy and branched molecular structures, respectively.

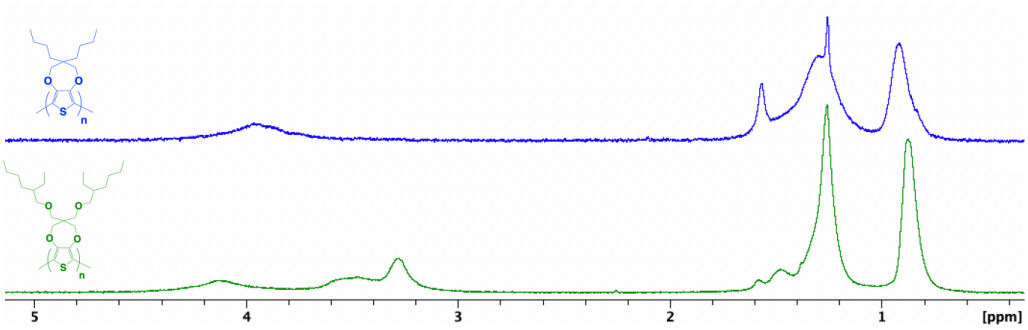

Figure 2.18. ^{1}H-NMR spectra of photopolymerized DBuProDOT and DEHProDOT oligomers.

Chemical composition of the copolymers of DBuProDOT and DEHProDOT was analyzed by NMR. As depicted in Figure 2.19, the chemical shifts in 2.8~4.4 ppm assigned to the propylene dioxy moieties can be deconvoluted into two different signals originated from the repeating units of DBuProDOT and DEHProDOT. As shown in Figure 2.20, the composition of the repeating units of DBuProDOT and DEHProDOT was determined by the integration ratio among the chemical shifts of (1) CH_2 in DBuProDOT and DEHProDOT, (2) CH_2 of the dimethoxy moiety of DEHProDOT, and (3) CH of the branched ethylhexyl side chain of DEHProDOT. The results show that the actual composition of the two monomers in the copolymers at the monomer conversion larger than 90% is consistent with the monomer feeding ratios of 1:2, 1:4, and 1:6.

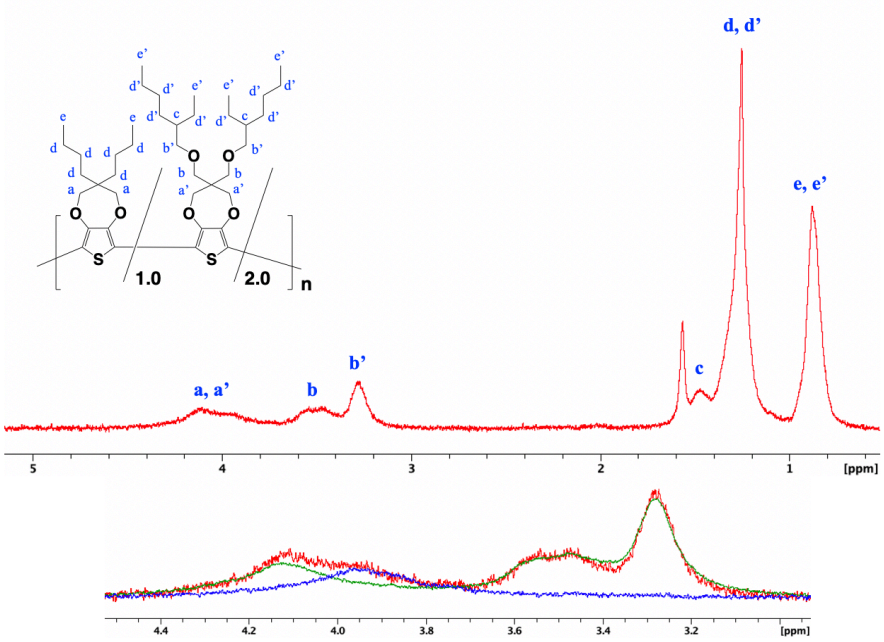

Figure 2.19. ^{1}H-NMR spectra of the photopolymerized copolymers of DBuProDOT and DEHProDOT.

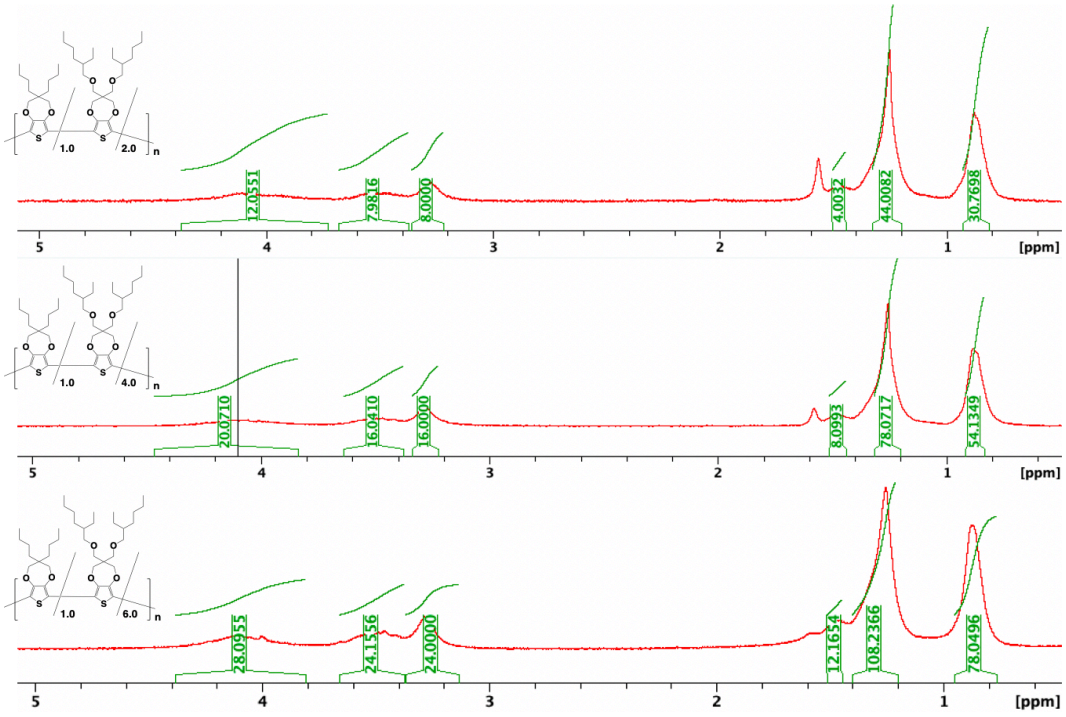

Figure 2.20. ^{1}H-NMR spectra of the copolymerized oligomers from DBuProDOT and DEHProDOT with different monomer feed ratios (1:2, 1:4, and 1:6).

After adding iodine (I_2) and perchloric acid ($HClO_4$) to the copolymer oligomers of DBuProDOT and DEHProDOT, we switched the light source to the 532nm pulse laser. Photopolymerization of the resulting diiodinated copolymer oligomers showed a gradual consumption of the oligomers (M_n=2,800 g/mol, PDI=1.20) and a simultaneously increasing peak corresponding to a larger molecular weight polymer (M_n=27,000 g/mol, PDI=1.25) in the GPC analysis shown in Figure 2.21. The GPC result is consistent with that of the photopolymerized homopolymer, poly(DEHProDOT), in Figure 2.12(b). The appearance and increasing amount of the larger molecular polymer having the same elution time rather than gradual increase in the molecular weight is apparently different from the conventional chain growth mechanism but is commonly observed in coupling reactions[60,61] between oligomeric or polymeric species or in the click reaction[62] of a grafted molecule. While the molecular weight of the coupled products should be doubled by each coupling reaction, almost 10 times increase in the molecular weight was achieved by the laser assisted photopolymerization. It is believed that the chain extension to both ends of ProDOT oligomers renders the higher molecular weight polymers.

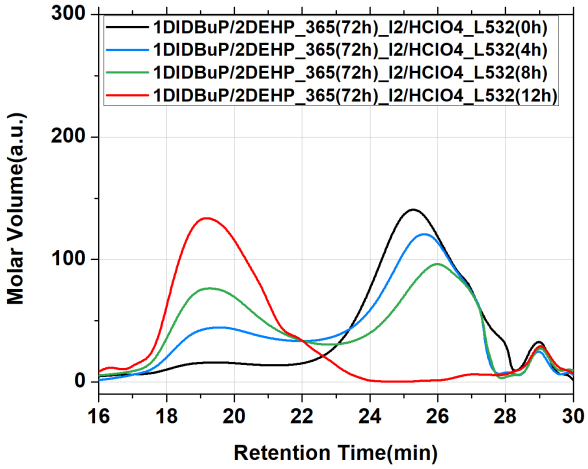

Figure 2.21. GPC traces of the photopolymerized samples from iodinated DBuProDOT/DEHProDOT by q-switched 532nm laser irradiation.

2.4 Conclusion

In summary, we have successfully developed a novel one-pot photo-mediated polymerization of ProDOT derivatives to achieve a conjugated polymer with a high molecular weight (M_n=27,000 g/mol) and narrow polydispersity (PDI=1.20). The polymerization initiated by photoarylation of diiodo-ProDOT and ProDOT under 365nm LED irradiation yields poly(ProDOT) oligomers with an excellent conversion ratio. During the photoarylation, the growing chain ends are replaced from C-I to C-H bonds by hydrogen substitution, which limits the molecular weight of the produced oligomers. However, further chain growth was achieved through the recovery of carbon-iodine bonds by iodine replenishment and adapting a q-switched 532nm pulse laser as a light source. The mechanism of the devised photo-polymerization was investigated by employing UV-vis absorption, GPC, and MALDI-TOF analysis on the polymerization products. Copolymers having the same monomer composition to the monomer feeding ratio were also successfully achieved, demonstrating feasible molecular structure engineering. To the best of our knowledge, this is the first systematic investigation on photo-polymerization of conjugated polymers in solution.

2.5 Synthesis

2.5.1 Synthetic schemes

The following thiophene derivatives were synthesized through the experimental procedures as presented below.

compound 1 and 2

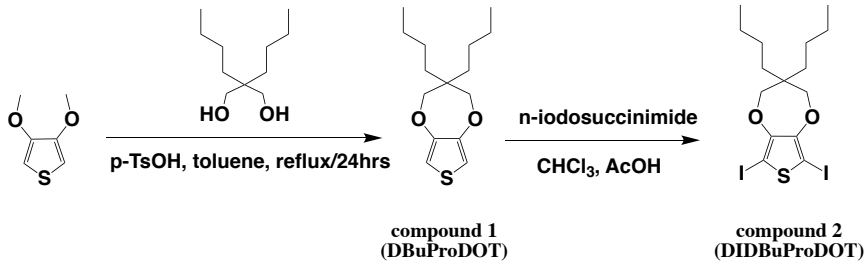

Figure 2.22. Synthetic scheme for DBuProDOT and DIDBuProDOT.

i) compound 1. 3,4-(3,3'-dibutylpropylenedioxy)thiophene (DBuProDOT)

6g of 3,4-dimethoxythiophene (41.61mmol, 1eq) and 10.187g of 2,2-dibutyl-1,3-propanediol (54.10mmol, 1.3eq) was dissolved in 200ml of toluene with 500mg of p-toluenesulfonic acid. The solution was refluxed at 120°C and the methanol produced by a transetherification of the reactants was removed by type 4A molecular sieves filled in a soxhlet extractor. The mixture was quenched by water after 24 hours reflux, extracted in ethyl acetate, then washed with brine and dried over $MgSO_4$. After evaporating the solvent with a rotary evaporator, the residue was purified by column chromatography with the elution of methylene chloride/hexane (1:4) to give 3,4-(3,3'-dibutylpropylenedioxy) thiophene (DBuProDOT) (69%, 7.70g). ^{1}H-NMR (300MHz, $CDCl_3$); 6.42(s, 2H), 3.85 (s, 4H), 1.46-1.15 (m, 12H), 0.98-0.86 (t, 6H)

ii) compound 2. 2,5-diiodo-[3,4-(3,3'-dibutylpropylenedioxy)]thiophene (DIDBuProDOT)

5g of 3,4-(3,3'-dibutylpropylenedioxy)thiophene (DBuProDOT) (18.63mmol, 1eq) was dissolved in chloroform and stirred with 9.22g of n-iodosuccinimide (40.98mmol, 2.2eq) with a few drops of acetic acid. The mixture was quenched with DI water, washed with sodium thiosulfate to remove excess iodine, and dried over $MgSO_4$, followed by the evaporation in vacuo. The residue was purified with the elution of methylene chloride and hexane (1:8) to yield DIDBuProDOT (85%, 12.68g), ^{1}H-NMR (300MHz, $CDCl_3$); 3.92 (s, 4H), 1.46-1.15 (m, 12H), 0.98-0.86 (t, 6H)

compound 3 and 4

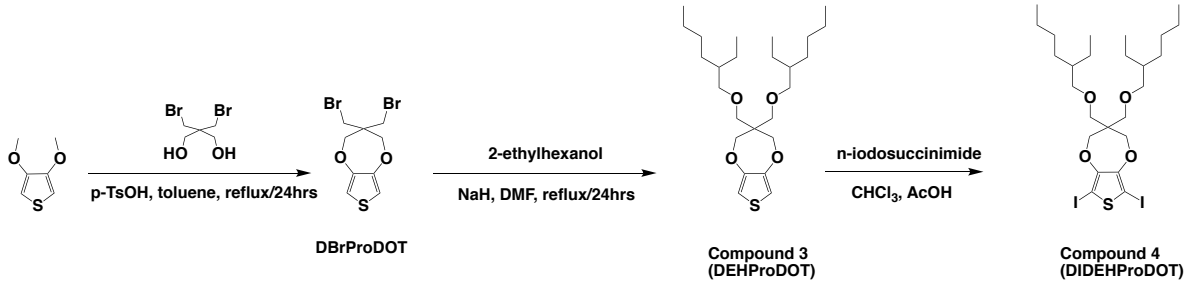

Figure 2.23. Synthetic scheme for DEHProDOT and DIDEHProDOT.

Compound 3 was synthesized through the experimental procedures as presented in the literature.[63]

i) 3,4-[2,2'-bis(bromomethyl)propylenedioxy]thiophene (DBrProDOT)

5g of 3,4-dimethoxythiophene (34.68mmol, 1eq) and 10.9g of 2,2-Bis(bromomethyl)-1,3-propanediol (41.61mmol, 1.2eq) was dissolved in 200ml of toluene with 500mg of p-toluenesulfonic acid. The solution was refluxed at 120^{o}C and the methanol produced by a transetherification of the reactants was removed by type 4A molecular sieves filled in a soxhlet extractor. The mixture was quenched by water after 24 hours reflux, extracted in ethyl acetate, then washed with brine and dried over $MgSO_4$. After evaporating the solvent with a rotary evaporator, the residue was purified by column chromatography with the elution of methylene

chloride/hexane (1:2) to give 3,4-(2,2'-bis(bromomethyl)propylenedioxy)thiophene (DBrProDOT) (45%, 5.34g), ^{1}H-NMR (300MHz, $CDCl_3$); 6.50(s, 2H), 4.10 (s, 4H), 3.62 (s, 4H)

ii) 3,4-[(2,2'-dimethoxyethylhexyl)propylenedioxy]thiophene (DEHProDOT)

2.924g of NaH (60% with oil, 73.09mmol, 5.0eq) were added to 250ml round bottom flask and purged by vacuum and filled with argon 3 times. After adding 100ml of anhydrous DMF at 0^{o}C, the cooled solution was stirred at room temperature for 2 hours. 4.19g of 2-ethylhaxanol (32.164mmol, 2.2eq) dissolved in 20ml of DMF and was added to the NaH solution dropwise and allowed to stir for 6 hours at room temperature. The solution of DBrProDOT (5g, 14.62mmol, 1eq)/DMF(20ml) was added to the mixture. The solution was refluxed at 80^{o}C for 24 hours and cooled down to room temperature, then quenched with 1N HCl dropwise, followed by the extraction with diethyl ether 3 times. The organic layer was washed 1N HCl and brine, then dried with $MgSO_4$ and evaporated under vacuo. The residue was purified by column chromatography with the elution of methylene chloride/hexane (1:4) to give DEHProDOT. (74%, 5.54g), ^{1}H-NMR (300MHz, $CDCl_3$); 6.45(s, 2H), 4.03(s,4H), 3.48(s, 4H), 3.28(s, 4H), 1.48(s, 2H), 1.35-1.15(m, 16H), 0.95-0.80 (m, 12H)

iii) 2,5-diiodo-[3,4-(2,2'-dimethoxyethylhexyl)propylenedioxy]thiophene (DIDEHProDOT)

5g of DEHProDOT) (11.35mmol, 1eq) was dissolved in chloroform and stirred with 5.615g of n-iodosuccinimide (24.96mmol, 2.2eq) with a few drops of acetic acid. The mixture was quenched with DI water, washed with sodium thiosulfate to remove excess iodine, and dried over $MgSO_4$, followed by the evaporation in vacuo. The residue was purified with the elution of methylene chloride and hexane (1:8) to yield DIDEHProDOT (85%, 6.678g), ^{1}H-NMR (300MHz, $CDCl_3$); 4.03(s,4H), 3.48(s, 4H), 3.28(s, 4H), 1.48(s, 2H), 1.35-1.15(m, 16H), 0.95-0.80 (m, 12H)

2.5.2 ^{1}H-NMR spectra of ProDOT derivatives

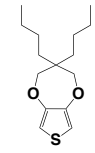

compound 1
(DBuProDOT)

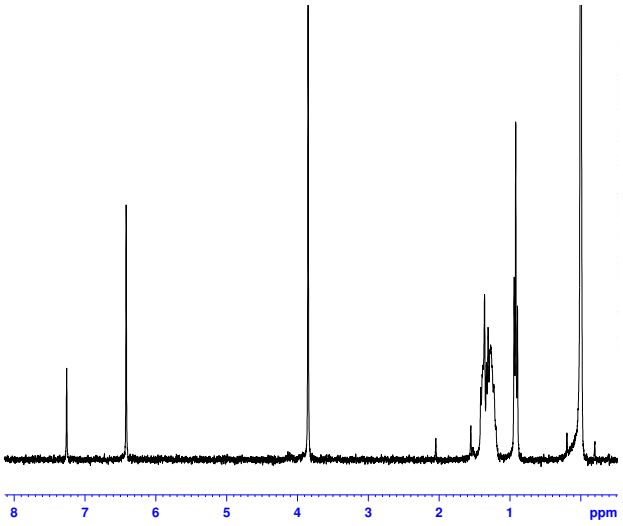

Figure 2.24. ^{1}H-NMR spectrum of 3,4-(3,3'-dibutylpropylenedioxy)thiophene (DBuProDOT). ^{1}H-NMR (300MHz, $CDCl_3$); 6.42(s, 2H), 3.85 (s, 4H), 1.46-1.15 (m, 12H), 0.98-0.86 (t, 6H)

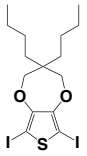

compound 2
(DIDBuProDOT)

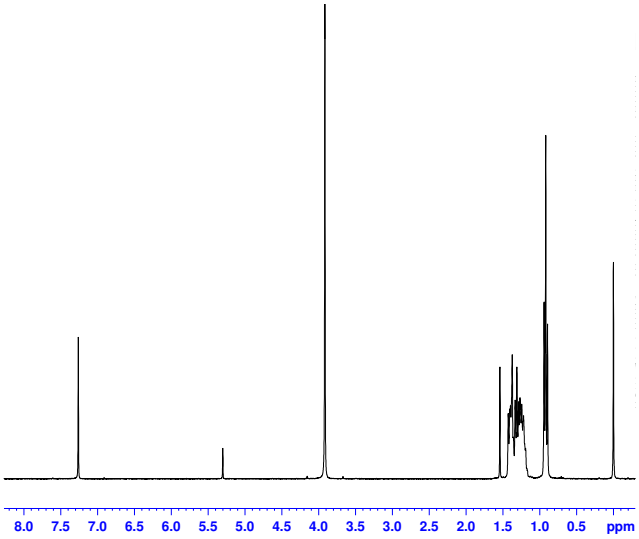

Figure 2.25. ^{1}H-NMR spectrum of 2,5-diiodo-[3,4-(3,3'-dibutylpropylenedioxy)] thiophene (DIDBuProDOT). ^{1}H-NMR (300MHz, $CDCl_3$); 3.92 (s, 4H), 1.46-1.15 (m, 12H), 0.98-0.86 (t, 6H)

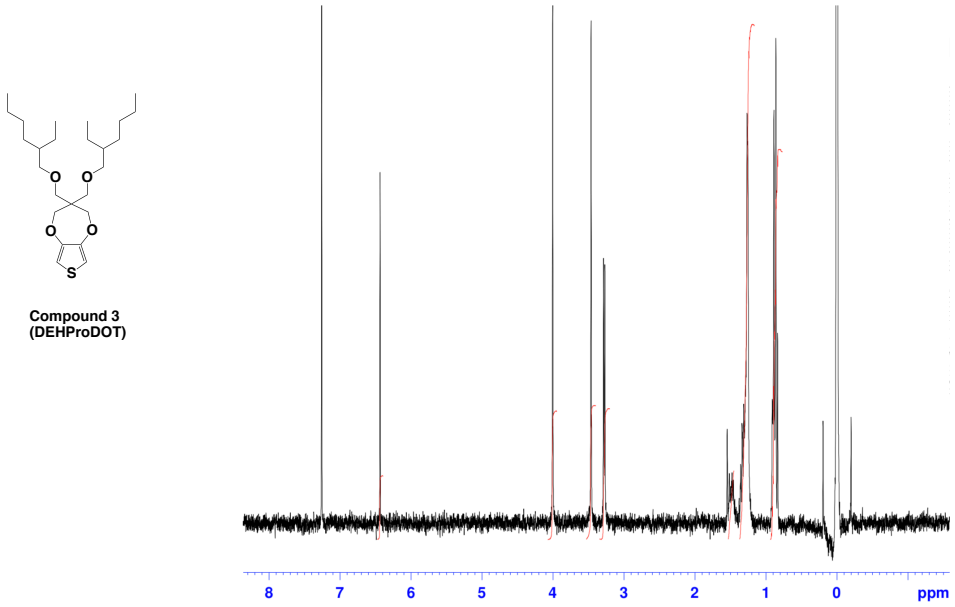

Figure 2.26. ^{1}H-NMR spectrum of 2,5-diiodo-3,4-[(2,2'-dimethoxyethylhexyl) propylenedioxy] thiophene (DEHProDOT). ^{1}H-NMR (300MHz, $CDCl_3$); 6.45(s, 2H), 4.03(s,4H), 3.48(s, 4H), 3.28(d, 4H), 1.48(s, 2H), 1.35-1.15(m, 16H), 0.95-0.80 (m, 12H)

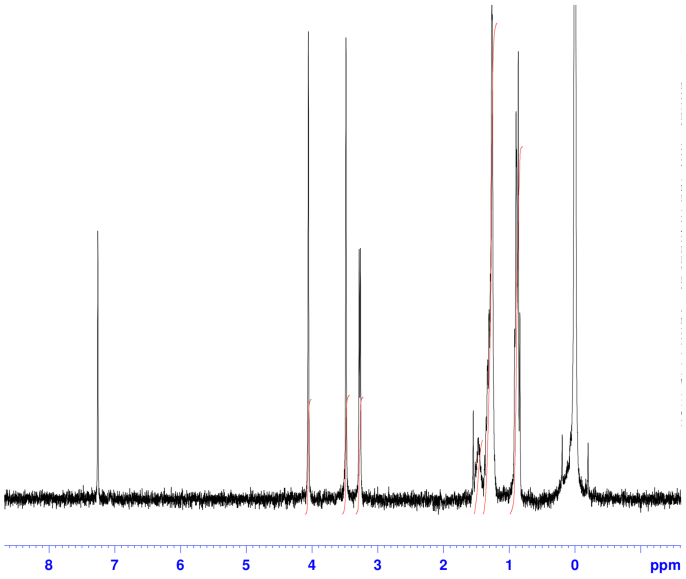

Figure 2.27. ^{1}H-NMR spectrum of 2,5-diiodo-[3,4-(2,2'-dimethoxyethylhexyl) propylenedioxy] thiophene (DIDEHProDOT). ^{1}H-NMR (300MHz, $CDCl_3$); 4.03(s,4H), 3.48(s, 4H), 3.28(d, 4H), 1.48(s, 2H), 1.35-1.15(m, 16H), 0.95-0.80 (m, 12H).

2.6 References

1. Jonas, F., Krafft, W., AG, B. EP440957. (1990).
2. Jonas, F., Krafft, W., Muys, B. Poly(3,4-ethylenedioxythiophene): Conductive coatings, technical applications and properties. in *Macromolecules Symposium* 169–173 (1995).
3. Heywang, B. G., Jonas, F. Poly(alkylenedioxythiophene)s-New, Very Stable Conducting Polymers. *Adv. Mater.* **4,** 116–118 (1992).
4. Im, S. G., Kusters, David, Choi, Wonjae, Baxamusa, Salmaan H., Sanden, M.C.M, Gleason, Karan K. Conformal coverage of poly(3,4-ethylenedioxythiophene) films with tunable nanoporosity via oxidative chemical vapor deposition. *ACS Nano* **2,** 1959–1967 (2008).
5. Merker, U., Kirchmeyer, S., Wussow, K. WO2004/088672. (2004).
6. Wang, Y., Lucht, B. L., Euler, W. B. Investigation of the oxidative coupling polymerization of 3-alkylthiophenes with iron(III) chloride. in *American Chemical Society, Polymer Preprints, Division of Polymer Chemistry* **43,** 1160 (2002).
7. Levermore, P. A., Chen, L., Wang, X., Das, R., Bradley, D. D. C. Highly conductive poly(3,4-ethylenedioxythiophene) films by vapor phase polymerization for application in efficient organic light-emitting diodes. *Adv. Mater.* **19,** 2379–2385 (2007).
8. Admassie, S., Zhang, Fengling, Manoj, A.G., Svensson, Mattias, Andersson, Mats R., Inganas, Olle. A polymer photodiode using vapour-phase polymerized PEDOT as an anode. *Sol. Energy Mater. Sol. Cells* **90,** 133–141 (2006).
9. Groenendaal, L., Zotti, G., Aubert, P. H., Waybright, S. M., Reynolds, J. R. Electrochemistry of poly(3,4-alkylenedioxythiophene) derivatives. *Adv. Mater.* **15,** 855–879 (2003).

10. Xia, J., Masaki, N., Lira-Cantu, M., Kim, Y., Jiang, K., Yanagida, S. Influence of doped anions on poly(3,4-ethylenedioxythiophene) as hole conductors for iodine-free solid-state dye-sensitized solar cells. *J. Am. Chem. Soc.* **130,** 1258–1263 (2008).

11. Yamamoto, T., Shiraishi, K., Abla, M., Yamaguchi, I., Groenendaal, L. B. Neutral poly(3,4-ethylenedioxythiophene-2,5-diyl)s: Preparation by organometallic polycondensation and their unique p-doping behavior. *Polymer (Guildf).* **43,** 711–719 (2001).

12. Welsh, D. M. Kloeppner, Leroy J., Madrigal, Luis, Pinto, Mauricio R., Thompson, Barry C., Schanze, Kirk S. Abboud, Khalil A., Powell, David, Reynolds, John R. Regiosymmetric dibutyl-substituted poly(3,4-propylenedioxythiophene)s as highly electron-rich electroactive and luminescent polymers. *Macromolecules* **35,** 6517–6525 (2002).

13. Shiraishi, K., Kanbara, T., Yamamoto, T., Groenendaal, L. Preparation of a soluble and neutral alkyl derivative of poly(3,4-ethylene- dioxythiophene) and its optical properties. *Polymer (Guildf).* **42,** 7229–7232 (2001).

14. Miyakoshi, R., Yokoyama, A., Yokozawa, T. Catalyst-transfer polycondensation. Mechanism of Ni-catalyzed chain-growth polymerization leading to well-defined poly(3-hexylthiophene). *J. Am. Chem. Soc.* **127,** 17542–17547 (2005).

15. Welsh, D. M., Kumar, A., Meijer, E. W., Reynolds, J. R. Enhanced contrast ratios and rapid switching in electrochromics based on poly(3,4-propylenedioxythiophene) derivatives. *Adv. Mater.* **11,** 1379–1382 (1999).

16. Romero, D. B., Schaer, M., Zuppiroli, L., Cesar, B., François, B. An iodine-doped polymer light-emitting diode. *Appl. Phys. Lett.* **67,** 1659 (1995).

17. Adachi, C., Baldo, M. A., Thompson, M. E., Forrest, S. R. Molecular organic light-emitting diodes using highly conducting polymers as anodes. *J. Appl. Phys.* **90,** 5048–5051 (2001).

18. Setiadi, D., He, Z., Hajto, J., Binnie, T. D. Application of a conductive polymer to self-absorbing ferroelectric polymer pyroelectric sensors. *Infrared Phys. Technol.* **40,** 267–278 (1999).

19. Yoon, H., Chang, M., Jang, J. Formation of 1D poly(3,4-ethylenedioxythiophene) nanomaterials in reverse microemulsions and their application to chemical sensors. *Adv. Funct. Mater.* **17,** 431–436 (2007).

20. Meskers, S. C. J., van Duren, J. K. J., Janssen, R. A. J., Louwet, F., Groenendaal, L. Infrared Detectors with Poly(3,4-ethylenedioxy thiophene)/Poly(styrene sulfonic acid) (PEDOT/PSS) as the Active Material. *Adv. Mater.* **15,** 613–616 (2003).

21. Fors, B. P., Hawker, C. J. Control of a living radical polymerization of methacrylates by light. *Angew. Chem. Int. Ed.* **51,** 8850–8853 (2012).

22. Treat, N. J. Sprafke, H. Kramer, J.W., Clark, P.G., Barton, B.E., Alaniz, J.R., Fors, B.P., Hawker, C.J. Metal-free atom transfer radical polymerization. *J. Am. Chem. Soc.* **136,** 16096–16101 (2014).

23. Xu, J., Jung, K., Atme, A., Shanmugam, S., Boyer, C. A robust and versatile photoinduced living polymerization of conjugated and unconjugated monomers and its oxygen tolerance. *J. Am. Chem. Soc.* **136,** 5508–5519 (2014).

24. Aydogan, B., Yagci, Y., Toppare, L., Jockusch, S., Turro, N. J. Photoinduced electron transfer reactions of highly conjugated thiophenes for initiation of cationic polymerization and conjugated polymer formation. *Macromolecules* **45,** 7829–7834 (2012).

25. Yagci, Y., Yilmaz, F., Kiralp, S., Toppare, L. Photoinduced polymerization of thiophene using iodonium salt. *Macromol. Chem. Phys.* **206,** 1178–1182 (2005).

26. Yagci, Y., Jockusch, S., Turro, N. J. Mechanism of photoinduced step polymerization of thiophene by onium salts: Reactions of phenyliodinium and diphenylsulfinium radical cations with thiophene. *Macromolecules* **40,** 4481–4485 (2007).

27. Laguitton-Pasquier, H., Martre, A., Deronzier, A. Photophysical properties of soluble polypyrrole-polypyridyl-ruthenium(II) complexes. *J. Phys. Chem. B* **105,** 4801–4809 (2002).

28. Segawa, H., Shimidzu, T., Honda, K. A novel photo-sensitized polymerization of pyrrole. *J. Chem. Soc. Chem. Commun.* 132–133 (1989).

29. Teshima, K., Yamada, K., Kobayashi, N., Hirohashi, R. Photopolymerization of aniline with a tris(2,2′-bipyridyl)ruthenium complex-methylviologen polymer bilayer electrode system. *Chem. Commun.* 829–830 (1996).

30. Natarajan, S., Kim, S. H. Photochemical oligomerization pathways in 2,5-diiodothiophene film. *J. Photochem. Photobiol. A Chem.* **188,** 342–345 (2007).

31. Natarajan, S., Kim, S. H. Photochemical conversion of 2,5-diiodothiophene condensed on substrates to oligothiophene and polythiophene thin films and micro-patterns. *Thin Solid Films* **496,** 606–611 (2006).

32. Wochnowski, C., Metev, S. UV-laser-assisted synthesis of iodine-doped electrical conductive polythiophene. in *Applied Surface Science* **186,** 34–39 (2002).

33. Dauria, M. & Mauriello, G. SYNTHESIS AND PHOTOCHEMICAL PROPERTIES OF NITROTHIENYL DERIVATIVES. *Photochem. Photobiol.* **60,** 542–545 (1994).

34. D'Auria, M., Distefano, C., D'Onofrio, F., Mauriello, G., Racioppi, R. Photochemical substitution of polyhalogenothiophene and halogenothiazole derivatives. *J. Chem. Soc. Perkin Trans.* **1**, 3513–3518 (2000).

35. D'Auria, M. Photochemical and Photophysical Behavior of Thiophene. *Adv. Heterocycl. Chem.* **104,** 127–390 (2011).

36. Wolf, W., Kharasch, N. Photolysis of Iodoaromatic Compounds in Benzene. *J. Org. Chem.* **30,** 2493–2498 (1965).

37. D'Auria, M., De Mico, A., D'Onofrio, F., Piancatelli, G. Italian Pat. Appl., 479799A90. (1990).

38. Lin, C., Endo, T., Takase, M., Iyoda, M., Nishinaga, T. Structural, Optical, and Electronic Properties of a Series of 3,4-Propylenedioxythiophene Oligomers in Neutral and Various Oxidation States. *J. Am. Chem. Soc* **133,** 11339–11350 (2011).

39. Reeves, B. D., Grenier, C.R., Argun, A.A., Cirpan, A., McCarley, T.D., Reynolds, J.R. Spray coatable electrochromic dioxythiophene polymers with high coloration efficiencies. *Macromolecules* **37,** 7559–7569 (2004).

40. Nishinaga, T., Sotome, Y. Stable Radical Cations and Their π-Dimers Prepared from Ethylene-and Propylene-3,4-dioxythiophene Co-oligomers: Combined Experimental and Theoretical Investigations. *J. Org. Chem* **82,** 7245-7253 (2017).

41. Herrera, O. S., Nieto, J. D., Olleta, A. C., Lane, S. I. The photoinduced reaction of 2-iodothiophene in solutions of n-heptane, dichloromethane and methanol. *J. Phys. Org. Chem.* **24,** 398–406 (2011).

42. Fox, R. J., Evans, F. W., Szwarc, M. Abstraction of Halogen Atoms by Methyl Radicals Part 2.--Reaction $RX+CH_3+R+XCH_3$ for R Different from Methyl. *Trans. Faraday Soc.* 1915–1927 (1961).

43. Tedder, J. M. The interaction of free radicals with saturated aliphatic compounds. *Quart. Rev. Chem. Soc.* **14,** 336–356 (1960).

44. Elisei, F., Latterini, L., Aloisi, G., D 'auria, M. Photoinduced Substitution Reactions in Halothiophene Derivatives. Steady State and Laser Flash Photolytic Studies. *J. Phys. Chem* **99,** 5365–5372 (1995).

45. Tedder, J. M. The interaction of free radicals with saturated aliphatic compounds. *Q. Rev. Chem. Soc.* **14,** 336–356 (1960).

46. Masini, J.J., Collier, B. US4978435A. (1990).

47. Jeffries, A. T., Párkányi, C., Parkanyi, C. Photodebromination of Bromothiophenes. *Z. Naturforsch* **31,** 345–347 (1976).

48. Welsh, D. M., Kloeppner, Leroy J., Madrigal L. Pinto, M.R., Thomson, B.C., Schanze, K.S., Abboud, K.A., Powell, D., Reynolds, J.R. Regiosymmetric dibutyl-substituted poly(3,4-propylenedioxythiophene)s as highly electron-rich electroactive and luminescent polymers. *Macromolecules* **35,** 6517–6525 (2002).

49. Ingana, O., Lundstro, I., Gadegaard, N., Österbacka, R. Two-Dimensional Electronic Excitations in Self-Assembled Conjugated Polymer Nanocrystals. *Science* **287,** 839–842 (2000).

50. Heinemann, M. D., Maydell, K.V., Zutz, F., Kolny-Olesiak, J., Borchert, H., Riedel, I. Parisi, J. Photo-induced charge transfer and relaxation of persistent charge carriers in polymer/nanocrystal composites for applications in hybrid solar cells. *Adv. Funct. Mater.* **19,** 3788–3795 (2009).

51. Jiang, X. M., Osterbacka, R., Korovyanko, O., An, C.P., Horovitz, B., Janssen, R.A., Vardeny, Z.V. Spectroscopic Studies of Photoexcitations in Regioregular and Regiorandom Polythiophene Films. *Adv. Funct. Mater.* **12,** 587–597 (2002).

52. Neto, N. M. B., Silva, M. D. R., Araujo, P. T., Sampaio, R. N. Photoinduced Self-Assembled Nanostructures and Permanent Polaron Formation in Regioregular Poly(3-hexylthiophene). *Adv. Mater.* 170505 (2018).

53. Sage, A. G. Oliver, T.A., Murdock, D., Crow, M.B., Ritchie, G.A., Harvey, J.N., Ashfold, N.R. nσ* and πσ* excited states in aryl halide photochemistry: a comprehensive study of the UV photodissociation dynamics of iodobenzene. *Phys. Chem. Chem. Phys.* **13,** 8075-8093 (2011).

54. Bonillo, B., Swager, T. M. Chain-growth polymerization of 2-chlorothiophenes promoted by lewis acids. *J. Am. Chem. Soc.* **134,** 18916–18919 (2012).

55. Goldberg, Y., Alper, H. *Biphasic Electrophilic Halogenation of Activated Aromatics and Heteroaromatics with JV-Halosuccinimides Catalyzed by Perchloric Acid*. *J. Org. Chem* **58,** 3072-3075 (1993).

56. Hintz, H., Egelhaaf, H.J., Luer, L., Hauch, J., Peisert, H., Chasse, T. Photodegradation of P3HT-A Systematic Study of Environmental Factors. *Chem. Mater* **23,** 145–154 (2011).

57. Ohta, H., Koizumi, H. Mechanisms of photo-induced degradation of polythiophene derivatives: re-examination of the role of singlet oxygen. *Polym. Bull.* **74,** 2319–2330 (2017).

58. Abdou, A., Holdcroft, S. Mechanisms of Photodegradation of Poly(3-alkylthiophenes) in Solution. *Macromolecules* **26,** 2954–2962 (1993).

59. Neto, N. M. B., Silva, M. D. R., Araujo, P. T., Sampaio, R. N. Photoinduced Self-Assembled Nanostructures and Permanent Polaron Formation in Regioregular Poly(3-hexylthiophene). *Adv. Mater.* **30,** (2018).

60. Leophairatana, P., Samanta, S., De Silva, C. C., Koberstein, J. T. Preventing Alkyne-Alkyne (i.e., Glaser) Coupling Associated with the ATRP Synthesis of Alkyne-Functional

Polymers/Macromonomers and for Alkynes under Click (i.e., CuAAC) Reaction Conditions. *J. Am. Chem. Soc.* **139,** 3756–3766 (2017).

61. Carnicom, E. M., Abruzzese, J. A., Sidibe, Y., Myers, K. D., Tillman, E. S. Effect of trapping agent and polystyrene chain end functionality on radical trap-assisted atom transfer radical coupling. *Polymers (Basel).* **6,** 2737–2751 (2014).

62. Altintas, O., Yankul, B., Hizal, G., Tunca, U. A3-type star polymers via click chemistry. *J. Polym. Sci. Part A Polym. Chem.* **44,** 6458–6465 (2006).

63. Kerszulis, J.A., Amb, C.M., Dyer, A.L., Reynolds, J.R. Supporting Information, Follow the Yellow Brick Road-Structural Optimization of Vibrant Yellow to transmissive Electrochromic Conjugated Polymers. *Macromolecules*, **47**, 5462-5469 (2014)

Chapter 3. Facile One-pot Fabrication of Transparent Conducting Polymer Thin Films through Photo-arylation based UV Polymerization of Thiophene Derivatives

3.1 Introduction

Conjugated polymers are widely investigated for a number of electronic device applications such as organic photovoltaics[1–4], OLED[3,4], and electrochromic devices[5–7] owing to their readily tunable optical and electronic properties, large molecular design window, and easy and economic processability. In addition, highly durable and flexible properties of the doped polymeric semiconductors are desirable to manufacture electronic devices in a roll-to-roll wet coating system[2]. In order to achieve solution processability for the thin film device fabrication, researchers have designed and engineered a myriad of conjugated polymers having various side chains on their repeating units. Although the side chains, due to their good miscibility with organic solvents, render excellent solubility to conjugated molecules, their insulating volumes and steric hinderance to molecular packing also give rise to the decrease in electrical properties. Therefore, in order to realize desirable electrical performance, minimizing the side chain length and bulkiness while maintaining good solubility of the conjugated molecules is required for any wet coating process.

Poly(3,4-ethylenedioxythiophene) (PEDOT) is one of distinguished conducting polymers having excellent optical and electrical properties along with high stability. In parallel, the molecular structure of PEDOT without any side chain can allow high intermolecular packing density in thin films as a consequence of strong π-π stacking interaction between their conjugated backbones. However, PEDOT is not soluble in common organic solvents due to the absence of side chains. Therefore, it is desirable to conduct in-situ polymerization to form conducting PEDOT thin films from pre-deposited EDOT precursor molecules on a given substrate.

Electrochemical polymerization is an archetypical method to prepare transparent conducting thin films from EDOT-contained electrolytes. It is challenging, however, to control physical and chemical properties such as thickness, morphology, and film compositions in electro-polymerization. Moreover, applicable substrates to be deposited are limited to conducting electrodes such as ITO-coated glasses.[8] To overcome these drawbacks, halogen radical mediated in-situ polymerization of 2,5-dibromo-3,4-ethylenedioxythiophene[9] or chemical vapor deposition of EDOT source and bromine[10] were suggested for the fabrication of doped PEDOT thin films affording well-ordered microstructures with competitive conductivity values.

In-situ photopolymerization is also a very promising strategy to fabricate conducting thin films. It is of great commercial and practical value since this polymerization method is not only instantaneous but also can be applied to non-conducting substrates different from electrochemical polymerization. In addition, it is less restricted by other experimental parameters such as temperature, pH, and type of required solvents. Moreover, mass production is achievable at a low cost and even in a limited space. Therefore, the preparation of a conducting polymer thin film through one-step in-situ UV polymerization from monomer precursors is desirable not only to make the fabrication process simpler and more practical, but also to extend applicable monomers whose polymers are insoluble in common organic solvents.

Polythiophene thin films have been fabricated from 2,5-diiodothiophene through UV-induced in-situ polymerization and their optical and electrical properties were characterized and compared to those of chemically synthesized polythiophenes.[11,12] The photodissociation of carbon-iodine bonds of precursor molecules plays a significant role in coupling between precursors to yield higher molecular weight species. The molecular weight distribution of the resulting oligomeric species follows the Flory model for linear step growth polymerization.[11] Despite of its simple and instant process, low degree of polymerization and the presence of cross-linked chains produced from α- β' coupling of the precursors are not favorable to achieve desirable electrical properties for the application of transparent electrodes. In addition, since iodine species originated from the photodissociation of carbon-iodine bonds of thiophene precursors is not sufficient to fully dope the oligomeric species, additional efforts for post-doping are required to demonstrate compelling optoelectronic properties of conducting polymer thin films.

The photoarylation between iodothiophene and other heterocyclic compounds has been widely investigated as an efficient synthetic route to give corresponding arylation complexes in good yield.[13–15] Several oligomeric thiophenes were synthesized in a high yield through photo-arylation, which is a photochemical coupling of halothienyl derivatives with other heteroaromatic compounds.[15–17] In particular, a 2,5-diiodothiophene is arylated in a good yield to give a thiophene trimer in the presence of thiophene when irradiated by UV light in acetonitrile solution.[18] In this regard, photo-arylation could be a promising synthetic strategy to fabricate conducting polymer thin films with a great conversion efficiency to polymers having a high molecular weight. Even though photo-arylation in solution can have good mobility of precursors and consequently good reaction yield, we presumed that photo-arylation would be also favorable in solid state where the precursors and radicals are sufficiently diffuse in the deposited matrix.

In this paper, we report newly developed photoarylation based copolymerization between ProDOT or EDOT derivatives and their iodine substituted compounds to realize conducting polymer thin films having high electrical conductivity and transparency. 2,5-diiodo-ProDOT or EDOT derivatives serve as photoinitiators to generate thienyl radicals by means of efficient dissociation of the weak carbon-iodine bond upon UV irradiation. Subsequently, coupling of the thienyl radical with neighboring EDOT or ProDOT monomers affords the corresponding larger molecular weight species. Alkyl or ethylene glycol side chains were incorporated on to the propylenedioxy moiety to afford good solubility of the precursors in organic solvents and to facilitate wet coating processability, while promoting homogeneous photochemical reaction.[19] The copolymerized thin films were post-doped chemically by protonic acids to give electrical conductivity and transparency to the resulting polymers. We carried out a systematic study to investigate physical and optoelectronic properties of the fabricated conducting thin films by UV polymerization followed by a post-doping process. The results provide insights into how to engineer conducting polymers for outstanding performances as transparent electrodes.

3.2 Experimental

EDOT and ProDOT derivatives including 2,5-diiodo-3,4-(3,3'-dibutylpropylenedioxy)thiophene (DIDBuProDOT) and 2,5-diiodo-[diethylene glycol monomethyl ether-5,7-diiodo-2,3-dihydrothieno[3,4-b][1,4]dioxine] (DIEDOT-DEG) (Figure 3.1) were synthesized as illustrated in the literatures.[19,20]

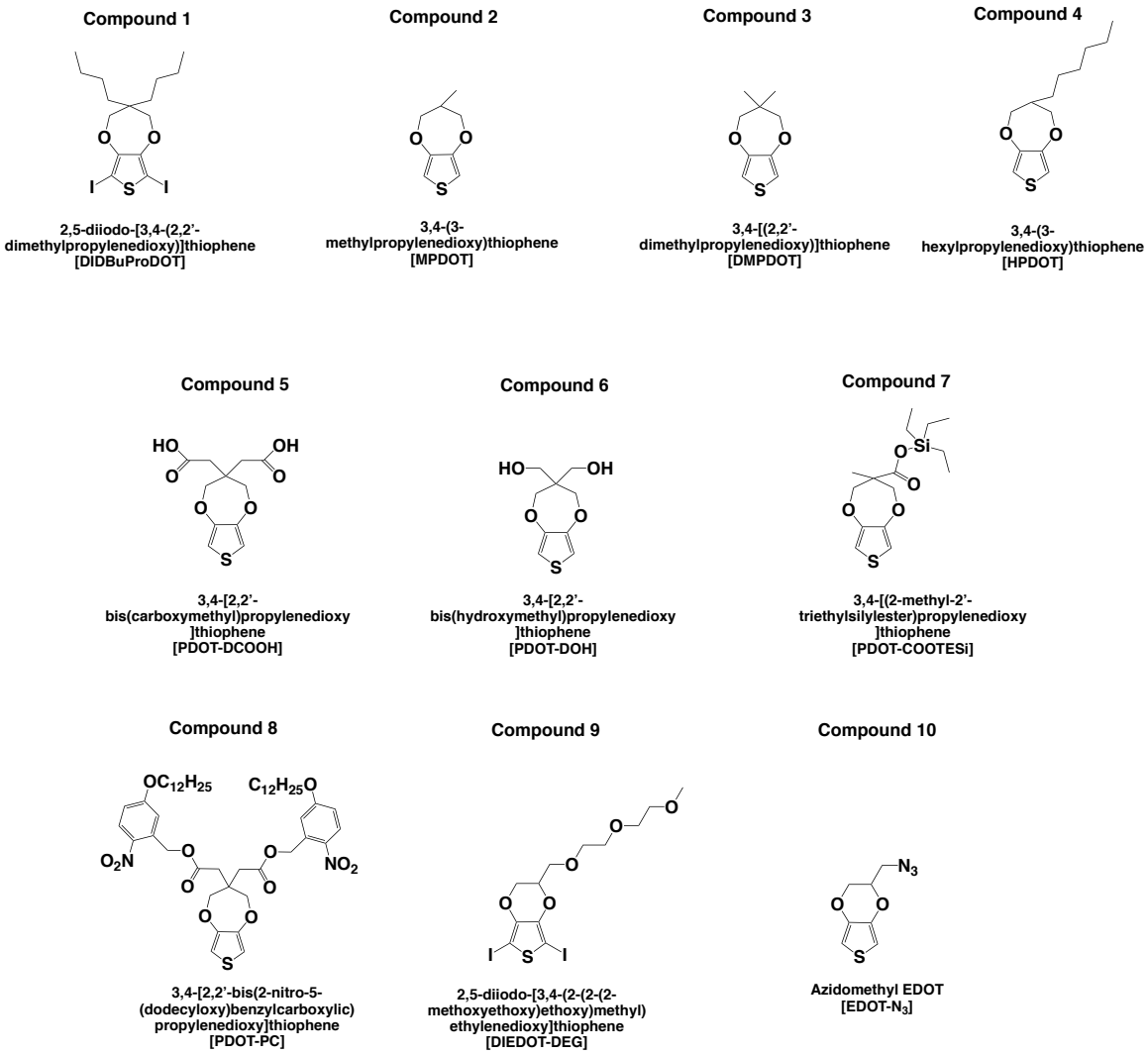

Figure 3.1. ProDOT and EDOT derivatives synthesized for photoarylation based UV polymerization.

For the conducting polymer thin film fabrication, DIDBuProDOT or DIEDOT-DEG dissolved in chloroform with other thiophene derivatives to prepare a 2wt% solution. Thin films were prepared by spin-casting the solutions on glass substrates (1inch x 1inch) that were cleaned by ultrasonication in dilute soap, acetone, and isopropanol, followed by ozone surface treatment before use. UV irradiation was applied to the spin-coated films with a 254nm UV lamp (4W or 35W) in a nitrogen purged glovebox. The UV-cured films were soaked in acetone and chloroform

and annealed at 80°C to eliminate small molecular weight species and iodine from the polymerized films. Then, the thin films were chemically doped by dipping in a 2M solution of sulfuric acid (H_2SO_4) or methanesulfonic acid (CH_3SO_3H) diluted with nitromethane for 15 minutes, rinsed with fresh nitromethane, and dried under vacuum. The detailed procedure is described in Figure 3.2.

The absorption spectra of the films were measured with UV-vis-NIR spectrophotometer before and after the chemical doping process. Transmittance and electric conductivity of the doped film were measured via UV-vis spectrometry and a four-point-probe method, respectively. Optical microscopy and AFM were employed to investigate the molecular packing and morphology of the films. The composition and polymerization efficiency were evaluated from XPS and FT-IR analyses of the photochemically synthesized films from DIEDOT-DEG and EDOT-N_3.

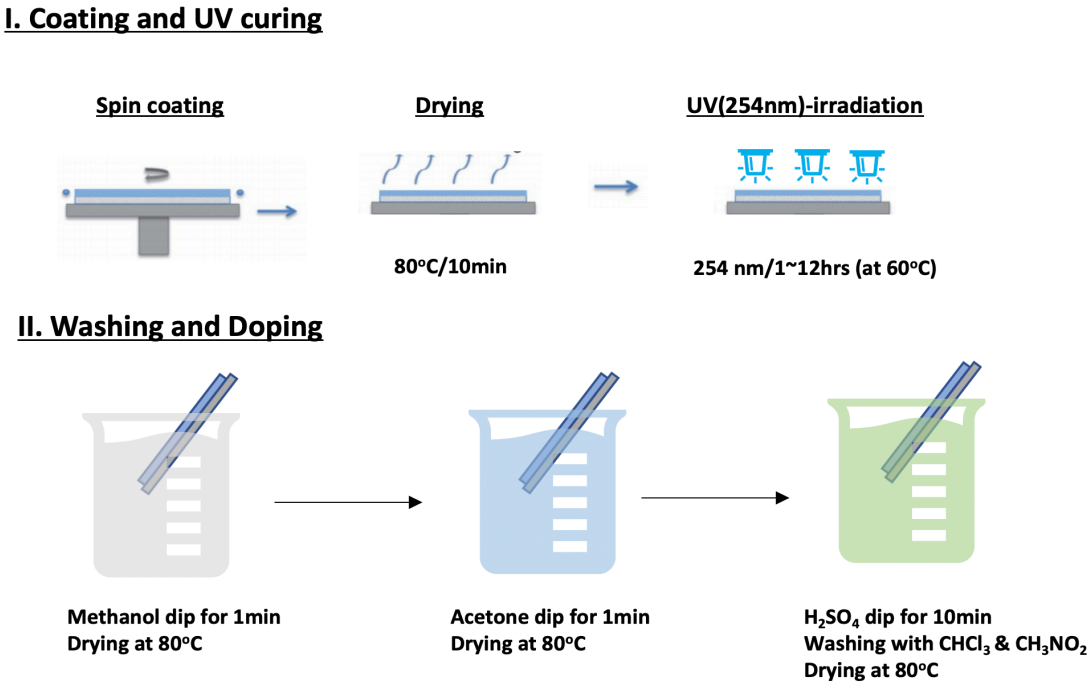

Figure 3.2. Schematic illustration of the fabrication of transparent conducting polymer thin films by means of UV-mediated polymerization, solvent rinsing, and acid doping.

3.3 Result and Discussion

In order to compare polymerization efficiency between photocondensation and photoarylation, DIDBuProDOT or 2,5-diiodo-3,4-dihexylthiophene (DIDHTh) were UV polymerized in toluene solely or together with DBuProDOT or 3,4-dihexylthiophene, respectively, by 6.8W 365nm LED lamp (Thorlab). As depicted in Figure 3.3(a) and (b), the UV polymerization of the thiophene derivatives yielded only minute amounts of oligomeric molecules with a low conversion rate under the UV light irradiation for 24 hours. In contrast, the UV polymerization of dibutyl-ProDOT derivatives exhibited much better reactivity with higher conversion rates under the same photo-irradiation condition (Figure 3.3(c) and (d)). This suggests that the propylenedioxy moiety on the thiophene plays an important role in the photochemical reaction owing to the electron-donating nature of the moiety and consequentially lowered oxidation potential of the ProDOT molecules. The molecular weight distribution by the UV-irradiated polymerization of DIDBuProDOT followed the Flory model for linear step growth polymerization, which is consistent with that of the in-situ UV polymerization of 2,5-diiodothiophene (Figure 3.3(c)).[11] In contrast, when DIDBuProDOT is copolymerized with DBuProDOT under the same UV irradiation condition, most monomers were consumed to produce oligomer species having a higher molecular weight as shown in Figure 3.3(d). These results imply that the later (photoarylation) is more efficient than the former (photocondensation) to yield oligomeric or polymeric species having a high molecular weight and a high conversion ratio.

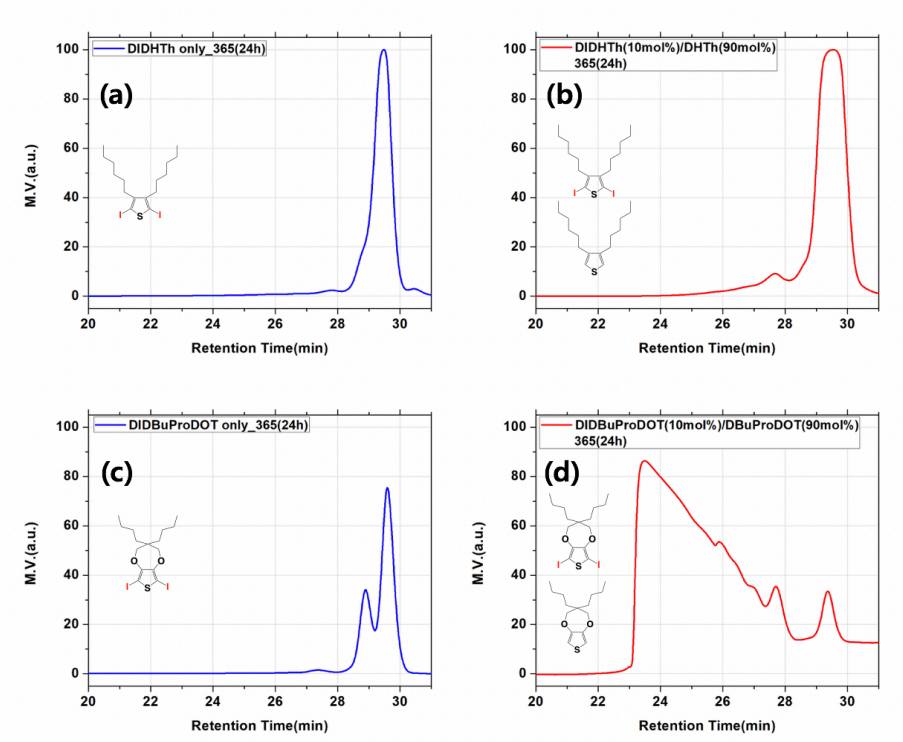

Figure 3.3. GPC data for (a) the photopolymerized sample from diiodo-dihexylthiophene (DIDHTh) only, (b) DIDHTh/DHTh, (c) DIDBuProDOT only, and (d) DIDBuProDOT/DBuProDOT.

Inspired by the one-pot photopolymerization based on the combination of sequential photoarylation and coupling described in the previous chapter and the reported works in references[15,18,21], we investigated the same one-pot photopolymerization in solid-state for the development of flexible and transparent conjugated polymer electrodes. We saw the feasibility if we design the system to allow good enough monomers' mobility in the solid state. Figure 3.4 shows UV-vis absorption spectrum of the copolymerized film of DIDBuProDOT and dimethyl substituted ProDOT (DMPDOT, compound 3) with an 1:2 feed ratio. After 12 hours of UV irradiation, the polymerized film exhibited absorption λ_{max} at 300 and 350nm and a broad absorption in a longer wavelength region. The first two absorption peaks are corresponding to

small oligomer molecules originated from the coupling between DIDBuProDOT precursors. The broad absorption band over 700nm, on the other hand, has to do with the doped conjugated polymers by iodine. After immersing the UV-cured film in chloroform and subsequent annealing at 80°C to eliminate small molecules and iodine, the main absorption band shifted to ~ 500nm, while the absorption bands of the small molecules and in the long wavelength region diminished. As the film develops charge transfer by chemical doping with sulfuric acid, the neutral states are bleached and new absorption bands simultaneously appear over the longer visible wavelength and near infrared (NIR) ranges. The doped film showed a high conductivity of 140 S/cm.

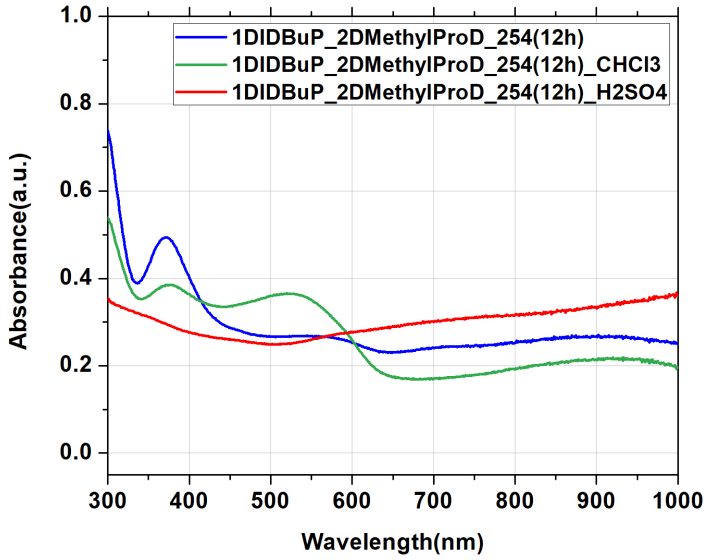

Figure 3.4. UV-vis absorption spectra for the UV-polymerized film from DIDBuProDOT and DMethylProDOT precursors and its post-treatment.

DIDBuProDOT was copolymerized with several thiophene derivatives as presented in Figure 3.1 under the same polymerization condition to examine and compare their electrical conductivities. As shown in Table 3.1, the 160nm-thick film of EDOT copolymerized with

DIDBuProDOT exhibited the best conductivity of 780 S/cm in the doped condition. This result indicates that minimizing the volume of insulating side chains appears to enhance the electrical properties because of the absence of otherwise insulating side chains of EDOT and consequent as well. Meanwhile, the copolymer of 3-hexylthiophene and DIDBuProDOT exhibited lower conductivity than any other UV-polymerized thin films. This suggested that the presence of ethylenedioxy or propylenedioxy moiety on the thiophene plays a very important role in enhancing electrical properties of the p-doped films by reducing the oxidation potential of the conjugated polymers.

Table 3.1. Conductivity depending on monomers copolymerized with DI-DBuProDOT

Monomer	MPDOT	DMPDOT	PDOT -DCOOH	PDOT -DOH	EDOT	EDOT -OH	3-HT
Conductivity (S/cm)	130	140	90	270	780	93	79

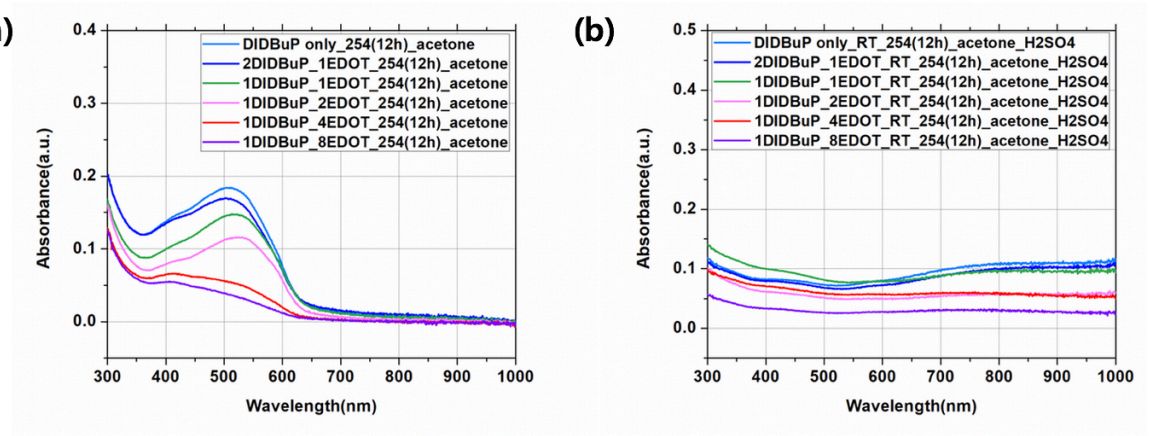

Figure 3.5. The absorption spectrum of UV-cured film with DIDBuProDOT and EDOT (a) in neutral state, and (b) in doped state.

The optical and electrical properties of copolymer thin films were also examined at different DIDBuProDOT/EDOT ratios. The absorption spectra of 50~100nm thick films in neutral

and doped states are shown in Figure 3.5. The spectra in Figure 3.5(a) showed main characteristic absorption bands at around 500nm corresponding to the π-π* transition of the neutral polymers. Increasing EDOT ratio makes the absorption maxima red-shifted while the extinction coefficient decreases. This implies that the incorporation of EDOT causes the copolymer thin films to form highly packed coplanar conjugated polymer backbones due to the reduction of the side chain volume. On the other hand, the reduction of the absorption intensity can be attributed to less efficient monomer to polymer conversion because of the reduced amount of iodine radicals that are essential for the photochemical reaction and the chain growth.

The absorption bands of the neutral states significantly decrease upon the chemical doping by sulfuric acid, while new absorption bands in the longer visible wavelength and NIR region appear, indicating the formation of charge transfer by the dopant. (Figure 3.5(b)) Accordingly, the doped films become transparent with more than 80% of transmittance along with the enhanced charge concentration. Figure 3.6 presents the conductivities of the doped copolymer thin films calculated from the sheet resistivity measured by the 4-point probe method and the film thicknesses determined by ellipsometry. The copolymer prepared from 1:1 ratio of DIDBuProDOT and EDOT showed the maximum conductivity. When a larger amount of DIDBuProDOT is used than EDOT, polycondensation becomes dominant by the UV irradiation so that the polymerization is likely to be less efficient. In the other regime where DIDBuProDOT/EDOT<1, electrical conductivities decrease with increasing EDOT molar ratios due to the reduced amount of iodine radicals and the consequently lower monomer to polymer conversion efficiency. When the two components are equivalent, efficient copolymerization via photoarylation between DIDBuProDOT and EDOT is anticipated.

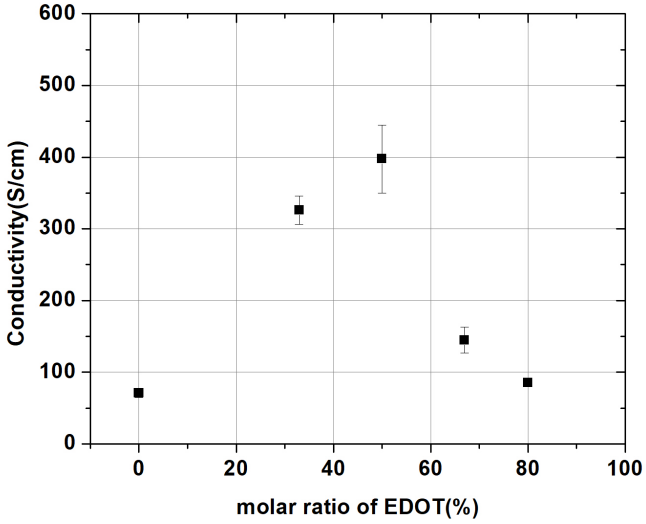

Figure 3.6. Conductivities as a function of the feed ratio between DIDBuProDOT and EDOT

Figure 3.7 describes the absorption changes of the spin-coated films during the UV polymerization at different temperatures. The completion of the solid-sate photo-induced copolymerization was determined by the saturation of the absorption bands at ~900nm corresponding to the iodine doped polymers. At room temperature, it commonly takes 6 to 12 hours to complete the solid-state photo-polymerization. This rather long reaction time is impractical for real applications, and also can induce photodegradation during the prolonged UV irradiation. In the solid states, the mobility of the precursors is prone to be limited. Due to this mobility limitation, monomers as well as the radical species of the bulky growing polymer chains would not be able to readily diffuse to each other to further extend the conjugation. In order to impart mobility to the growing chains and precursors and enhance the propagation rate, the reaction mixture was heated up to 60^{o}C during the UV irradiation. The reaction time is reduced from 6~12 hours to 4 hours in all compositions of DIDBuProDOT and EDOT. As depicted in Figure 3.8, the absorption peak of the neutral states for the heated samples at 60^{o}C is stronger and

slightly red-shifted than that of the samples prepared at room temperature in all compositions, indicating that thermal energy renders more efficient UV polymerization by imparted better molecular mobility at the higher temperature.

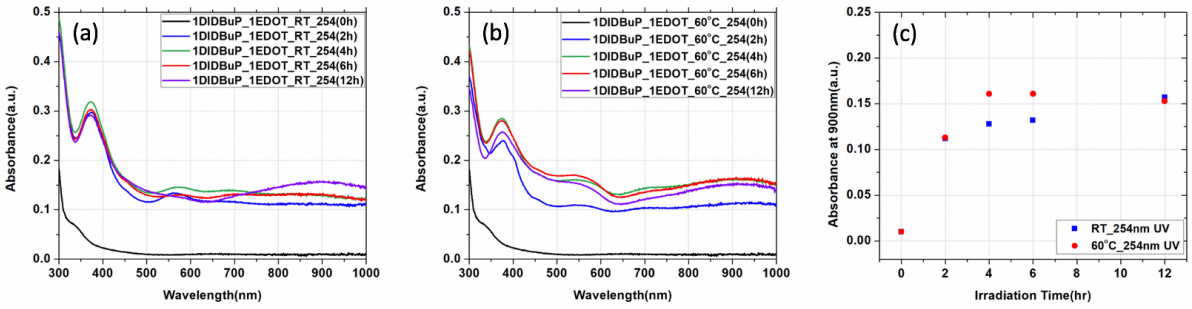

Figure 3.7. UV-vis spectra of the polymerized thin films at (a) room temperature, (b) 60°C, and (c) the plot of absorption changes depending on UV irradiation times.

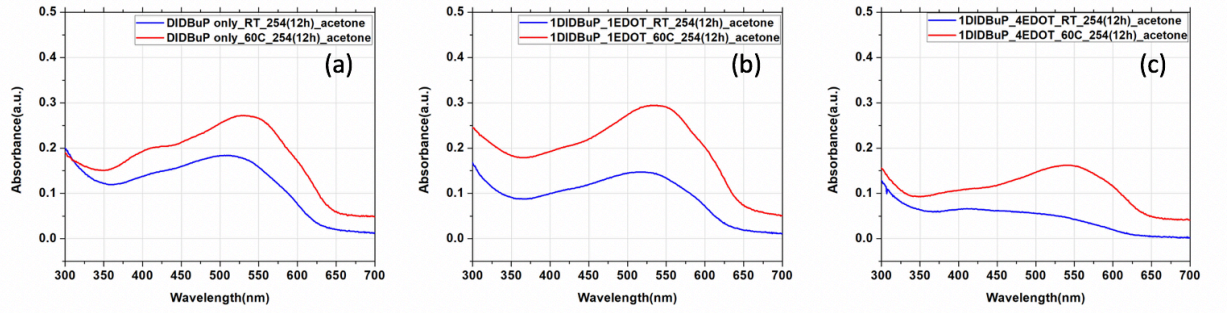

Figure 3.8. Absorption spectra of the UV-polymerized thin films at room temperature (blue) and 60°C (red) with different feed ratios of DIDBuProDOT/EDOT; (a)100:0, (b)50:50, and (c)20:80.

The developed UV polymerization based on photoarylation allows a variety of heteroaromatic molecules to be copolymerized with diiodo-thiophene derivatives. Under the same scheme of DIDBuProDOT copolymerization with EDOT, three different monomers, ProDOT incorporating photocleavable side chains (PDOT-PC, compound 8), 9H-fluorene, and 4H-Cyclopenta[1,2-b:5,4-b']bisthiophene (CyPBTh) are used to yield copolymers as depicted in

Figure 3.9 The copolymer thin films exhibited their own unique absorption spectra both in the neutral states and in the doped states as depicted in Figure 3.10. The films show higher than 80% transmittance. While the conductivities of the ProDOT-fluorene and ProDOT-CyPBTh copolymers are 400~500 S/cm, which is comparable to that of DBuProDOT-EDOT copolymer, ProDOT-PDOT-PC copolymer demonstrates lower conductivity of 160~180 S/cm due to the presence of the cleavable bulky side chains, implicating the photo-cleavage of the side chains was not fully carried out (Figure 3.11).

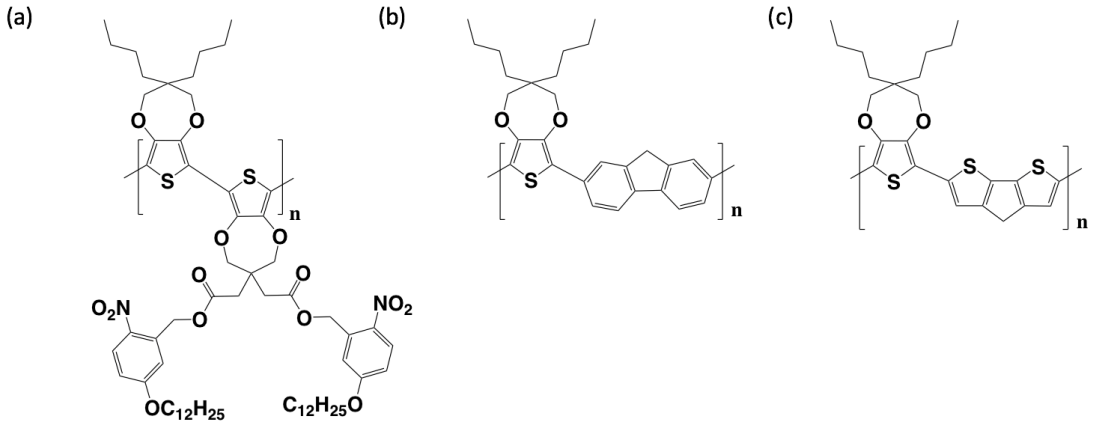

Figure 3.9. Copolymers of ProDOT and (a) ProDOT-PC, (b) 9H-fluorene, and (c) benzothiazole.

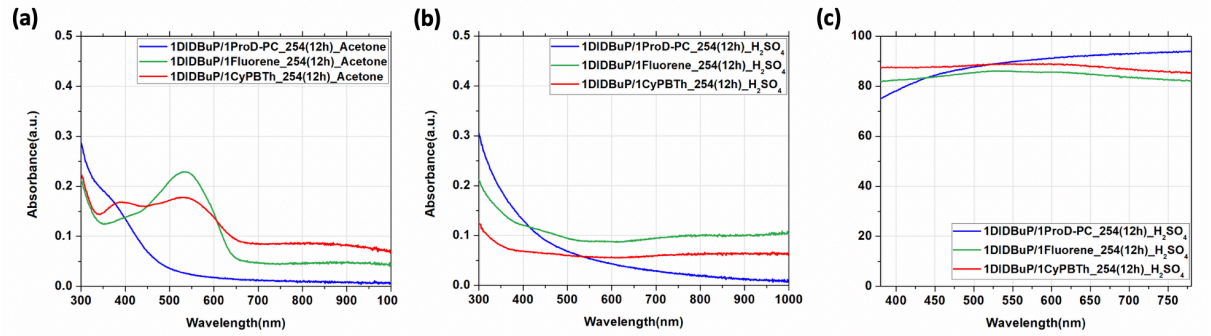

Figure 3.10. UV-vis absorption spectra of copolymers (a) in the neutral states, (b) in doped states, and (c) their transmittance spectra.

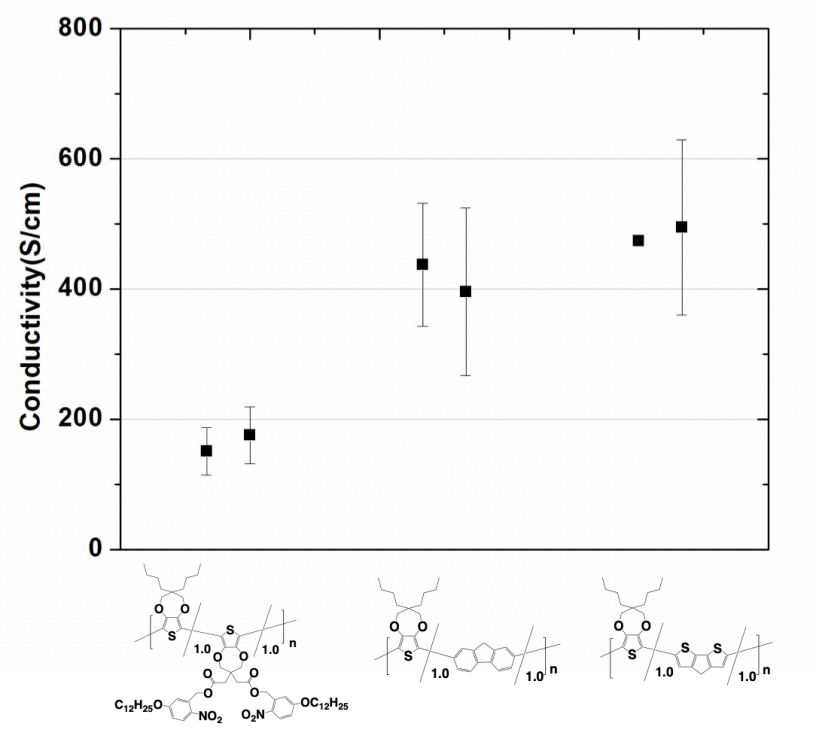

Figure 3.11. Conductivities for the copolymers of DBuProDOT and three different monomers, ProDOT incorporating photocleavable side chains (PDOT-PC), 9H-fluorene, and 4H-Cyclopenta[1,2-b:5,4-b']bisthiophene(CyPBTh).

In order to enhance the conductivity by reducing the side chain volume from the resulting polymer backbone, we employed 2,5-diiodo-3,4-ethylenedioxythiophene (DI-EDOT) instead of DIDBuProDOT and copolymerize with EDOT under the same condition. The deposited film, however, underwent crystallization upon drying on a hot plate at 60°C. As previously reported, in a solid-state polymerization of dihalo-EDOTs,[9] short intermolecular interactions between iodine atoms yield high degree of stacks of the EDOT monomers. As depicted in Figure 3.12, a very weak absorption band at 400nm appeared after the UV irradiation but diminished by acetone washing. This suggests that the crystallization of precursors is detrimental to the polymerization efficiency owing to the restricted molecular mobility in the crystalline state. In other words, successful UV

polymerization in a solid-state thin film can be realized by attaining good enough mobility of precursours during the photochemical reaction as the more efficient copolymerization of DIDBuProDOT and EDOT at 60°C than room temperature testified.

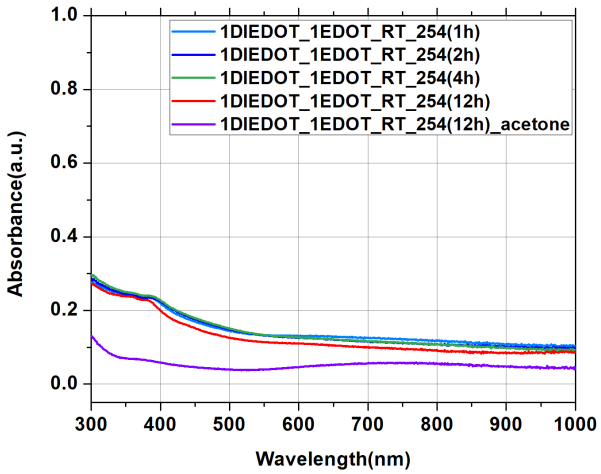

Figure 3.12. UV-vis spectra of an UV polymerized PEDOT thin film from DIEDOT and EDOT.

We anticipated that the molecular mobility of the reaction mixture can be largely enhanced by incorporating an oligomeric ethylene glycol side chain in the diiodo-EDOT framework. Owing to their more flexible features than any other alkyl side chains, ethylene glycol side chains offer more mobility so as to promote the chain propagation during the UV polymerization. The synthesized DIEDOT-DEG incorporating a diethylene glycol monomethyl ether unit as a side chain (compound 9) was copolymerized with EDOT derivatives with an 1:1 feed ratio under the same UV curing condition and the result was compared with the copolymer of DBuProDOT and EDOT as depicted in Figure 3.13.

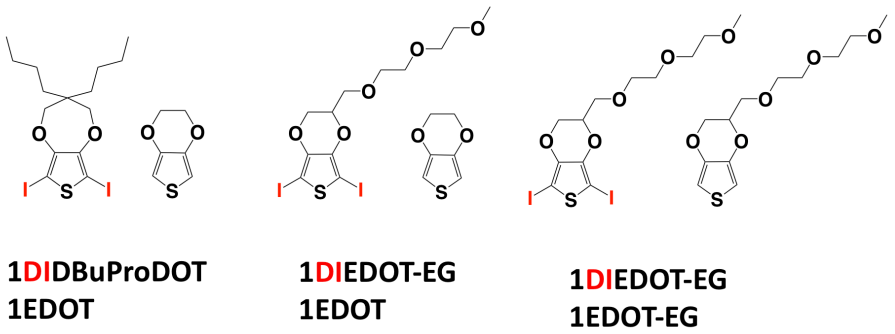

Figure 3.13. The precursors used in the UV polymerization for the conducting polymer thin film fabrication.

The polymerization efficiency is also affected by the intensity of the employed light source. A new 254nm UV lamp with 35W intensity was used to copolymerize DIEDOT-DEG, EDOT, and EDOT-DEG. The polymerized films exhibited broad absorption bands in the longer visible wavelength and NIR regions after the chemical doping with sulfuric acid, but their λ_{max} is shorter than that of the copolymer thin film of DIDBuProDOT and EDOT as shown in Figure 3.14(a). Surprisingly, the conductivity of the PEDOT thin films copolymerized with DIEDOT-DEG and EDOT is nearly 10 times higher than that of DIDBuProDOT-EDOT copolymer (Figure 3.14(b)). This result implies that the mobility of the reaction mixture during the solid-state polymerization plays a crucial role in forming the conducting polymer thin films with a high molecular weight. The results also reveal that EDOT-based copolymer is more advantageous than EDOT-ProDOT copolymer to achieve excellent electrical properties due to the absence of side chains.

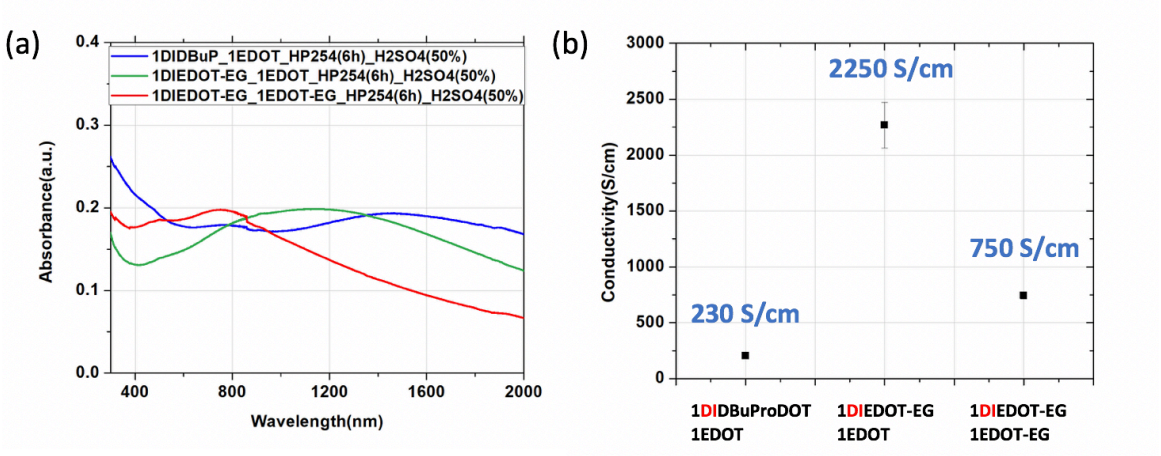

Figure 3.14. Characterization of doped copolymerized thin films from DIDBuProDOT/EDOT, DIEDOT-DEG/EDOT, and DIEDOT-DEG/EDOT-DEG by (a) UV-vis absorption spectra of and (b) their conductivities.

The optical and electrical properties of the UV polymerized thin films were examined as a function of the feed ratio between DIEDOT-DEG and EDOT as shown in Figure 3.15. When the amount of DIEDOT-DEG is twice larger than that of EDOT, high degree of absorption is observed in near IR range corresponding to polaron states in the film where the obtained polymers were doped by iodine molecules to a great extent. While increasing the EDOT feed ratio leads to the decrease in the absorption in NIR, conductivity of the film is optimized at 1:1 ratio of DIEDOT-DEG: EDOT with maximum conductivity of 2000 S/cm, which is consistent with the previously identified optimum 1:1 ratio of DIDBuProDOT and EDOT precursors. As we discussed from the previous results, polycondensation is dominant when DIEDOT-DEG is rich in the film so that most precursors participate in yielding small oligomers doped with iodine molecules resulting in a high doping level of the film but low transparency and poor conductivity. On the contrary, as the amount of EDOT becomes rich in the system, photoarylation is dominant but the chain extension is limited due to the scarce amount of iodine source to maintain the photochemical reaction.

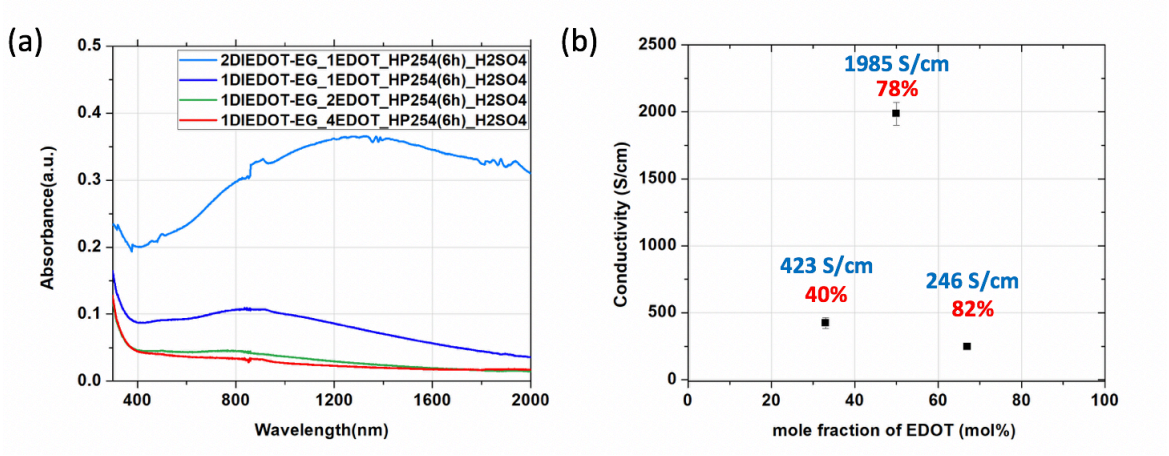

Figure 3.15. Characterization of doped copolymerized thin films from DIEDOT-DEG/EDOT with different ratios by (a) UV-vis-NIR absorption spectra and (b) electrical conductivity and optical transmittance (blue letters: conductivity, red letters: transmittance).

DIDBuProDOT and DIEDOT-DEG are copolymerized with ProDOT and EDOT derivatives having different side chains, respectively, to investigate the relationships between the molecular structures of the produced copolymers and the optical and electrical properties. As depicted in Figure 3.16, the doped copolymers thin films from DIDBuProDOT and ProDOT derivatives show analogous absorption without having any notable absorption band in the longer visible wavelength and NIR ranges. At the same time, the films maintain relatively high transparency in the visible range with a higher than 70% of transmittance value when the thickness of the doped films is 50~100nm. The doped polymer films copolymerized from DIEDOT-DEG and EDOT derivatives except for EDOT-DEG also show similar optical properties to those of the ProDOT copolymers.

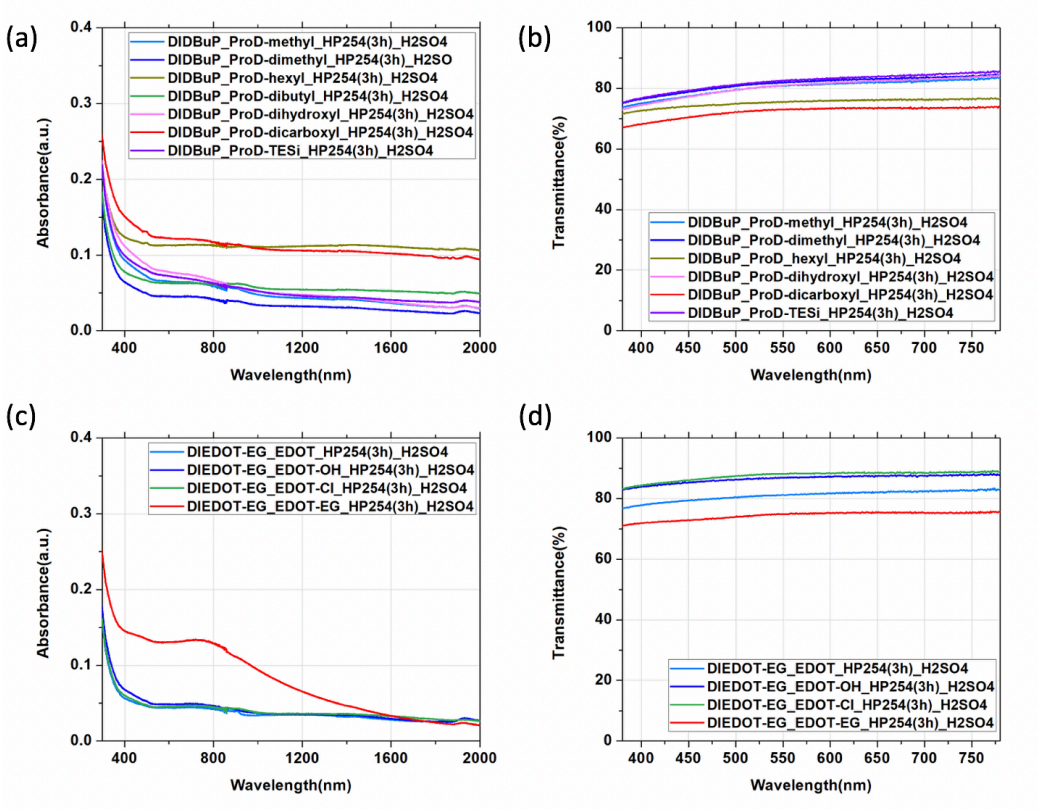

Figure 3.16. Characterization of doped copolymerized thin films from DIDBuProDOT and ProDOT derivatives, and DIEDOT-DEG and EDOT derivatives by (a),(c) UV-vis-NIR absorption spectra and (b),(d) optical transmittance.

Different from their similar optical properties regardless of ProDOT or EDOT derivatives, conductivities of the doped films are significantly affected by their molecular structures as compared in Figure 3.17(a). While the film polymerized only from DIDBuProDOT displays relatively low conductivity (144 S/cm) due to its dominant polycondensation to yield lower molecular weight species, copolymer thin films of ProDOT having short methyl or dimethyl side chains provide much higher conductivity of ~1,000 S/cm. When a long hexyl side chain is attached to the ProDOT unit, corresponding conductivity lowers down to ~200 S/cm, likely because the steric hinderance by the longer hexyl chains obstructs the molecular packing. In addition, the

copolymers from ProDOT with hydroxyl or carboxyl side chains show low conductivity. The polar moeiteies are likely to hamper the polymerization by interacting with iodine or growing chain radical species. Hydroxyl or carboxyl side chains on the ProDOT monomer reduce the degree of polymerization due to the nucleaophilic attack by the functional groups to radical cation intermediates.[22] Hence, polymerization of protected functional monomers followed by subsequent deprotection of the functional groups looks to be necessary in order to achieve large molecular weight conjugated polymers having neucleophilic side chains. When the ProDOT derivative having a triethylsilyl-protected carboxylic side chain is employed for the copolymerization with DIDBuProDOT, indeed 5 times higher conductivity was achieved than that of the ProDOT polymer film copolymerized from non-protected ProDOT-carboxylic acid and DIDBuProDOT as depicted in Figure 3.17(a).

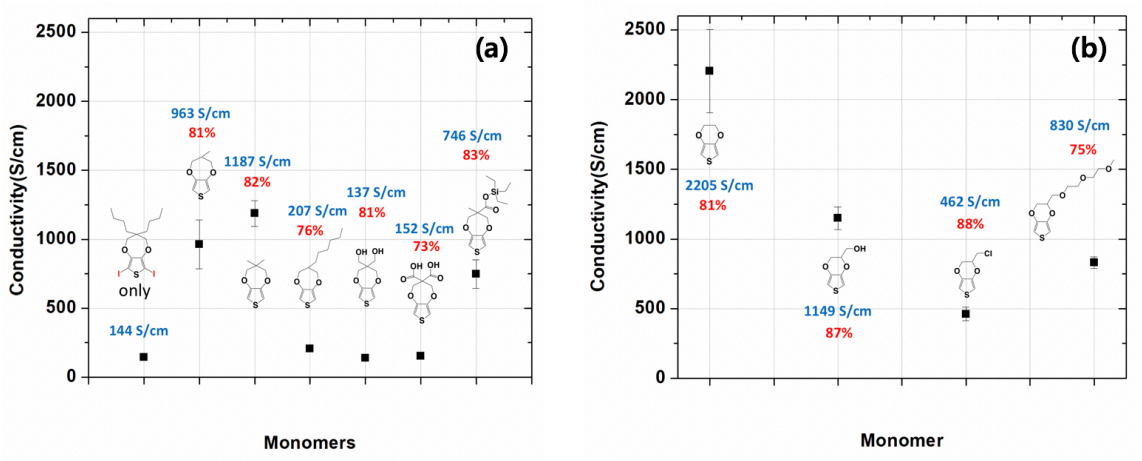

Figure 3.17. Conductivity and transmittance of doped polymer thin films copolymerized from (a) DIDBuProDOT and ProDOT derivatives and (b) DIEDOT-DEG and EDOT derivatives. (blue letters: conductivity, red letters: transmittance).

Conductivity data of the thin films copolymerized from DIEDOT-DEG and EDOT derivatives exhibit a similar trend with those of PProDOT copolymer thin films (Figure 3.17(b)). The copolymer thin film employing EDOT shows the best conductivity due to the absence of side chains and the resulting highly packed molecular structures. Therefore, as one can anticipate, the PEDOT copolymer thin films incorporating EDOT having any side chain indeed have lower conductivities even though the overall conductivities of PEDOT copolymers are higher than those of PProDOT copolymers.

Interestingly, when DIDBuProDOT and EDOT were copolymerized, a unique morphology was observed from the thin film in optical microscopy as shown in Figure 3.18. Randomly oriented patterns were formed in the middle of the polymerized thin film by UV irradiation. Figure 3.18(c) showing an AFM image and its height profile reveals that the bright regions rise up with 200~300nm heights of elevation from the darker areas. We believe that the patterns are formed due to the combined effects of shrinkage of the deposited film and the loss of adhesion from the glass substrate. When the film is polymerized to form conducting polymer films, the polymer chains become hydrophobic due to the increasing volume of butyl side chains. The change in the surface tension of the film could be attributed to the change in adhesion between the film and the substrate, resulting in the wrinkle formation. On the contrary, the thin film copolymerized from DIEDOT-DEG and EDOT exhibited very smooth morphology in optical microscopy with the height profile with only a few nanometers in the AFM image (Figure 3.18(b) and (d)). The smooth morphology implies that the polymerized thin film maintains a good adhesion with the glass substrate owing to the hydrophilic diethylene glycol side chain of DIEDOT-DEG.

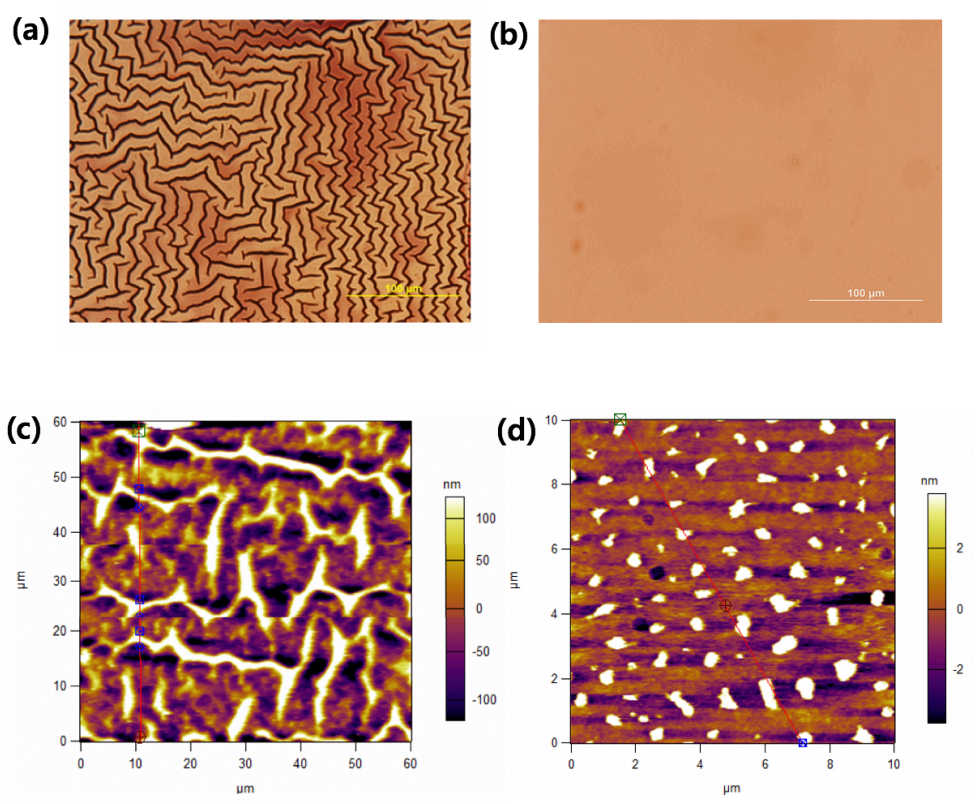

Figure 3.18. Optical microscopic and AFM images of the copolymerized films of (a), (c) DIDBuProDOT and EDOT and (b), (d) DIEDOT-DEG and EDOT.

To confirm the copolymerization between two different EDOT derivatives through the photoarylation, X-ray photoelectron spectroscopy (XPS) analysis was conducted for the thin films copolymerized from DIEDOT-DEG and 2-(Azidomethyl)-2,3-dihydrothieno[3,4-b][1,4]dioxine (EDOT-N_3) and washed with chloroform to remove small molecules (Figure 3.19). As shown in Figure 3.20, XPS survey and core scans for the copolymerized films reveal analogous distributions of the functional groups of C 1s, S 2p, and O 1s spectra as in the previously reported PEDOT polymer films.[10]

The oxygen rich diethyleneglycol side chain of DIEDOT-DEG and the presence of nitrogen on the side chain of EDOT-N_3 are expected to show the elemental change of the copolymers

depending on the feed ratios of the two constituent monomers. It is noteworthy that an azide group on EDOT-N_3 unit also undergoes a photolysis by UV irradiation to yield an amine (-NH_2) group.[23] Assuming that EDOT-N_3 precursors are equivalently copolymerized with DIEDOT-DEG molecules and their azide groups are completely transformed to amine groups by UV-irradiation, two sulfur atoms per every nitrogen atom on the polymer chains are anticipated as depicted in Figure 3.19.

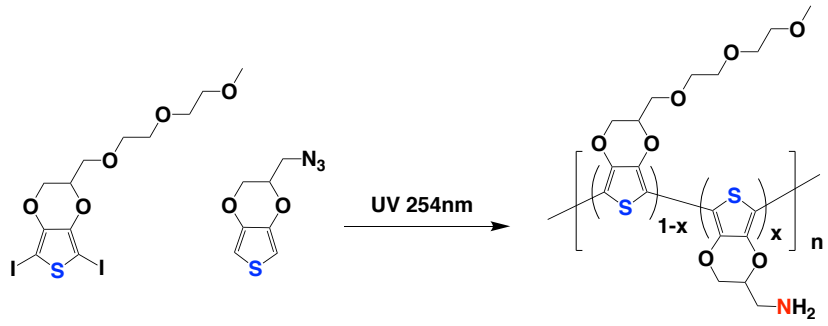

Figure 3.19. UV mediated copolymerization of DIEDOT-DEG and EDOT-N_3.

The core scan for N 1s in Figure 3.20(b) shows that the intensity of N 1s peak enhances as the feed ratio of EDOT-N_3 increases. In particular, the quantitative analysis of N 1s and C 1s by XPS scan survey shows that the atomic ratio of sulfur to nitrogen is 2:1 under an 1:1 feed ratio of DIEDOT-DEG and EDOT-N_3, implying quantitative photoarylation-based copolymerization. Interestingly, the copolymerized film from an 1:2 feed ratio of DIEDOT-DEG/EDOT-N_3 also has an 2:1 of S/N atomic ratio. This result implies that one DIEDOT-DEG molecule reacts equivalently with one EDOT-N_3 and extra EDOT-N_3 molecule remains intact and is removed by chloroform washing. This also implicates that the movement of radical species running the photopolymerization is significantly restricted in solid state.

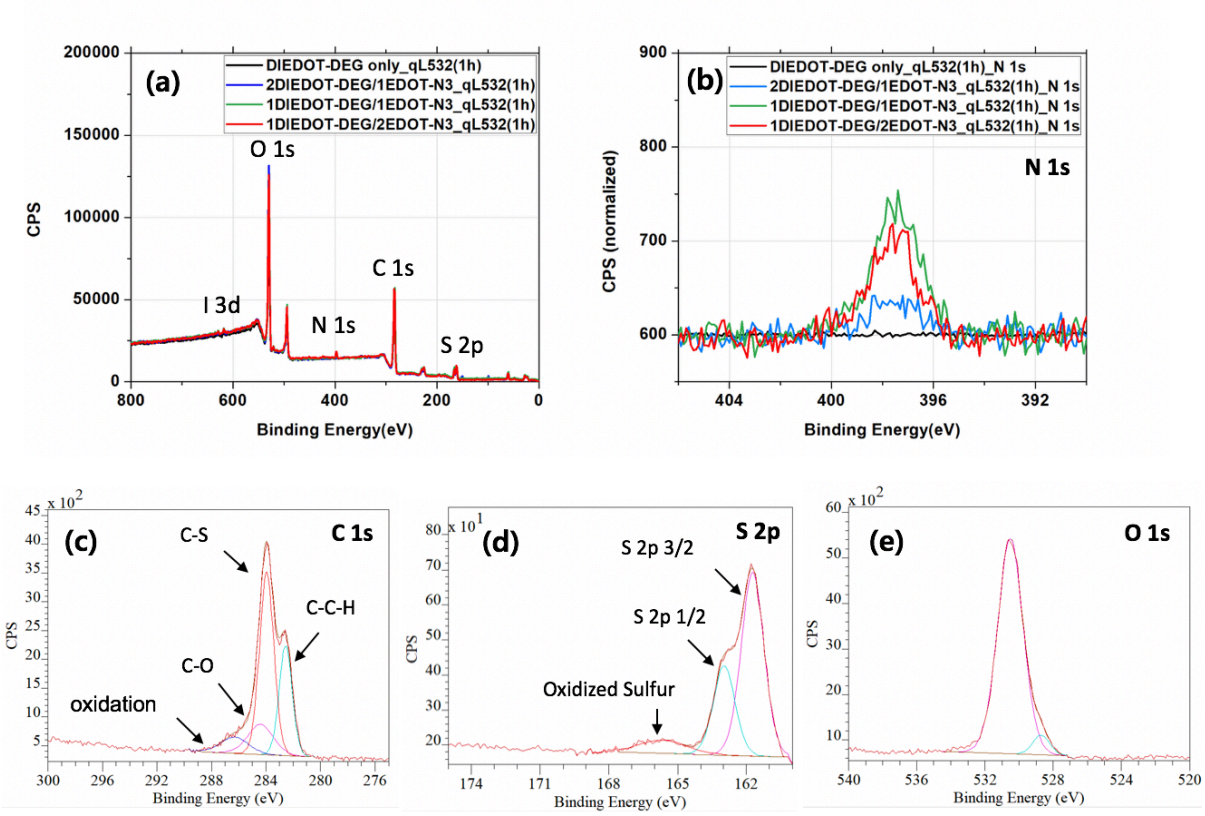

Figure 3.20. XPS spectra of copolymers of DIEDOT-DEG and EDOT-N_3; (a) survey scan, core scans of (b) N 1s, (c) C 1s, (d) S 2p, and (e) O 1s.

The FT-IR spectra in Figure 3.21 additionally support the copolymerization of the same precursors. The copolymerized films commonly exhibited absorption bands corresponding to the stretching modes of C=C and C-C in the thiophene ring (1473, 1439, and 1373 cm^{-1}) and of C-O-C in the ethylenedioxy group on the thiophene ring (1245 and 1142 cm^{-1}) or diethyleneglycol side chains from DIEDOT-DEG. Besides the absorption bands from the conjugated backbone of PEDOT, the characteristic absorption bands from the side chains of the copolymers are observed in the FT-IR spectra. The broad bands between 1500 and 1750 cm^{-1} ascribed to in-plane NH_2 scissoring become stronger with an increasing feed ratio of EDOT-N_3 but saturated at 1:1 feed

ratio of DIEDOT-DEG/EDOT-N_3. This result is in good agreement with the atomic ratios of S/N in XPS spectra for the same samples.

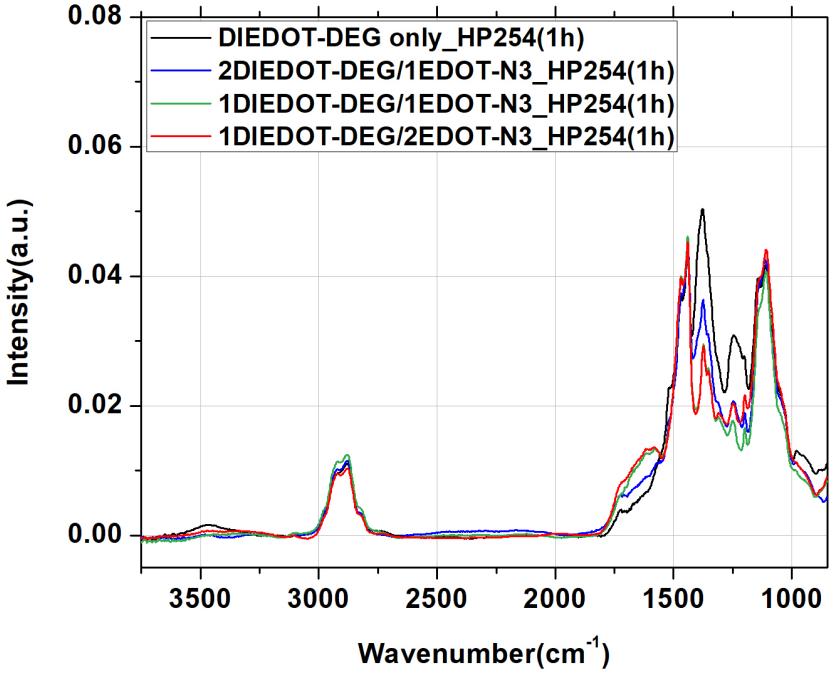

Figure 3.21. FT-IR spectra of the copolymerized thin films from different feed ratios of DIEDOT-DEG and EDOT-N_3.

3.4 Conclusion

In summary, the newly investigated UV-mediated solid-state copolymerization between 2,5-diiodothiophene derivatives and a series of heterocyclic molecules in solid states rendered solvent-resistant conducting polymer thin films on glass substrates. We took advantage of a facile photoarlyation between 2,5-diiodo thiophene derivatives and other heterocyclic compounds to form robust and solvent resistant polymer thin films by UV irradiation. Besides the light source intensity, polymerization temperature also largely affects the solid-state photo-polymerization, implying that the mobility of the precursors is the critical determining factor for the degree of

polymerization. By incorporating a flexible and mobile diethylene glycol side chain to EDOT (DIEDOT-DEG), the polymerization efficiency was greatly enhanced to afford a PEDOT polymer thin film with excellent optical transparency and electrical conductivity after subsequent chemical doping with protonic acid. Eventually, we have successfully developed a novel one-pot UV photo-polymerization to fabricate a transparent conducting polymer thin film with outstanding electrical conductivity (~2,200 S/cm) and high transparency (> 80%). To our knowledge, this optoelectronic value has not been reported in the conducting polymer thin films through photopolymerization. Considering the facile and simple thin film fabrication process and the corresponding excellent optical and electrical performances, the developed photoarylation-based solid-state polymerization is a promising strategy for the convenient and roll-to-roll fabrication of flexible transparent electrodes.

3.5 Synthesis

3.5.1 Synthetic Schemes for thiophene derivatives

compound 1. 2,5-diiodo-[3,4-(3,3'-dibutylpropylenedioxy)]thiophene (DIDBuProDOT)

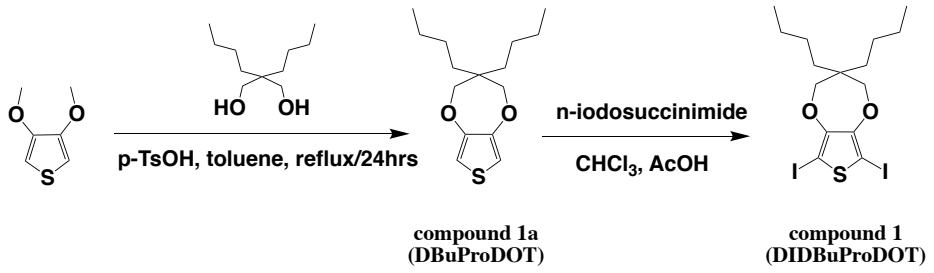

Figure 3.22. Synthetic scheme for DIDBuProDOT

i) compound 1a. 3,4-(3,3'-dibutylpropylenedioxy)thiophene (DBuProDOT)

6g of 3,4-dimethoxythiophene (41.61mmol, 1eq) and 10.187g of 2,2-dibutyl-1,3-propanediol (54.10mmol, 1.3eq) was dissolved in 200ml of toluene with 500mg of p-toluenesulfonic acid. The solution was refluxed at 120°C and the methanol produced by a transetherification of the reactants was removed by type 4A molecular sieves filled in a soxhlet extractor. The mixture was quenched by water after 24 hours reflux, extracted in ethyl acetate, then washed with brine and dried over $MgSO_4$. After evaporating the solvent with a rotary evaporator, the residue was purified by column chromatography with the elution of methylene chloride/hexane (1:4) to give 3,4-(3,3'-dibutylpropylenedioxy) thiophene (DBuProDOT) (69%, 7.70g). ^{1}H-NMR (300MHz, $CDCl_3$); 6.42(s, 2H), 3.85 (s, 4H), 1.46-1.15 (m, 12H), 0.98-0.86 (t, 6H)

ii) compound 1. 2,5-diiodo-[3,4-(3,3'-dibutylpropylenedioxy)]thiophene (DIDBuProDOT)

5g of 3,4-(3,3'-dibutylpropylenedioxy)thiophene (DBuProDOT) (18.63mmol, 1eq) was dissolved in chloroform and stirred with 9.22g of n-iodosuccinimide (40.98mmol, 2.2eq) with a few drops of acetic acid. The mixture was quenched with DI water, washed with sodium thiosulfate to remove excess iodine, and dried over $MgSO_4$, followed by the evaporation in vacuo. The residue was purified with the elution of methylene chloride and hexane (1:8) to yield DIDBuProDOT (85%, 12.68g), ^{1}H-NMR (300MHz, $CDCl_3$); 3.92 (s, 4H), 1.46-1.15 (m, 12H), 0.98-0.86 (t, 6H)

compound 2. 3,4-(3-methylpropylenedioxy)thiophene (MPDOT)

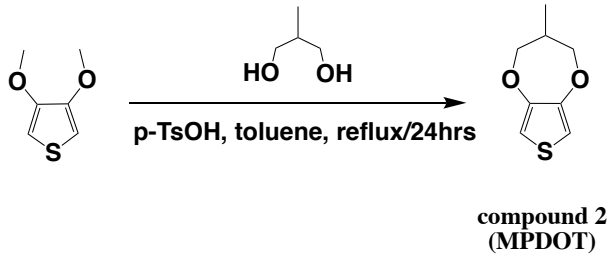

Figure 3.23. Synthetic scheme for MPDOT.

5g of 3,4-dimethoxythiophene (34.68mmol, 1eq) and 3.75g of 2-methyl-1,3-propanediol (41.61mmol, 1.2eq) was dissolved in 200ml of toluene with 500mg of p-toluenesulfonic acid. The solution was refluxed at 120°C and the methanol produced by a transetherification of the reactants was removed by type 4A molecular sieves filled in a soxhlet extractor. The mixture was quenched by water after 24 hours reflux, extracted in ethyl acetate, then washed with brine and dried over $MgSO_4$. After evaporating the solvent with a rotary evaporator, the residue was purified by column chromatography with the elution of methylene chloride/hexane (1:4) to give 3,4-(3-methylpropylenedioxy)thiophene (MPDOT) (55%, 3.25g), ^{1}H-NMR (300MHz, $CDCl_3$); 6.50(s, 2H), 4.18-4.09(q, 2H), 3.75-3.64(q, 2H), 2.46-2.31(m, 1H), 1.03-0.95 (d, 3H)

compound 3. 3,4-[3,3'-(dimethylpropylenedioxy)]thiophene (DMPDOT)

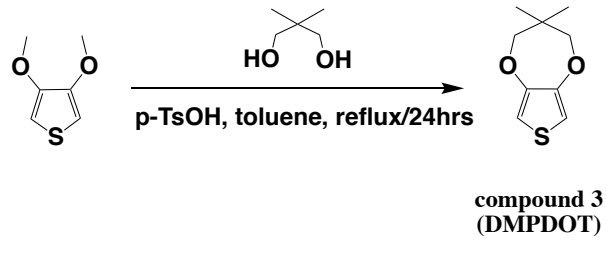

Figure 3.24. Synthetic scheme for DMPDOT.

5g of 3,4-dimethoxythiophene (34.68mmol, 1eq) and 4.72g of 2,2-dimethyl-1,3-propanediol (41.61mmol, 1.2eq) was dissolved in 200ml of toluene with 500mg of p-toluenesulfonic acid. The solution was refluxed at 120°C and the methanol produced by a transetherification of the reactants was removed by type 4A molecular sieves filled in a soxhlet extractor. The mixture was quenched by water after 24 hours reflux, extracted in ethyl acetate, then washed with brine and dried over $MgSO_4$. After evaporating the solvent with a rotary evaporator, the residue was purified by column chromatography with the elution of methylene chloride/hexane (1:4) to give 3,4-(3,3'-dimethylpropylenedioxy) thiophene (DMPDOT) (60%, 3.86g), ^{1}H-NMR (300MHz, $CDCl_3$); 6.48(s, 2H), 3.73(s, 4H), 1.03(s, 6H)

compound 4. 3,4-(3-hexylpropylenedioxy)thiophene (HPDOT)

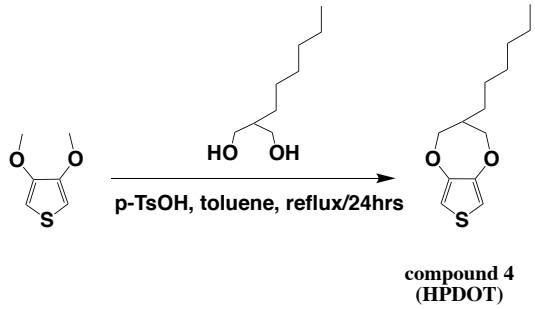

Figure 3.25. Synthetic scheme for HPDOT.

5g of 3,4-dimethoxythiophene (34.68mmol, 1eq) and 6.67g of 2-n-hexyl-1,3-propanediol (41.61mmol, 1.2eq) was dissolved in 200ml of toluene with 500mg of p-toluenesulfonic acid. The solution was refluxed at 120°C and the methanol produced by a transetherification of the reactants was removed by type 4A molecular sieves filled in a soxhlet extractor. The mixture was quenched by water after 24 hours reflux, extracted in ethyl acetate, then washed with brine and dried over $MgSO_4$. After evaporating the solvent with a rotary evaporator, the residue was purified by column chromatography with the elution of methylene chloride/hexane (1:4) to give 3,4-(3-

hexylpropylenedioxy)thiophene (HPDOT) (36%, 3g), ^{1}H-NMR (300MHz, $CDCl_3$); 6.47(s, 2H), 4.21-4.05(m, 2H), 3.93-3.81(m, 2H), 2.35-2.05(m, 1H), 1.47-1.18 (m, 10H), 0.97-0.81 (t, 3H)

compound 5. 3,4-[2,2'-bis(carboxymethyl)propylenedioxy]thiophene (PDOT-DCOOH)

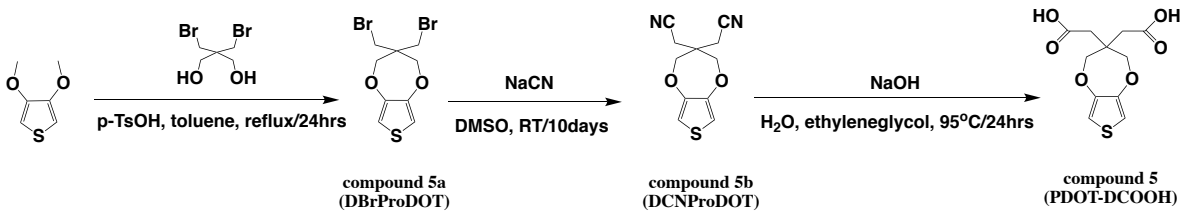

Figure 3.26. Synthetic scheme for PDOT-DCOOH.

i) compound 5a. 3,4-[2,2'-bis(bromomethyl)propylenedioxy]thiophene (DBrProDOT)

5g of 3,4-dimethoxythiophene (34.68mmol, 1eq) and 10.9g of 2,2-Bis(bromomethyl)-1,3-propanediol (41.61mmol, 1.2eq) was dissolved in 200ml of toluene with 500mg of p-toluenesulfonic acid. The solution was refluxed at 120°C and the methanol produced by a transetherification of the reactants was removed by type 4A molecular sieves filled in a soxhlet extractor. The mixture was quenched by water after 24 hours reflux, extracted in ethyl acetate, then washed with brine and dried over $MgSO_4$. After evaporating the solvent with a rotary evaporator, the residue was purified by column chromatography with the elution of methylene chloride/hexane (1:2) to give 3,4-(2,2'-bis(bromomethyl)propylenedioxy)thiophene (DBrProDOT) (45%, 5.34g), ^{1}H-NMR (300MHz, $CDCl_3$); 6.50(s, 2H), 4.10 (s, 4H), 3.62 (s, 4H)

ii) compound 5b. 3,4-[2,2'-bis(cyanomethyl)propylenedioxy]thiophene (DCNProDOT)

5g of 3,4-(2,2'-bis(bromomethyl)propylenedioxy)thiophene (21.34mmol, 1eq) and 2.15g of sodium cyanide (25.61mmol, 1.2 eq) were dissolved in 150ml of DMSO and stirred at room temperature for 10 days. The mixture was quenched by water and extracted in methylene chloride, then washed with brine and dried over $MgSO_4$. After evaporating the solvent with a rotary evaporator, the residue was purified by column chromatography with the elution of methylene chloride/hexane (2:1) to give 3,4-(2,2'-bis(cyanomethyl)propylenedioxy)thiophene (DCNProDOT) (70%, 2.40g), ^{1}H-NMR (300MHz, $CDCl_3$); 6.61(s, 2H), 4.02 (s, 4H), 2.74 (s, 4H)

iii) compound 5. 3,4-[2,2'-bis(carboxymethyl)propylenedioxy]thiophene (PDOT-DCOOH)

2g of 3,4-(2,2'-bis(cyanomethyl)propylenedioxy)thiophene (8.54mmol, 1eq) was dissolved in 100ml of NaOH aqueous solution (2M) and 100ml of ethyleneglycol. The solution was refluxed at 95^{o}C and cooled down to room temperature after 24 hours, then hydrochloric acid aqueous solution (1N) was added. The quenched solution was extracted 3 times with diethylether and washed with brine, followed by drying with $MgSO_4$ and evaporation in vacuo. The residue was precipitated in chloroform to give a crystal form of 3,4-(2,2'-bis(carboxymethyl)propylenedioxy)thiophene. (PDOT-DCOOH) (55%, 1.28g), ^{1}H-NMR (300MHz, DMSO-d_6); 12.34(s, 2H), 6.77(s, 2H), 4.03 (s, 4H), 3.34 (s, 4H)

compound 6. 3,4-[2,2'-bis(hydroxymethyl)propylenedioxy]thiophene (PDOT-DOH)

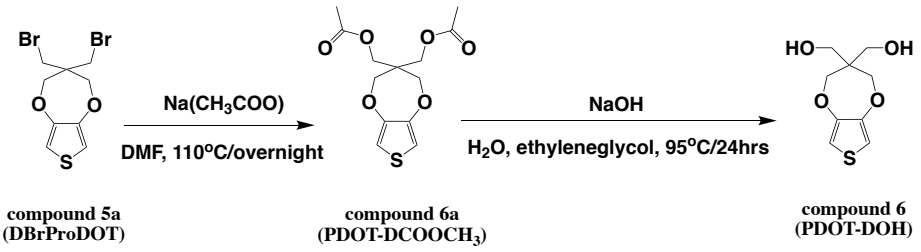

Figure 3.27. Synthetic scheme for PDOT-DOH

i) compound 6a. 3,4-[2,2'-bis(methylethanoate)propylenedioxy]thiophene (PDOT-DCOOCH$_3$)

5g of 3,4-(2,2'-bis(bromomethyl)propylenedioxy)thiophene (DBrProDOT, compound 5a, 14.62mmol, 1eq) and 12g of sodium acetate (0.146mol, 10eq) were dissolved in 150ml of DMF and refluxed at 110^{o}C overnight. After cooling down to room temperature, the solution was quenched with water and extracted 3 times into ethyl acetate, then washed with brine and dried with $MgSO_4$, followed by evaporation in vacuo. The residue was purified with column chromatography with ethyl acetate/hexane (1:2) to give 3,4-(2,2'-bis(methylethanoate)propylenedioxy)thiophene (PDOT-DCOOCH$_3$). (80%, 3.51g), ^{1}H-NMR (300MHz, $CDCl_3$); 6.49(s, 2H), 4.19 (s, 4H), 4.05 (s, 4H), 2.08 (s, 6H)

ii) compound 6. 3,4-(2,2'-bis(hydroxymethyl)propylenedioxy)thiophene (PDOT-DOH)

3g of 3,4-(2,2'-bis(methylethanoate)propylenedioxy)thiophene (PDOT-DCOOCH$_3$, 9.99mmol, 1eq) was dissolved in 15ml of NaOH aqueous solution(2M) and 15ml of acetonitrile and stirred at room temperature overnight. The solution was diluted with 2N H_2SO_4, extracted with

ethyl acetate, and washed with brine. After drying the residue with $MgSO_4$, the residue was purified with chloroform precipitation to give 3,4-(2,2'-bis(hydroxymethyl) propylenedioxy)thiophene (PDOT-DOH) (77%, 1.66g), ^{1}H-NMR (300MHz, DMSO-d_6); 6.69(s, 2H), 4.65 (t, 2H), 3.88 (s, 4H), 3.49-3.40(d, 4H)

compound 7. 3,4-[(2-methyl-2'-triethylsilylester)propylenedioxy]thiophene (PDOT-COOTESi)

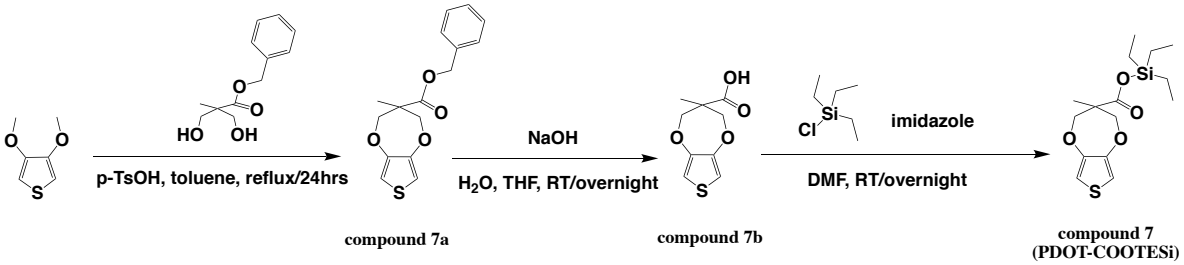

Figure 3.28. Synthetic scheme for PDOT-COOTESi.

i) compound 7a. 3,4-((2-methyl-2'-phenylmethylester)propylenedioxy)thiophene

5g of 3,4-dimethoxythiophene (34.68mmol, 1eq) and 9.33g of 2,2-Bis(hydroxymethyl)propionic acid (41.61mmol, 1.2eq) was dissolved in 200ml of toluene with 500mg of p-toluenesulfonic acid. The solution was refluxed at 120^{o}C and the methanol produced by a transetherification of the reactants was removed by type 4A molecular sieves filled in a soxhlet extractor. The mixture was quenched by water after 24 hours reflux, extracted in ethyl acetate, then washed with brine and dried over $MgSO_4$. After evaporating the solvent with a rotary evaporator, the residue was purified by column chromatography with the elution of methylene

chloride/hexane (1:2) to give 3,4-((2-methyl-2'-phenylmethylester)propylenedioxy)thiophene. (25%, 2.64g), ^{1}H-NMR (300MHz, $CDCl_3$); 7.35(m, 5H), 6.47(s, 2H), 4.59-4.45 (d, 2H), 4.00-3.90 (d, 2H), 1.28 (t, 3H)

ii) compound 7b. 3,4-((2-methyl-2'-carboxyl)propylenedioxy)thiophene

2.5g of 3,4-((2-methyl-2'-phenylmethylester)propylenedioxy)thiophene (8.21mmol, 1eq) was dissolved in 20ml of THF and 20ml of sodium hydroxide aqueous solution (2M) and stirred overnight. The solution was extracted with ethyl acetate and washed with brine. After drying the organic layer with $MgSO_4$ and evaporating in vacuo, the residue was purified with chloroform precipitation to give 3,4-((2-methyl-2'-carboxyl)propylenedioxy) thiophene. (60%, 1.06g), ^{1}H-NMR (300MHz, DMSO-d_6); 12.96(s, 1H), 6.79(s, 2H), 4.42-4.30 (d, 2H), 3.94-3.79 (d, 2H), 1.18(s, 3H)

iii) compound 7. 3,4-((2-methyl-2'-triethylsilylester)propylenedioxy)thiophene (PDOT-COOTESi)

1g of 3,4-((2-methyl-2'-carboxyl)propylenedioxy)thiophene (4.67mmol, 1eq) and 0.477g of imidazole (7.00mmol, 1.5eq) was dissolved in DMF and stirred. To the solution, 0.352ml of chlorotriethylsilane was added dropwise and stirred overnight. The solution was quenched with water and extracted with ethyl acetate. After drying the organic layer with $MgSO_4$ and evaporating in vacuo, the residue was purified with chloroform precipitation to give 3,4-((2-methyl-2'-triethylsilylester)propylenedioxy)thiophene (80%, 1.23g), ^{1}H-NMR (300MHz, $CDCl_3$); 6.49(s, 2H), 4.56-4.46 (d, 2H), 3.98-3.87 (d, 2H), 1.31(s, 3H), 1.04-0.90(m, 9H), 0.66-0.54(m, 6H)

compound 8. 3,4-[2,2'-bis(2-nitro-5-(dodecyloxy)benzylcarboxylic)propylenedioxy] thiophene (PDOT-PC)

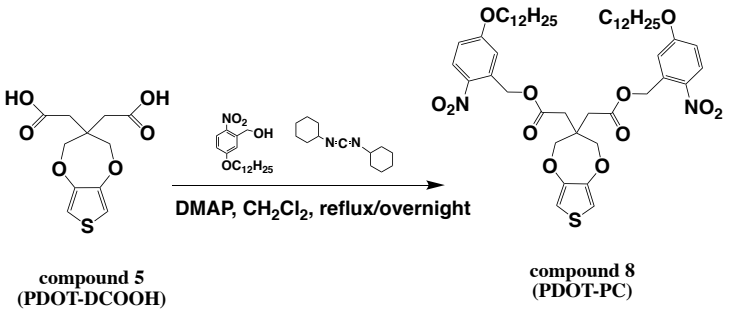

Figure 3.29. Synthetic scheme for PDOT-PC.

i) (2-Nitro-5-(dodecyloxy)phenyl)methanol

The synthesis was carried out according to the reference.[24] ^{1}H-NMR (300MHz, $CDCl_3$); 8.20-8.17(d, 1H), 7.20(d, 1H), 6.90-6.87(dd, 1H), 5.00(d, 2H), 4.09-4.06(m, 2H), 1.84-1.81(m, 2H), 1.47(m, 2H), 0.91-0.87(t, 3H)

ii) Compound 8 (PDOT-PC)

1g of 3,4-(2,2'-bis(carboxylmethyl)propylenedioxy)thiophene (3.67mmol, 1eq), 2.73g of 2-Nitro-5-(dodecyloxy)phenyl)methanol (8.08mmol, 2.2eq) prepared in the reference[25], and 2.27g of DMAP(8.08mmol, 2.2eq) was dissolved in anhydrous methylene chloride under argon purging. To the solution, 1.67g of N,N'-dicyclohexylcarbodiimide (8.08mmol, 2.2eq) dissolved in 15ml of anhydrous methylene chloride was added. The mixture was refluxed overnight and cooled down to room temperature. The solution was quenched with 1N of HCl and $NaHCO_3$, then the organic layer was dried with $MgSO_4$ and evaporated in vacuo. The residual was purified with column

chromatography on silica using methylene chloride/hexane(1:1) to give 3,4-(2,2'-bis(2-nitro-5-(dodecyloxy)benzylcarboxylic)propylenedioxy)thiophene. (50%, 1.67g), ^{1}H-NMR (300MHz, $CDCl_3$); 8.16-8.13(d, 2H), 7.00-6.99(d, 2H), 6.81-6.80(dd, 2H), 6.49(s, 2H), 5.50(s, 4H), 4.12(s, 4H), 4.01-3.99(t, 4H), 2.90(s, 4H), 1.81-1.77(m, 4H), 1.43(m, 4H), 0.97-0.85(t, 6H)

compound 9. 2,5-diiodo-[3,4-(2-(2-(2-methoxyethoxy)ethoxy)methyl)ethylenedioxy] thiophene (DIEDOT-DEG)

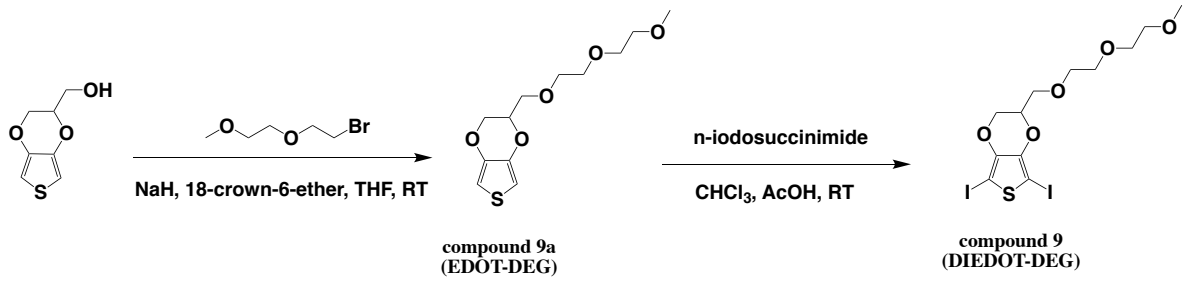

Figure 3.30. Synthetic scheme for DIEDOT-DEG.

i) compound 9a. [(2-(2-(2-methoxyethoxy)ethoxy)methyl)ethylenedioxy]thiophene (EDOT-DEG)

0.581g of NaH (60% with oil, 14.52mmol, 5.0eq) and 76.8mg of 18-crown-6-ether(0.29mmol, 0.1eq) were added and stirred in 15ml of THF purged with argon. To the cooled solution with iced water, 0.5g of hydroxymethyl EDOT(2.90mmol, 1eq) was added and stirred for 1 hour at room temperature. The solution was cooled down to 0^{o}C with ice and 0.47ml of 1-bromo-2-(2-methoxyethoxy)ethane (3.48mmol, 1.2eq)was added dropwise. The solution was refluxed at 80^{o}C for 24 hours and cooled down to room temperature, then quenched with 1N HCl dropwise, followed by the extraction with diethyl ether 3 times. The organic layer was washed 1N HCl and

brine, then dried with $MgSO_4$ and evaporated under vacuo. The residue was purified with column chromatography to give EDOT-DEG. (50%, 400mg), ^{1}H-NMR (300MHz, $CDCl_3$); 6.32(s, 2H), 4.39-4.29 (m, 2H), 4.12-3.99(m, 1H), 3,84-3.62(m, 8H), 3.59-3.49(m, 2H), 3.38 (t, 3H)

ii) compound 9. 2,5-diiodo-[(2-(2-(2-methoxyethoxy)ethoxy)methyl)ethylenedioxy] thiophene (DIEDOT-DEG)

300mg of EDOT-DEG (1.09mmol, 1eq) was dissolved in chloroform and stirred with excess n-iodosuccinimide (2.41mmol, 2.2eq) with a few drops of acetic acid. The mixture was quenched with DI water, washed with sodium thiosulfate to remove excess iodine, and dried over $MgSO_4$, followed by the evaporation in vacuo. The residue was purified with the elution of methylene chloride and hexane (1:8) to yield DIEDOT-DEG. (84%, 0.48g) ^{1}H-NMR (300MHz, $CDCl_3$); 4.40-4.28 (m, 2H), 4.20-4.07(m, 1H), 3.91-3.60(m, 8H), 3.60-3.50(m, 2H), 3.38 (t, 3H)

compound 10. Azidomethyl EDOT (EDOT-N_3)

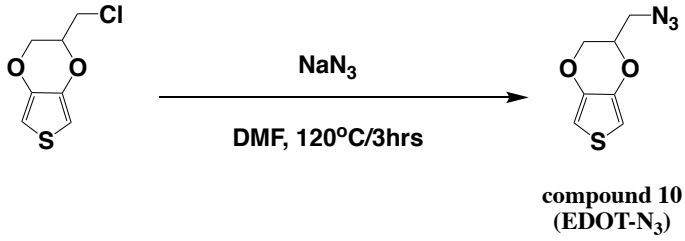

Figure 3.31. Synthetic scheme for EDOT-N_3.

0.5g of chloromethyl EDOT(2.62mmol, 1.0eq, 95%, Sigma Aldrich) was dissolved in 25ml of DMF under argon and 0.341g of sodium azide (5.24mmol, 2.0eq) was added. The mixture was refluxed at 120°C for 3 hours and cooled down to room temperature, followed by quenching with

water. The mixture was extracted into diethylether and the resulting organic layer was washed with brine, dried by $MgSO_4$, and evaporated in vacuo. The residue was purified with methylene chloride/hexane (1:2) to give azidomethyl EDOT. (74%, 0.38g), ^{1}H-NMR (300MHz, $CDCl_3$); 6.45-6.22(q, 2H), 4.39-4.13 (m, 2H), 4.13-3.97(m, 1H), 3.66-3.41(m, 2H)

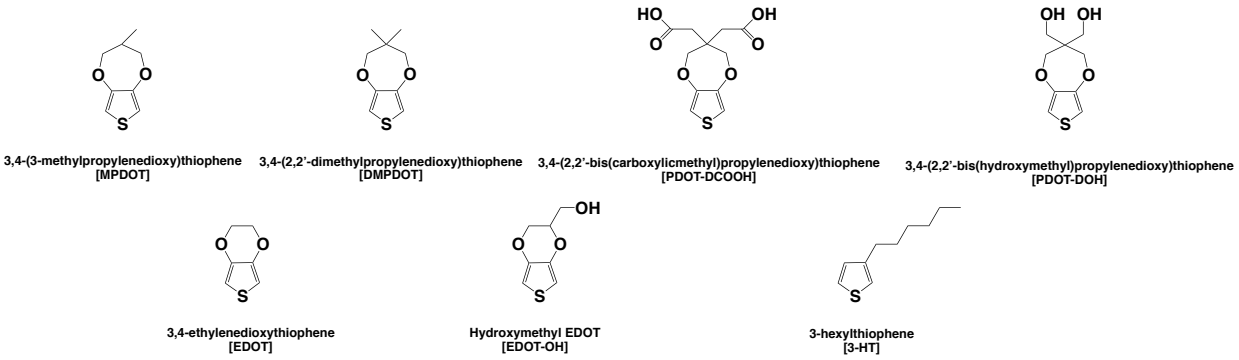

Figure 3.32. Monomers copolymerized with DIDBuProDOT.

3.5.2 ^{1}H-NMR spectra of thiophene derivatives

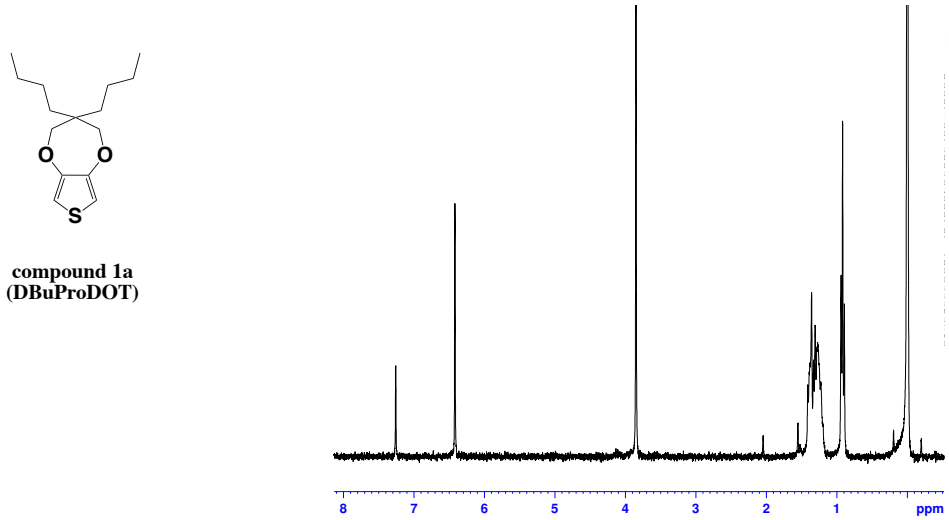

Figure 3.33. ^{1}H-NMR spectrum of 3,4-(3,3'-dibutylpropylenedioxy)thiophene (DBuProDOT). ^{1}H-NMR (300MHz, $CDCl_3$); 6.42(s, 2H), 3.85 (s, 4H), 1.46-1.15 (m, 12H), 0.98-0.86 (t, 6H)

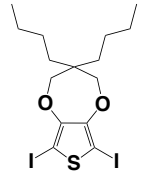

compound 1
(DIDBuProDOT)

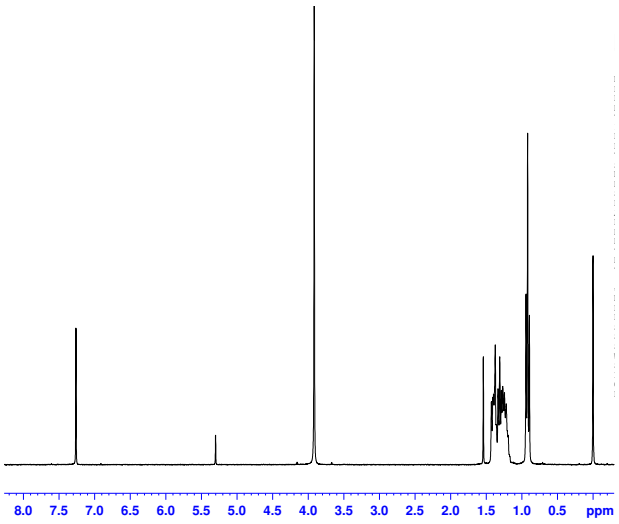

Figure 3.34. ^{1}H-NMR spectrum of 2,5-diiodo-[3,4-(3,3'-dibutylpropylenedioxy)] thiophene (DIDBuProDOT).^{1}H-NMR (300MHz, $CDCl_3$); 3.92 (s, 4H), 1.46-1.15 (m, 12H), 0.98-0.86 (t, 6H)

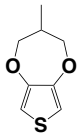

compound 2
(MPDOT)

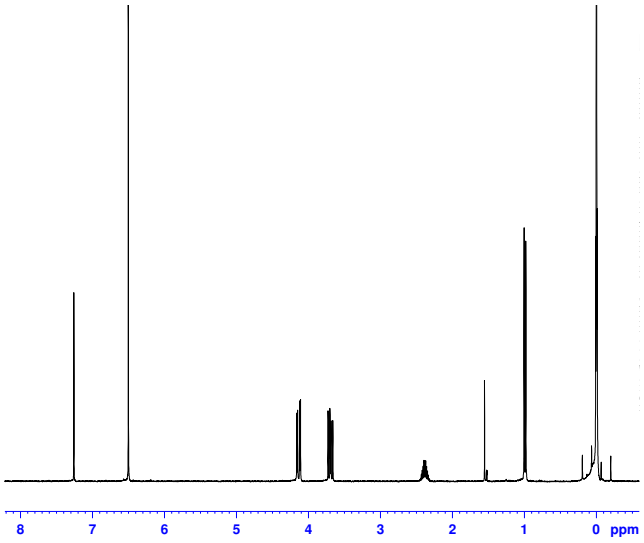

Figure 3.35. ^{1}H-NMR spectrum of 3,4-(3-methylpropylenedioxy)thiophene (MPDOT). ^{1}H-NMR (300MHz, $CDCl_3$); 6.50(s, 2H), 4.18-4.09(q, 2H), 3.75-3.64(q, 2H), 2.46-2.31(m, 1H), 1.03-0.95 (d, 3H)

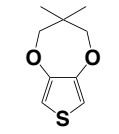

compound 3 (DMPDOT)

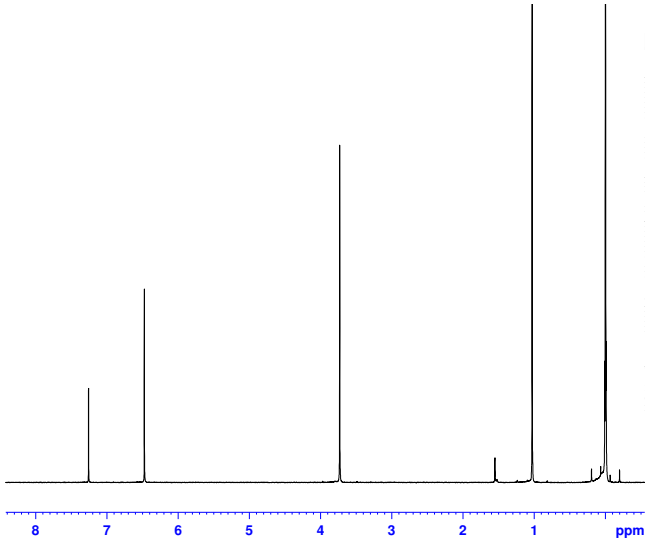

Figure 3.36. ^{1}H-NMR spectrum of 3,4-[3,3'-(dimethylpropylenedioxy)]thiophene (DMPDOT). ^{1}H-NMR (300MHz, $CDCl_3$); 6.48(s, 2H), 3.73(s, 4H), 1.03(s, 6H)

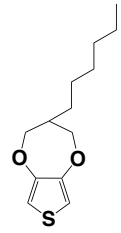

compound 4 (HPDOT)

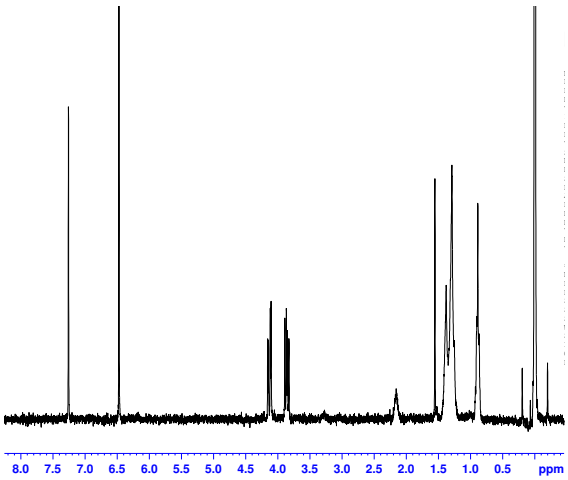

Figure 3.37. ^{1}H-NMR spectrum of 3,4-(3-hexylpropylenedioxy)thiophene (HPDOT). ^{1}H-NMR (300MHz, $CDCl_3$); 6.47(s, 2H), 4.21-4.05(m, 2H), 3.93-3.81(m, 2H), 2.35-2.05(m, 1H), 1.47-1.18 (m, 10H), 0.97-0.81 (t, 3H)

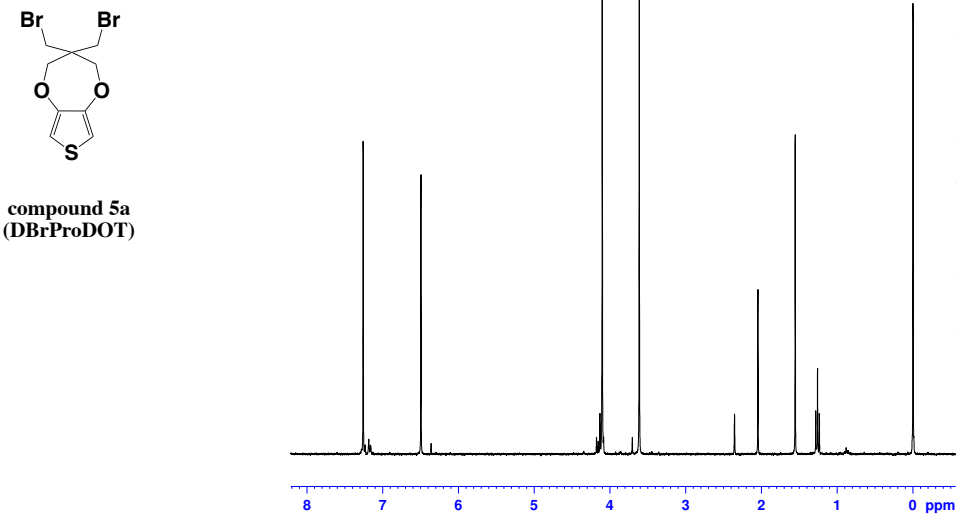

compound 5a (DBrProDOT)

Figure 3.38. ^{1}H-NMR spectrum of 3,4-[2,2'-bis(bromomethyl)propylenedioxy] thiophene (DBrProDOT), ^{1}H-NMR (300MHz, $CDCl_3$); 6.50(s, 2H), 4.10 (s, 4H), 3.62 (s, 4H)

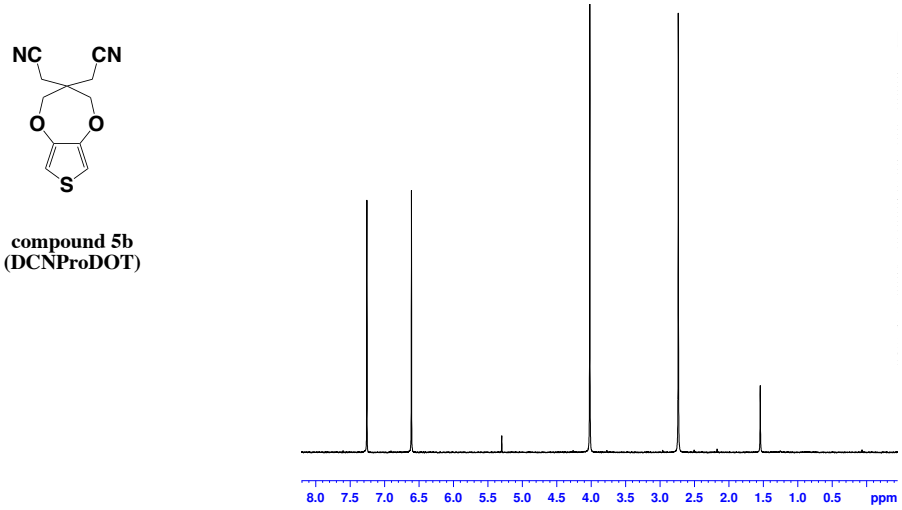

compound 5b (DCNProDOT)

Figure 3.39. ^{1}H-NMR spectrum of 3,4-[2,2'-bis(cyanomethyl)propylenedioxy] thiophene (DCNProDOT). ^{1}H-NMR (300MHz, $CDCl_3$); 6.61(s, 2H), 4.02 (s, 4H), 2.74 (s, 4H)

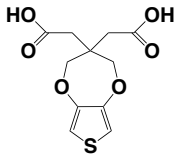

compound 5
(PDOT-DCOOH)

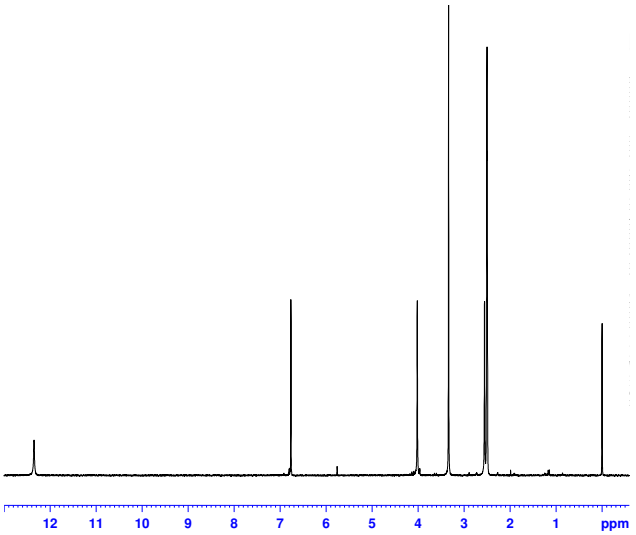

Figure 3.40. ^{1}H-NMR spectrum of 3,4-[2,2'-bis(carboxymethyl)propylenedioxy] thiophene (PDOT-DCOOH). ^{1}H-NMR (300MHz, DMSO-d_6); 12.34(s, 2H), 6.77(s, 2H), 4.03 (s, 4H), 3.34 (s, 4H)

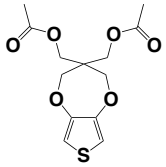

compound 6a
(PDOT-DCOOCH$_3$)

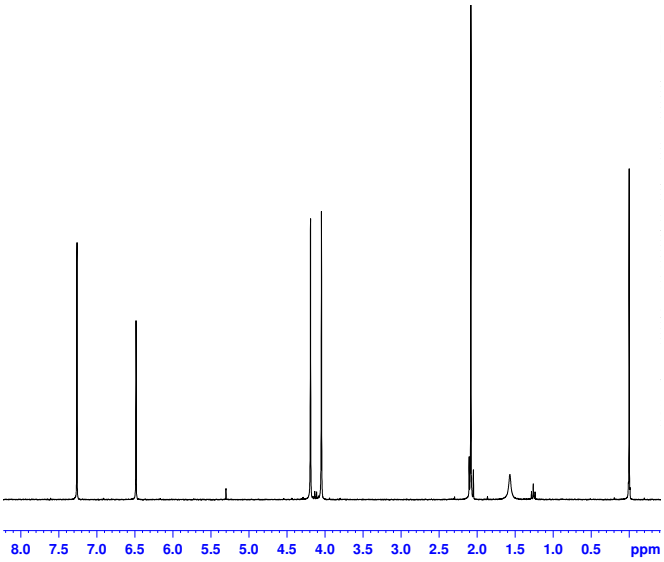

Figure 3.41. ^{1}H-NMR spectrum of 3,4-[2,2'-bis(methylethanoate)propylenedioxy] thiophene (PDOT-DCOOCH$_3$). ^{1}H-NMR (300MHz, $CDCl_3$); 6.49(s, 2H), 4.19 (s, 4H), 4.05 (s, 4H), 2.08 (t, 6H)

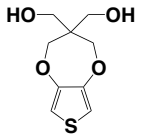

compound 6
(PDOT-DOH)

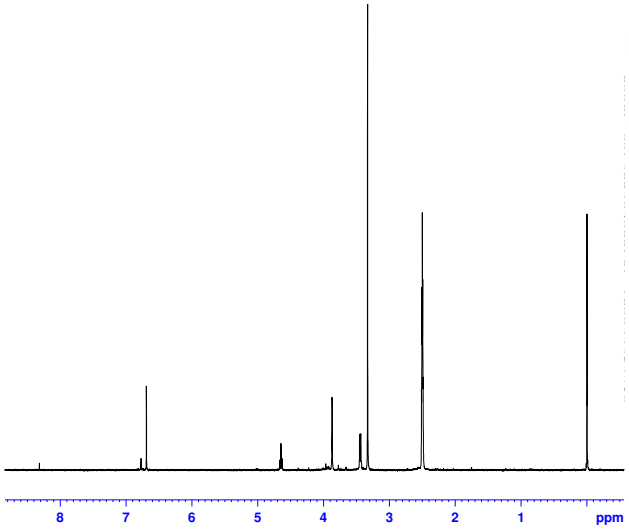

Figure 3.42. ^{1}H-NMR spectrum of 3,4-(2,2'-bis(hydroxymethyl)propylenedioxy) thiophene (PDOT-DOH). ^{1}H-NMR (300MHz, DMSO-d_6); 6.69(s, 2H), 4.65 (t, 2H), 3.88 (s, 4H), 3.49-3.40(d, 4H)

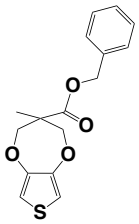

compound 7a

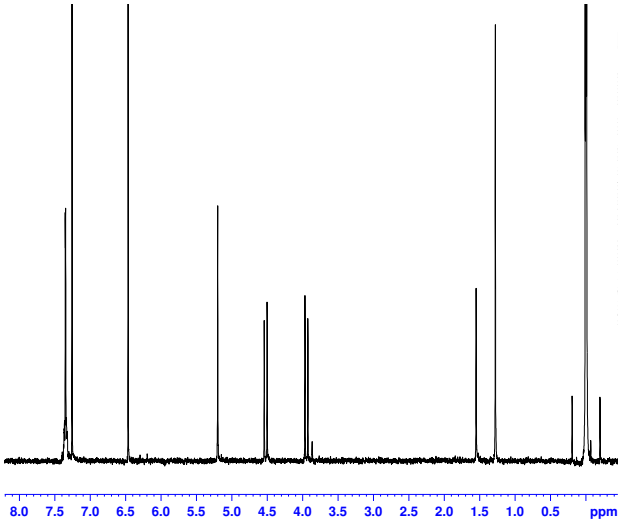

Figure 3.43. ^{1}H-NMR spectrum of 3,4-((2-methyl-2'-phenylmethylester)propylenedioxy) thiophene. ^{1}H-NMR(300MHz, $CDCl_3$); 7.35(m, 5H),6.47(s, 2H),4.59-4.45(d, 2H),4.00-3.90(d, 2H), 1.28(t, 3H)

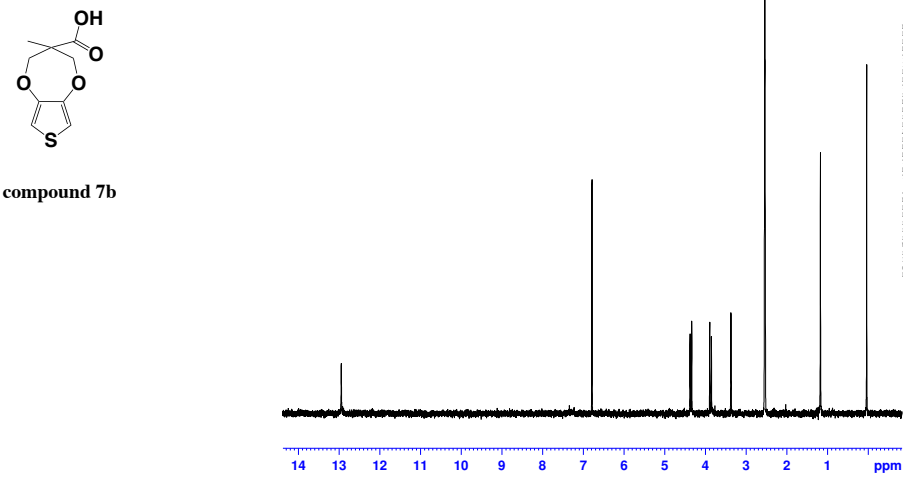

Figure 3.44. [1]H-NMR spectrum of 3,4-((2-methyl-2'-carboxyl)propylenedioxy) thiophene. [1]H-NMR(300MHz,DMSO-d_6);12.96(s,1H),6.79(s,2H),4.42-4.30(d,2H),3.94-3.79(d,2H),1.18(s, 3H)

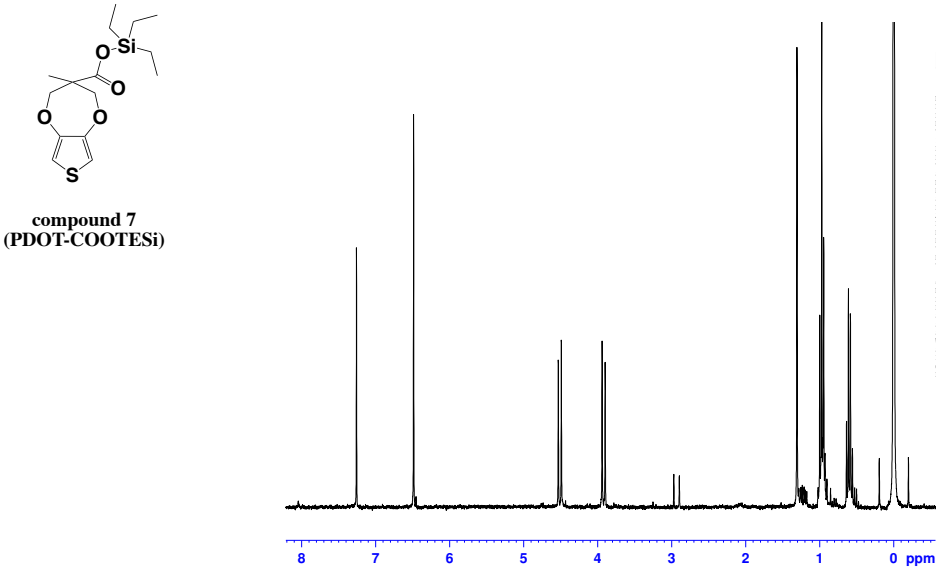

Figure 3.45. [1]H-NMR spectrum of 3,4-((2-methyl-2'-triethylsilylester)propylenedioxy) thiophene (PDOT-COOTESi). [1]H-NMR (300MHz, $CDCl_3$); 6.49(s, 2H), 4.56-4.46 (d, 2H), 3.98-3.87 (d, 2H), 1.31(s, 3H), 1.04-0.90(m, 9H), 0.66-0.54(m, 6H)

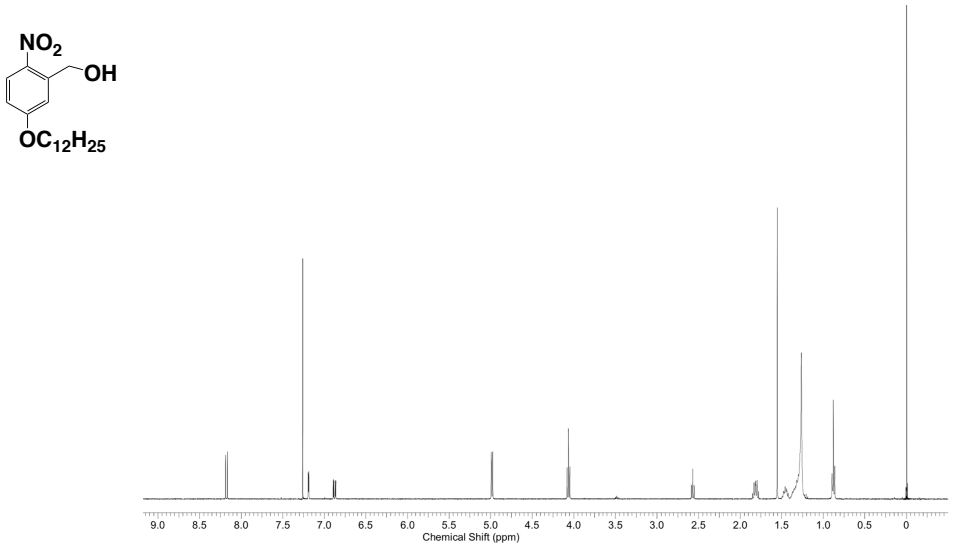

Figure 3.46. ^{1}H-NMR spectrum of 2-Nitro-5-(dodecyloxy)phenyl)methanol. ^{1}H-NMR (300MHz, $CDCl_3$); 8.20-8.17(d, 1H), 7.20(d, 1H), 6.90-6.87(dd, 1H), 5.00(d, 2H), 4.09-4.06(m, 2H), 1.84-1.81(m, 2H), 1.47(m, 2H), 0.91-0.87(t, 3H)

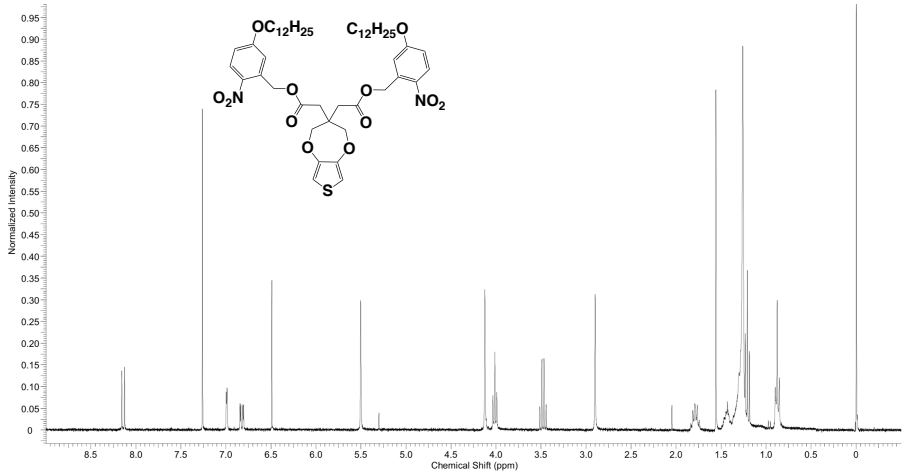

Figure 3.47. ^{1}H-NMR spectrum of 3,4-(2,2'-bis(2-nitro-5-(dodecyloxy) benzylcarboxylic) propylenedioxy)thiophene. ^{1}H-NMR (300MHz, $CDCl_3$); 8.16-8.13(d, 2H), 7.00-6.99(d, 2H), 6.81-6.80(dd, 2H), 6.49(s, 2H), 5.50(s, 4H), 4.12(s, 4H), 4.01-3.99(t, 4H), 2.90(s, 4H), 1.81-1.77(m, 4H), 1.43(m, 4H), 0.97-0.85(t, 6H)

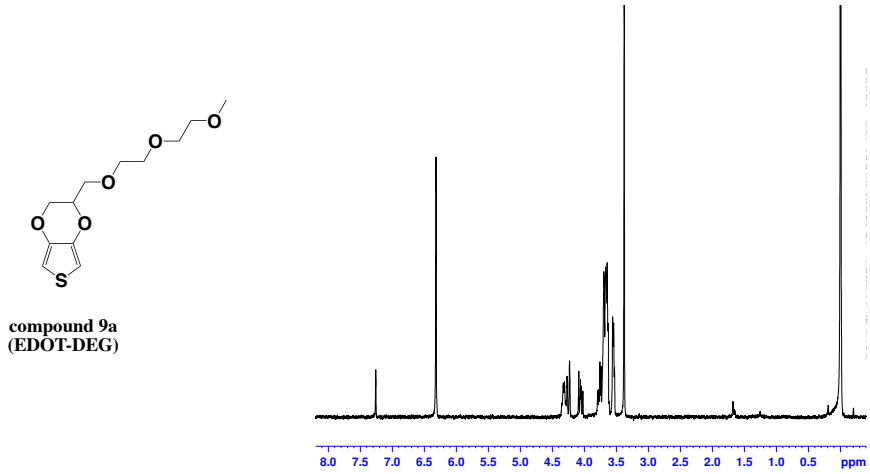

Figure 3.48. ^{1}H-NMR spectrum of [(2-(2-(2-methoxyethoxy)ethoxy)methyl) ethylenedioxy] thiophene (EDOT-DEG). ^{1}H-NMR (300MHz, $CDCl_3$); 6.32(s, 2H), 4.39-4.29 (m, 2H), 4.12-3.99(m, 1H), 3,84-3.62(m, 8H), 3.59-3.49(m, 2H), 3.38 (t, 3H)

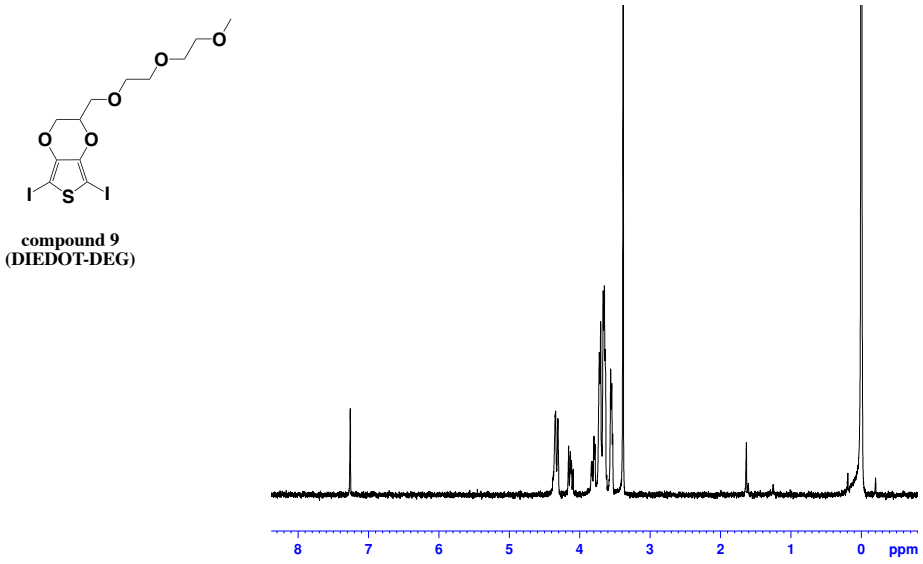

Figure 3.49. ^{1}H-NMR spectrum of 2,5-diiodo-[(2-(2-(2-methoxyethoxy)ethoxy)methyl) ethylenedioxy]thiophene (DIEDOT-DEG). ^{1}H-NMR (300MHz, $CDCl_3$); 6.32(s, 2H), 4.39-4.29 (m, 2H), 4.12-3.99(m, 1H), 3,84-3.62(m, 8H), 3.59-3.49(m, 2H), 3.38 (t, 3H)

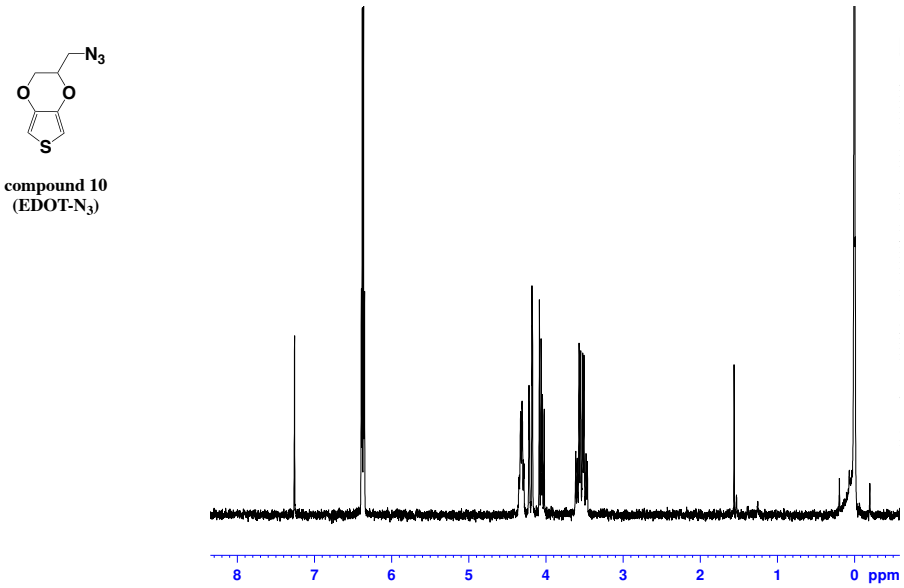

Figure 3.50. ^{1}H-NMR spectra of Azidomethyl EDOT (EDOT-N_3). ^{1}H-NMR(300MHz,$CDCl_3$); 6.45-6.22(q, 2H),4.39-4.13 (m, 2H),4.13-3.97(m, 1H),3.66-3.41(m, 2H)

3.6 References

1. Vosqueritchian, M., Lipomi, D., Bao, Z. Highly Conductive and Transparent PEDOT:PSS Films with a Fluorosurfactant for Stretchable and Flexible Transparent Electrodes. *Adv. Funct. Mater.* **22**, 421–428 (2012).
2. Cho, C. K., Hwang, W. J., Eun, K., Choa, S. H., Na, S. I., Kim, H. K. Mechanical Flexibility of Transparent PEDOT:PSS Electrodes Prepared by Gravure Printing for Flexible Organic Solar Cells. *Sol. Energy Mater. Sol. Cells* **95**, 3269–3275 (2011).
3. Ziebarth, J. M., Saafir, A. K., Fan, S., McGehee, M. D. Extracting Light from Polymer Light-Emitting Diodes Using Stamped Bragg Gratings. *Adv. Funct. Mater.* **14**, 451–456 (2004).
4. Lambropoulos, Maragakis, P., Zhang, P., Fittinghoff, J., Bolton, D. N., Chang, P. R., Kulander, B., Walker, K. C. Improving the Performance of Doped π-Conjugated Polymers for Use in Organic Light-Emitting Diodes. *Nature* **405**, 661–665 (2000).
5. Rosseinsky, D. R., Mortimer, R. J. Electrochromic Systems and the Prospects for Devices. *Adv. Mater.* **13**, 783–793. (2001).
6. Argun, A. A., Cirpan, A., Reynolds, J. R. The First Truly All-Polymer Electrochromic Devices. *Adv. Mater.* **15***,* 1338–1341 (2003).
7. Jensen, J., Hösel, M., Kim, I., Yu, J. S., Jo, J., Krebs, F. C. Fast Switching ITO Free Electrochromic Devices. *Adv. Funct. Mater.* **24**, 1228–1233 (2014).
8. Li, H., Decoster, M. E., Ireland, R. M., Song, J., Hopkins, P. E., Katz, H. E. Modification of the Poly(Bisdodecylquaterthiophene) Structure for High and Predominantly Nonionic Conductivity with Matched Dopants. *J. Am. Chem. Soc.* **139**, 11149–11157 (2017).

9. Meng, H., Perepichka, D. F., Bendikov, M., Wudl, F., Pan, G. Z., Yu, W., Dong, W., Brown, S. Solid-State Synthesis of a Conducting Polythiophene via an Unprecedented Heterocyclic Coupling Reaction. *J. Am. Chem. Soc.* **125** (49), 15151–15162 (2003).

10. Pistillo, B. R., Menguelti, K., Desbenoit, N., Arl, D., Leturcq, R., Ishchenko, O. M., Kunat, M., Baumann, P. K., Lenoble, D. One Step Deposition of PEDOT Films by Plasma Radicals Assisted Polymerization via Chemical Vapour Deposition. *J. Mater. Chem. C* **4**, 5617–5625 (2016).

11. Natarajan, S., Kim, S. H. Photochemical Oligomerization Pathways in 2,5-Diiodothiophene Film. *J. Photochem. Photobiol. A Chem.* **188**, 342–345 (2007).

12. Natarajan, S., Kim, S. H. Photochemical Conversion of 2,5-Diiodothiophene Condensed on Substrates to Oligothiophene and Polythiophene Thin Films and Micro-Patterns. *Thin Solid Films* **496**, 606–611 (2006).

13. D'Auria, M., Distefano, C., D'Onofrio, F., Mauriello, G., Racioppi, R. Photochemical Substitution of Polyhalogenothiophene and Halogenothiazole Derivatives. *J. Chem. Soc. Perkin Trans. 1* **20**, 3513–3518 (2000).

14. Elisei, F., Latterini, L., Aloisi, G. G., D'Auria, M. Photoinduced Substitution Reactions in Halothiophene Derivatives. Steady State and Laser Flash Photolytic Studies. *J. Phys. Chem.* **99**, 5365–5372 (1995).

15. D'Auria, M. Photochemical and Photophysical Behavior of Thiophene. *Adv. Heterocycl. Chem.,***104**, 127–390 (2011).

16. D'Auria, M., Distefano, C., D'Onofrio, F., Mauriello, G., Racioppi, R. Photochemical Substitution of Polyhalogenothiophene and Halogenothiazole Derivatives. *J. Chem. Soc. Perkin Trans. 1* **20**, 3513–3518 (2000).

17. Dauria, M., Mauriello, G. Synthesis and Photochemical Properties of Nitrothienyl Derivatives. *Photochem. Photobiol.* **60**, 542–545 (1994).

18. D'Auria, M., De Mico, A., D'Onofrio, F., Piancatelli, G. Italian Pat. Appl. 479799A90. (1990).

19. Welsh, D. M., Kloeppner, L. J., Madrigal, L., Pinto, M. R.,Thompson, B. C., Schanze, K. S., Abboud, K. A., Powell, D., Reynolds, J. R. Regiosymmetric Dibutyl-Substituted Poly(3,4-Propylenedioxythiophene)s as Highly Electron-Rich Electroactive and Luminescent Polymers. *Macromolecules* **35**, 6517–6525 (2002).

20. Perepichka, I. F., Besbes, M., Levillain, E., Sallé, M., Roncali, J. Hydrophilic Oligo(Oxyethylene)-Derivatized Poly(3,4-Ethylenedioxythiophenes): Cation-Responsive Optoelectroelectrochemical Properties and Solid-State Chromism. *Chem. Mater.* **14**, 449–457 (2002).

21. Elisei, F., Latterini, L., Aloisi, G., D 'auria, M. Photoinduced Substitution Reactions in Halothiophene Derivatives. Steady State and Laser Flash Photolytic Studies. *J. Phys. Chem*. **99**, 5365–5372 (1995).

22. Kang, S. K., Kim, J.-H., An, J., Lee, E. K., Cha, J., Lim, G., Park, Y. S., Chung, D. J. Synthesis of Polythiophene Derivatives and Their Application for Electrochemical DNA Sensor. *Polym. J.* **36**, 937–942 (2004).

23. Kyba, E. P., Abramovitch, R. A. Photolysis of Alkyl Azides. Evidence for a Nonnitrene Mechanism. *J. Am. Chem. Soc.* **102**, 735–740 (1980).

24. Smith, Z. C., Pawle, R. H., Thomas, S. W. Photoinduced Aggregation of Polythiophenes. *ACS Macro Lett.* **1**, 825–829 (2012).

25. Smith, Z. C., Meyer, D. M., Simon, M. G., Staii, C., Shukla, D., Thomas, S. W. Thiophene-Based Conjugated Polymers with Photolabile Solubilizing Side Chains. *Macromolecules* **48**,956-966 (2015).

Chapter 4. Conclusions and Future Outlook

4.1 Research Summary

Photoarylation is systematically examined as an essential tool for the photopolymerization of EDOT or ProDOT monomers. Photoarylation of 2,5-diiodo-EDOT (or ProDOT) with thiophene derivatives by UV light leads to the formation of conjugated molecules in a high yield. The photochemical reaction is substantially attractive in the sense that only monomers and light irradiation are involved in the coupling reaction without any photochemical catalysts or photoinitiators. By expanding the photoarylation scheme to a polymer regime, we have successfully achieved a variety of conjugated polymers through one-pot photopolymerization. Mechanistic studies on the devised solution photo-polymerization of conjugated polymers revealed the photopolymerization mechanism (**chapter 2**) and the photo-reaction scheme was adapted to the development of solid-state photopolymerization to fabricate highly transparent and conducting polymer thin films (**chapter 3**).

A new light-controlled polymerization system was established in two consecutive photochemical reactions: i) photoarylation of diiodo-ProDOT and ProDOT derivatives by 365nm UV irradiation to yield ProDOT oligomers, ii) after reviving carbon-iodine end groups subsequent coupling of the oligomers by 532nm pulsed laser for chain extension. The conversion efficiency

of the ProDOT derivatives by photoarylation in hydrogen-free $CBrCl_3$ is high enough to consume most monomers in 72 hours of UV irradiation, yielding ProDOT oligomers with narrow polydispersity. The limited chain growth up to an oligomer level caused by the formation of carbon-hydrogen end groups of the oligomers, which is not reactive anymore to UV light, was resolved by the iodine replenishment for C-I end group restoration and subsequent photo-irradiation with 532nm pulsed laser. We achieved ProDOT polymers with a high molecular weight (M_n=27,000 g/mol) and narrow polydispersity (PDI=1.20) by applying the newly devised one-pot photopolymerization.

Inspired by the excellent photochemical reactivity of the ProDOT derivatives in the photoarylation scheme in solution, one-pot solid-state photopolymerization of ProDOT or EDOT derivatives has been successfully devised to achieve highly robust and solvent-resistant conjugated polymer thin films. UV irradiation on DIProDOT(or DIEDOT) and ProDOT(EDOT) derivatives in solid state and subsequent acid doping afford transparent conducting polymer thin films. In particular, the incorporation of flexible oligomeric ethylene glycol side chains to EDOT monomers promotes the movement of the precursors and chain propagation during the UV polymerization, resulting in a dramatic increase in conductivity up to 2,200 S/cm. To the best of our knowledge, such a high value has not been realized by means of any photo-mediated polymerization and is comparable to the best conductivity (1,600~2,400 S/cm) of PEDOT:PSS films post-treated with ethylene glycol[1] or acids[2,3] or ITO coated PET films or glasses (10^3~10^4 S/cm)[4].

4.2 Future work

4.2.1 Research development

Although the solution photopolymerization provides a great opportunity to synthesize conjugated polymers with a high molecular weight and narrow polydispersity, the repeating units

of the resulting polymers were incorporated in random fashion. When the photopolymerization is adapted to copolymerization of two different monomers, it is evident that the resulting polymer gives a disordered distribution of the two repeating units along the polymer chain. Photo-controlled radical polymerization (photo-CRP) is a compelling strategy to devise highly ordered molecular architectures rendering efficient packing of the 2D polymer chains to enhance optical and electrical properties. Since the chain growth is accomplished by sequential addition of monomer "A" to the pre-synthesized polymer "B",[5] it is advantageous to synthesize conjugated block-copolymers having two different side chains affording self-assembled and highly oriented nanostructures in solid state. We believe that a photochemical coupling reaction of iodinated ProDOT oligomers and neighboring ProDOT monomers by 532nm pulsed laser has great potential to establish a photo-CRP for conjugated polymers with a well-defined molecular structure.

Considering that there is a great demand in thin, light-weight, and foldable displays,[6] a polymeric substrate is regarded as an indispensable platform to fabricate flexible electronic devices. As we established the new UV polymerization scheme of conjugated polymers on glass substrates, it would be feasible and desirable to demonstrate excellent optical and electrical performances of conjugated thin films on plastic substrates as well. Among myriad of polymeric substrates, polyimide is a compelling material because of the outstanding stability against thermal and mechanical stresses, not to mention high chemical resistance.[7] Since polymer substrates have distinctive physical and chemical properties from glass such as adhesion at the interface and UV induced aging/coloration, careful control of fabrication conditions including UV polymerization, solvent rinsing, and acid doping is required to achieve a high quality conducting polymer thin film with outstanding optical and electrical properties.

4.2.2 Future Applications of photopolymerized conjugated polymers

We can take advantage of the simple fabrication procedure and the outstanding electrical properties of the photopolymerized conjugated polymer thin films to explore several promising energy harvesting or storage applications, such as battery, supercapacitors, thermoelectric generator (TEG), etc.

Owing to the great redox capacitance, fast switching between redox states, and outstanding chemical or thermal stability, conducting polymers are of the surge in attention to flexible and light-weight charge storage devices such as supercapacitors or batteries. Although solid-state electrolytes are considered as an excellent substitute for liquid electrolytes, whose stability issues have been a great concern due to the electrolyte leakage and dendrite growth.[8] In addition, substantial electrical resistance in solid states at electrolyte/electrode interface and poor ionic conductivity lowers electrochemical performances.[9] In contrast, conducting polymers can serve as solid-state electrolytes having both ionic and electronic conductivities since they can hold two opposite electrochemical properties through n-doping and p-doping. The rigid characteristics of conjugated polymers can be compensated by incorporating gel-like oligomeric ethylene glycol side chains to release mechanical stresses at the interface as well as promote ionic charge transfer. By means of the UV polymerization of PEDOT incorporating oligoethylene glycol side chains, we anticipate breakthrough results to resolve the stability issue of lithium-ion batteries while maintaining electrochemical performances.

Despite excellent ZT values (1.0~2.2) of inorganic thermoelectric materials such as Bi_2Te_3[10], nearly all current high-efficiency TE materials are expensive, brittle, based on elements of low abundance, limiting their practical use and scale-up, in particular for applications in wearable energy harvesting and mobile electronic devices. Organic semiconductors, on the other hand, are based on earth-abundant elements and are mostly synthesized at near room temperature,

leading to the attractive low cost and easy processability. They provide high mechanical toughness and elasticity as well as other practical advantages such as light weight and capability for large-area deposition, making them suitable for flexible thermoelectric generators. Since thermal conductivity (κ) is generally low in organic materials, improving ZT in organic semiconductor materials primarily relies on increasing the thermoelectric power factor ($S^2\sigma$) and carrier mobility (μ). These values can be significantly enhanced by engineering molecular structures of a modified PEDOT system through the UV polymerization from EDOT and its derivatives.

4.3 References

1. Kim, Y. H., Sachse, C., Machala, M. L., May, C., Muller-Meskamp, L., Karl, L. Highly Conductive PEDOT:PSS Electrode with Optimized Solvent and Thermal Post-Treatment for ITO-Free Organic Solar Cells. *Adv. Funct. Mater.* **21**, 1076–1081 (2011).
2. Xia, Y., Sun, K., Ouyang, J. Solution-Processed Metallic Conducting Polymer Films as Transparent Electrode of Optoelectronic Devices. *Adv. Mater.* **24**, 2436–2440 (2012).
3. Ouyang, J. Solution-Processed PEDOT:PSS Films with Conductivities as Indium Tin Oxide through a Treatment with Mild and Weak Organic Acids. *Appl. Mater. Interfaces*. **5**, 13082–13088 (2013).
4. Na, S.I., Kim, S.S., Jo, J., Kim, D.Y. Efficient and Flexible ITO-Free Organic Solar Cells Using Highly Conductive Polymer Anodes. *Adv. Mater.* **20** (21), 4061–4067. (2008)
5. Chen, M., Zhong, M., Johnson, J. A. Light-Controlled Radical Polymerization: Mechanisms, Methods, and Applications. *Chem. Rev.* **116** (17), 10167–10211 (2016).
6. Chen, J., Liu, C. T. Technology Advances in Flexible Displays and Substrates. *IEEE Access.* **1**, 150–158 (2013).
7. Rana, R., Chakraborty, J., K., Tripathi, Santosh K., Nasim, M. Study of Conducting ITO Thin Film Deposition on Flexible Polyimide Substrate Using Spray Pyrolysis. *J. Nanostruct. Chem.* **6**, 65-74 (2016).
8. Lu, D., Tao, J., Yan, P., Henderson, W. A., Li, Q., Shao, Y., Helm, M. L., Borodin, O., Graff, G. L., Polzin, B. Formation of Reversible Solid Electrolyte Interface on Graphite Surface from Concentrated Electrolytes. *Nano Lett.* **17**, 1602–1609 (2017).
9. Wu, J., Hao, S., Lan, Z., Lin, J., Huang, M., Huang, Y., Li, P., Yin, S., Sato, T. An All-Solid-State Dye-Sensitized Solar Cell-Based Poly(N-Alkyl-4-Vinyl-Pyridine Iodide) Electrolyte with Efficiency of 5.64%. *J. Am. Chem. Soc.* **130**, 11568–11569 (2008).

10. Biswas, K., He, J., Blum, I. D., Wu, C. I., Hogan, T. P., Seidman, D. N., Dravid, V. P., Kanatzidis, M. G. High-Performance Bulk Thermoelectrics with All-Scale Hierarchical Architectures. *Nature*. **489**, 414–418 (2012).